



CONFORMATIONAL DYNAMICS AND EQUILIBRIA IN AMIDES

JAAN LEIS

DISSERTATIONES CHIMICAE UNIVERSITATIS TARTUENSIS

10

**CONFORMATIONAL DYNAMICS AND
EQUILIBRIA IN AMIDES**

JAAN LEIS



**TARTU UNIVERSITY
PRESS**

Department of Chemistry, University of Tartu, Estonia

Dissertation is accepted for the commencement of the Degree of Doctor of Philosophy in Chemistry on October 6th, 1998 by the Doctoral Committee of the Department of Chemistry, University of Tartu.

Opponents: Professor Dr. Ülo Lille, Tallinn
 Professor Dr. Jaak Järv, Tartu

Commencement: November 19th, 1998

Publication of this dissertation is granted by the University of Tartu

CONTENTS

LIST OF ORIGINAL PUBLICATIONS	6
INTRODUCTION	7
1. CONFORMATIONAL TRANSITION BARRIERS	9
1.1. Activation Parameters	9
1.2. Origin of Rotation and Inversion Barriers	9
2. METHODS USED IN THE STUDIES OF DYNAMIC PROCESSES	12
2.1. NMR Spectroscopy	12
2.2. Quantum-Chemical Methods	16
3. CONFORMATIONAL STUDIES IN AMIDES	18
3.1. Nitrogen Inversion in Amides. Is the Nitrogen Planar?	18
3.2. Slow Rotation around the Amide N-C(O) Bond	20
3.3. Dynamic Processes at the Other than Amide Bond	30
4. SUMMARY OF ORIGINAL PAPERS	32
4.1. <i>N</i> -Arylamides	32
4.2. <i>N</i> -Acylated 1,2-Dihydrobenzo(<i>h</i>)quinolines	35
REFERENCES	38
SUMMARY IN ESTONIAN	42
ACKNOWLEDGMENTS	44
PUBLICATIONS	45

LIST OF ORIGINAL PUBLICATIONS

- I Leis, J., Karelson, M., Schiemenz, G. P. "Stereochemistry of arylamides, 1. NMR spectra of some *N*-(1-naphthyl)amides", *ACH-Models in Chemistry* **1998**, *135* (1–2), 157–171.
- II Leis, J., Maran, U., Schiemenz, G. P., Karelson, M. "Stereochemistry of arylamides, 2. AM1 SCF and SCRF quantum chemical modelling of some *N*-(1-naphthyl)amides", *ACH-Models in Chemistry* **1998**, *135* (1–2), 173–181.
- III Leis, J., Klika, K. D., Karelson, M. "Solvent polarity effects on the *E/Z* conformational equilibrium of *N*-1-naphthylamides", *Tetrahedron* **1998**, *54*, 7497–7504.
- IV Karelson, M., Leis, J. "Quantum-chemical study of the stereochemistry of some *N,N*-diaryl amides", *Proceedings of the Estonian Academy of Sciences (Chem.)*, submitted.
- V Leis, J., Pihl, A., Pihlaja, K., Karelson, M. "Reaction of 1-naphthyl amine with methyl ketones: a possible route to the one-pot syntheses of substituted 1,2-dihydrobenzo(h)quinolines", *ACH-Models in Chemistry* **1998**, *135* (4), 573–581.
- VI Leis, J., Klika, K. D., Pihlaja, K., Karelson, M. "High inversion barrier in *N*-acylated 1,2-dihydrobenzo(h)quinolines", *Tetrahedron*, submitted.

INTRODUCTION

The life is a continuum of a variety of dynamic systems. The better knowledge about the character and rate of different motions in these systems is of a great importance as determining the stability and different properties of respective dynamic systems. The investigation of the dynamics in the chemical systems such as solutions, mixtures, but also in the single molecules enables to explain as well as to predict the stability and various useful properties of these systems.

Important issues of the physical organic chemistry are connected with the intramolecular transformations such as rotation along the chemical bonds, inversion at atoms and tautomerism. Provided that these processes are slow enough, the respective conformers or tautomers can be experimentally observed by NMR spectroscopy. The method called the variable temperature NMR or the dynamic NMR, introduced by Gutowsky and Holm [1], has become a powerful tool [2] to study the intramolecular processes characterised by the rate constants within the range of $10^{-4} \leq k \leq 10^{10} \text{ s}^{-1}$ [3]. The slower processes with the rate constants smaller than 10^{-4} s^{-1} , which correspond to the activation free energies $\Delta G^\ddagger > 23 \text{ kcal mol}^{-1}\#$, may lead to the isomers separable at the room temperature.

Although the experimental methods for the studies of exchange processes including the measurements of rates and activation energies have been continually improved, there are still uncertainties caused by the experimental limitations. Also, an insufficient knowledge about the possible substituent effects and the effects arising from the intermolecular solute-solvent or solute-solute interactions is often responsible for inadequate interpretation of experimental results. Notably, the quantum-chemical calculations could be helpful to solve the problems arising from complications in experiment. The modelling of potential surfaces of exchange processes provides valuable information about essential changes in the structural and electronic properties of the respective molecule during the transformation process. Also, the effects arising from the interaction of the molecular system under the study with the surrounding environment can be estimated using modern theoretical methods based on quantum mechanics and molecular dynamics. Therefore, a substantial support in both the planning of experiments and interpretation of experimental results is provided by theoretical chemistry.

This thesis presents a comparative NMR and quantum chemical study of conformational dynamics in the molecules with an amide functionality. In the first part of the thesis, Chapters 1 and 2, we introduce to the basics of the conformational transition barriers with a brief overview about the more widely

1 kcal = 4.184 kJ

used methods in the studies of dynamic processes. In Chapter 3, the literature overview about the stereochemistry in amides is given. In Chapter 4, the results of our own study are discussed, followed by the reprints of original publications.

1. CONFORMATIONAL TRANSITION BARRIERS

1.1. Activation Parameters

The studies of dynamic processes involve both the structural and energetic aspects. The energy barriers needed to pass to realise the conformational transitions are well defined numeric values which characterise quantitatively the dynamics of the processes. Two important equations relate the experimentally observable rate constants, k , to the activation barriers.

Eq. (1) reflects the *Arrhenius activation theory*, which is based on the assumption that the molecules require a certain excess energy, the activation energy E_A , in order to react, and that the activated and non-activated molecules are in equilibrium.

$$k = A \cdot e^{-E_A/RT} \quad (1)$$

The pre-exponential or frequency factor, A , has been interpreted as reflecting the number of “effective” collisions per unit volume and unit time.

The *Eyring equation* (Eq. (2)) is the fundamental equation of the *absolute rate theory* which is derived from the basic principles of the statistical thermodynamics.

$$k = \kappa \frac{k_B T}{h} e^{-\Delta G^\ddagger/RT} \quad (2)$$

Here, κ is the transmission coefficient, i.e. the fraction of all reacting molecules reaching the transition state that proceed to deactivated product molecules. The transmission coefficient is usually assumed to be unity.

The activation free energy, ΔG^\ddagger , is a thermodynamic characteristic of the process. The Arrhenius’ parameters can be related to the activation enthalpy ΔH^\ddagger and activation entropy ΔS^\ddagger according to the following equations:

$$\Delta H^\ddagger = E_A - RT \quad (3)$$

$$\Delta S^\ddagger = R \left(\ln A - \ln \frac{ek_B T}{h} \right) \quad (4)$$

1.2. Origin of Rotation and Inversion Barriers

This chapter gives a short overview about the origin and the most important factors affecting the conformational transition barriers in molecules. The *inversion* at atoms is connected with the rehybridisation of the central atom at

which the chemical bonds and uncoupled electron-pairs rearrange. This process can be presented by the model: $sp^3 \rightleftharpoons sp^2 \rightleftharpoons sp^3$. Consequently, the factors affecting the rehybridisation at the inverting atom affect the rate of the respective inversion process. The general rule is that the stronger is the s character of the electron-pair (n), the more energy is needed for the rehybridisation of respective atom, i.e., to planarise the pyramidal atom [4]. The inversion barriers have been observed to increase in the order: $N < P < As$, which is consistent with the magnitude of the s character at hybrid orbitals in these atoms. The electronegative substituents, e.g. halogens, at these atoms are known to increase the inversion barriers. It has been explained by the inductive effect stabilising the pyramidal ground state. The accompanying effect is the repulsion between the electron pairs of the inverting atom and the electronegative substituent in the planar transition state, respectively. On the contrary, the electron-withdrawing substituents substantially decrease the inversion barriers due to the stabilisation of the transition state, i.e., the latter substituents increase the p character of inverting atoms.

The steric effects upon the inversion barriers associate with the geometrical changes during the rehybridisation of the inverting atoms. For instance, the ring effects in aziridines substantially increase the inversion barriers due to the geometry of the three-membered ring unfavouring the 120° bond angle at the sp^2 -nitrogen in the planar transition state. The steric effects are associated with the size of the substituents. It has been observed that the inversion barriers decrease with the increasing size of the substituent. This is caused by the destabilisation of the inverted atom in sp^3 ground state due to the stronger repulsion between the substituents. However, this effect is usually small as compared to the ring-effects and inductive effects of the electronegative substituents.

The rotational barriers about the sp^3 - sp^3 bonds (e.g., the ethane derivatives) as well as the sp^3 - sp^2 bonds (e.g., the alkylarenes) are mainly caused by the steric restrictions, i.e., the larger substituents at the rotating atoms, the higher is the barrier.

The rotation around the sp^2 - sp^2 bonds may be also sterically hindered as for instance in the *ortho*-substituted biphenyls. In the case of conjugated double bonds, the resonance interactions are, however, predominant in determining the rotational barriers at these bonds. In this case, the origin of rotational barriers arises from the disappearance of the resonance stabilisation during rotation. It has been, however, been a subject of discussion in the case of amides [5; 6]. The quantum chemical calculations on formamide have revealed that the electron population at the nitrogen atom is highest in the planar ground state which is an opposite to that predicted by the resonance model. Also, the electronic population and geometric properties of an oxygen atom are almost unaffected during the rotation around the amide bond. Furthermore, as based on the cal-

culations of the attractive and repulsive components of the potential energy, it has been proposed that the origin of the amide bond rotation barriers (as well as barriers for several other rotational processes [7]) arises from the more substantial increase of the attractive potential energy as compared to the smaller decrease of the repulsive energy at the rotational transition state [7]. Even if this is correct for the rotational barriers in the gas phase, the resonance model cannot be ruled out for the amide bond rotation in polar media. The comparative gas-phase and liquid-phase *ab initio* study on rotation in formamide confirmed that the direct electronic (resonance) interaction between the nitrogen and oxygen atom is substantially stronger in polar solvents, particularly in water [8]. It was shown that in high dielectric media, both the C-O and C-N bonds are affected by the C-N bond rotation.

2. METHODS USED IN THE STUDIES OF DYNAMIC PROCESSES

2.1. NMR Spectroscopy

The NMR spectroscopy is probably the most common experimental tool to measure the exchange rates in molecular systems [2; 9–11]. The respective application is generically called as the dynamic NMR (DNMR). A wide variety of different conformational exchange processes can be examined using this methodology.

1. *Mutual exchange*, where the energetic levels for the initial (E_A) and the final (E_B) state of exchange (rotation) are equal, i.e. $E_A = E_B$. The rotation around the N-C(O) bond in *N,N*-dimethylamides, presented on Fig. 1, is one example for this type of exchange.
2. *Non-mutual exchange* occurs, for instance, in *N,N*-asymmetrically substituted amides. In this case $E_A \neq E_B$ and the two minima on the potential curve for the N-C(O) bond rotation may be considered as two different conformational isomers (cf. Fig. 2).

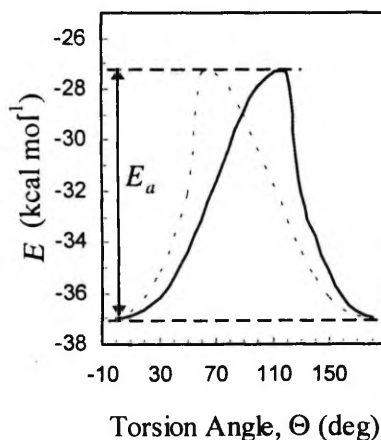


Figure 1. AM1 calculated potential energy curve characterising the amide bond rotation of *N,N*-dimethylformamide in gas phase.

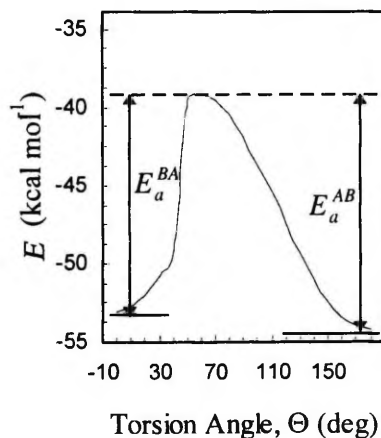


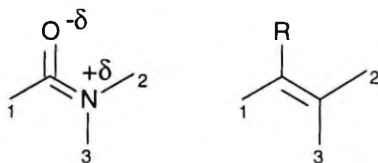
Figure 2. AM1 calculated potential energy curve characterising the amide bond rotation of *N-tert*-butylformamide in gas phase.

3. The substituted ethanes present a more complicated case. In these molecules, the rotation around the central C-C bond leads to the three energy minima (E_A , E_B and E_C). Depending on the height of the rotational barriers up to all three conformations can be distinguished by NMR.
4. The *enantiomerisation barriers* can be defined for the molecules carrying the diastereotopic groups, such as methylene protons in ethyl and neopentyl groups or methyls in isopropyl group. In the case of the slow rotation, the respective diastereotopic groups are surrounded by non-equivalent environments with different magnetic shielding.
5. The *ring-inversion* occurs in cyclic molecules, e.g. in cyclohexanes. The exchange of the magnetically non-equal axial and equatorial protons in the most stable chair conformation can be examined by DNMR.
6. The *atom inversion* takes place at pyramidal atoms, e.g., nitrogen or phosphorus. However, this process is usually too fast at the nitrogen atom even at low temperatures and only few cases (e.g. benzo(h)quinolines) are known with the inversion barrier high enough to be observed by DNMR.

Making the signal assignments

A crucial step in the conformational studies by NMR spectroscopy is the correct assignment of the signals corresponding to the different conformers. In the following, the main criteria used in making the signal assignments are listed:

1) *Inequality of cis-trans coupling constants*. It has been found [12–14], that in most cases the coupling between protons in *trans* position (J_{1-2}) is greater than in *cis* position (J_{1-3}).



Scheme 1

However, there are several examples where this relation is reversed [15; 16], and thus the signal assignments have to be supported by using additional proofs. Another restriction to this method is that the effect is observable only for couplings over three or (of smaller magnitude) over four bonds, i.e. for couplings J^3 and J^4 , respectively.

2) *Differential solvent shifts*. The resonance peaks in NMR spectra of the amides are substantially shifted in the aromatic solvents as compared to the respective peaks in the non-aromatic solvents. The useful phenomenon is that the resonance peaks of the alkyl group *trans* to oxygen appear at higher field in aromatic solvents as compared to those in non-aromatic solvents. Alternatively,

the resonance of the alkyl group *cis* to oxygen is almost unaffected. It has been proposed [17; 18] that the differential aromatic solvent induced shift (ASIS) is caused by a specific interaction between the π electrons of aromatic ring and the positively charged amide nitrogen atom, with the negatively charged carbonyl oxygen being turned away from the centre of the benzene ring.

3) *Intramolecular Overhauser effect*. The method is based on the nuclear Overhauser effect (NOE) which states that the main mechanism for proton spin-lattice relaxation, T_1 , is the direct intramolecular dipole-dipole interaction [19; 20]. The contribution to T_1 from the intramolecular dipole-dipole interactions of nuclei A and B is given by Eq. (5):

$$\frac{1}{T_1^{AB}} = \frac{\hbar^2 \gamma_A^2 \gamma_B^2 \tau}{d^6} \quad (5)$$

where T_1^{AB} is the contribution to T_1 for nuclei A or B, τ is the correlation time of the random molecular rotation, d is the internuclear distance between A and B and $\gamma_{A(B)}$ is the gyromagnetic ratio for nuclei A and B, respectively.

4) *Shifts induced by anisotropic groups in the molecule*. If the molecule contains fragments for which the contours of anisotropic magnetic field are known (as for the benzene ring [21]), the conformational assignment using the differential chemical shifts of protons is possible. It has been widely used in *N*-aryl substituted formamides with restricted rotation around the nitrogen-aryl bond [22]. In these molecules, the aromatic ring is turned out of amide plane and the formyl proton *cis* to aryl group resonates at higher field as compared to the formyl proton in *trans* position.

Determination of kinetic parameters and activation energies of the conformational transitions

Signal shape analysis

Several methods have been applied to determine the activation energies of conformational transitions. Most frequently, the dependence of the NMR signal shape on the temperature has been used. The simplest case is the equally populated two site system with the lifetime of the resonating nuclei in states A and B equal (i.e. $\tau_A = \tau_B$). The formula for the shape of the resonance lines can then be derived from the Bloch equations as follows [9; 23]:

$$g(\nu) = \frac{2\tau_A(\nu_A - \nu_B)^2}{[\nu - \frac{1}{2}(\nu_A + \nu_B)]^2 + \pi^2 \tau_A^2 (\nu - \nu_A)^2 (\nu - \nu_B)^2} \quad (6)$$

where τ is the lifetime of the nucleus in state A (B), and ν_A and ν_B are the resonance frequencies of nucleus in states A and B, respectively, under conditions of a slow exchange or in the absence of exchange.

A common procedure in the line shape analysis is the calculation of the theoretical spectrum for a series of rate constants, k (s^{-1}), using experimentally determined chemical shifts, ν_A and ν_B (Hz). Thereupon the temperature of NMR probe is raised to the value at which the shape of the experimental spectrum will be identical to the calculated spectrum. This method is also called as a *complete line shape analysis*. By determining the rate constants at different temperatures, the activation energy of the respective dynamic process can be calculated using Arrhenius equation.

Several computer programs are available to compare the theoretical and experimental spectra iteratively to achieve the best match of spectral shapes.

Approximate analysis

A complete line shape analysis is usually recommended, especially for the systems with more than one exchange process or in the case of two or more non-equally populated sites participating in the exchange process. However, some useful relations have been derived from the line shape equation (Eq. (6)). For instance, at the coalescence point of equally populated uncoupled two site system, the rate constant is

$$k_c = \frac{1}{\tau} = \frac{\pi \delta \nu_{AB}}{\sqrt{2}} \quad (7)$$

where $\delta \nu_{AB} = \nu_A - \nu_B$. Similarly, for the AB coupled two site system:

$$k_c = \frac{\pi \sqrt{\delta \nu_{AB}^2 + 6J_{AB}^2}}{\sqrt{2}} \quad (8)$$

where J_{AB} is the A-B coupling constant. The substitution of the expressions for k_c into Eyring' equation produces the following relationships (Eq. (9) and (10)) for the activation free energy of the exchange process:

$$\Delta G_c^* = 4.57 \cdot 10^{-3} T_c (9.972 + \log \frac{T_c}{\delta \nu_{AB}}) \quad (9)$$

$$\Delta G_c^* = 4.57 \cdot 10^{-3} T_c (9.972 + \log \frac{T_c}{\sqrt{\delta \nu_{AB}^2 + 6J_{AB}^2}}) \quad (10)$$

Equilibration method

This method is applicable when the characteristic NMR signals for the conformers at equilibrium are well separated and the activation energy is about 20 kcal/mol or higher. In this case, the mixture of respective isomers is displaced from the equilibrium and the sum of the rate constants of isomerisation are obtained from the time-dependence of the intensity ratio, $I_{A/B}$, of characteristic NMR signals of isomers using Eq. (11):

$$\ln \left[\frac{I_{A/B} - I_{eq}}{I_{A/B} + 1} \right] = (k_1 + k_2)t + C \quad (11)$$

where I_{eq} is the ratio at equilibrium.

2.2. Quantum-Chemical Methods

Schrödinger equation

The potential energy surface (PES), $E(R)$, of a molecule [24] is fundamental for a quantitative description of intramolecular geometrical transitions. Any given point on the $E(R)$ can be calculated by solving the Schrödinger equation (Eq. (12)) for the many-electron system:

$$\hat{H}_E \Psi_E(R, r) = E_E(r) \Psi_E(R, r) \quad (12)$$

where $\Psi_E(R, r)$ is the electronic wave function depending on both the electronic (r) and nuclear (R) coordinates. The electronic *Hamiltonian*, \hat{H}_E , can be presented as a sum of kinetic (\hat{T}_E) and potential (\hat{V}_E) energy operators:

$$\hat{H}_E = \hat{T}_E + \hat{V}_E = \sum_i^E \hat{T}_i + \sum_i^E \sum_{j \neq i}^E \frac{e_i e_j}{r_{ij}} + \sum_i^E \sum_a^N \frac{z_a e_i}{r_{ia}} \quad (13)$$

In the last equation, the potential energy is presented as a sum of electrostatic electron-electron and electron-nuclear interactions. By applying the Born-Oppenheimer approximation, the motion of electrons can be considered as in the field of “fixed” nuclei and the total energy, E , for the molecule can be presented as a sum of electronic, E_E , and the nuclear-nuclear interaction energies.

$$E = E_E + \frac{1}{2} \sum_a^N \sum_{b \neq a}^N \frac{z_a z_b}{r_{ab}} \quad (14)$$

The overview of mathematical techniques and different approximations made to solve the Schrödinger equation can be found in any quantum chemistry textbook [24].

Account for the Solvent Effects

Most of the chemical reactions as well the conformational transitions occur in solutions, i.e. in condensed media, where the solute molecule is surrounded by the other solvent and/or solute molecules. In this case, the different intermo-

lecular interactions may affect the geometry and electronic properties of molecules, and result in a changed chemical potential values as compared to those in the gas phase at low pressures. This difference is conventionally called the *solvent effect* and presented as follows:

$$\Delta G_{sol}^{\circ} = \Delta G_l^{\circ} - \Delta G_g^{\circ} , \quad (15)$$

where ΔG_l° and ΔG_g° are the chemical potentials in liquid and gas phase, respectively.

The solvent effects are usually classified as the specific and the non-specific effects [25]. The first of them include the directional, induction and dispersion effects. The second group includes the effects caused by the hydrogen bonding, the charge transfer or electron-pair donor-acceptor forces between the solute and solvent molecules. The non-specific solvent effects, particularly the solvent electrostatic polarisation effects, can be accounted for in the quantum-chemical calculations using the *self-consistent-reaction-field* (SCRF) approach [26; 27]. In the dipolar approximation, the SCRF *Hamiltonian* for the electroneutral polar solute molecule in a polarisable dielectric continuum is given as follows:

$$\hat{H} = \hat{H}_0 + \Gamma \hat{\mu}^2 \quad (16)$$

where \hat{H}_0 is the *Hamiltonian* for the isolated molecule and $\hat{\mu}$ is the dipole moment operator. The multiplier, Γ , in the perturbation term is a function of both the dielectric properties of the solvent and the size and shape of the solute molecule. The spherical cavities have been frequently assumed for the model systems, with the dielectric factor given as

$$\Gamma = \frac{(\epsilon - 1)}{(2\epsilon + 1)a_0^3} \quad (17)$$

The cavity radius a_0 can be calculated from the molar volume as follows:

$$a_0 = \left(\frac{3V_m}{4\pi N_A} \right)^{1/3} \quad (18)$$

Apart from the single-cavity models (SCa) [28] which have been shown to give a satisfactory solvation energies for tautomeric transformations, a multi-cavity model (MCa) [29] has been proposed for modelling the conformationally flexible molecules. In this case, the molecule is divided into rotationally active fragments, each of which is expected to interact with the solvent dielectric field independently. The method for the calculation of the cavity radii for the molecular fragments has been described elsewhere [29].

3. CONFORMATIONAL STUDIES IN AMIDES

The amides represent a class of compounds which stereochemistry is one of the most thoroughly investigated. The great interest in these compounds is caused by the importance of amide N-C(O) group in the determination of the conformation of polypeptides and proteins. The structure and biological activity of those compounds are directly related to the conformational preferences at the N-C(O) bond.

The most widespread explanation for the hindered rotation at the amide bond proceeds from the Pauling's resonance model, which predicts that the main contribution to the stabilisation of the planar amides arises from the shift of the electronic charge from the amide nitrogen to the carbonyl oxygen. The resulting N-C(O) partial double bond provides the hindrance to the rotation. However, recent investigations have shown that the main contribution to the barrier arises not from the charge transfer to the oxygen but rather from charge transfer between the nitrogen and the electron deficient carbonyl carbon [6]. The traditional explanation was suggested to be more appropriate for the thioamides than for amides [30] due to the larger perturbations during the rotation at the sulphur as compared to the oxygen. However, further studies revealed that in both compounds the barrier is determined by the loss in attraction due to the increase of the C-N bond length [31]. It was found that the main difference between the formamide and thioformamide is the greater donation of charge from the thioformyl group to the amino group in the latter compound. Accordingly, the pyramidalisation of nitrogen is more costly and leads to higher barrier to the rotation about the C-N bond in thioformamide.

The rotational barriers in amides are much dependent on the nature of the nitrogen environment, and hybridisation in the rotational ground state. Therefore, we will at first give a short overview on the pyramidalisation and inversion processes at the nitrogen atom, followed by the overview on the gas-phase and condensed-phase studies of the C-N bond rotation in the amides and related systems.

3.1. Nitrogen Inversion in Amides. Is the Nitrogen Planar?

According to both the resonance and hybridisation models, the amide nitrogen is expected to have a planar environment due to the partially double carbon-nitrogen bond. The microwave studies of formamide suggest a planar [32] or nearly planar molecule [33]. Also, the gas-phase *ab initio* calculations of the global minimum on the potential surface predict the planar nitrogen atom in the

amides [34; 35]. An evidence for a small degree of pyramidalisation was reported for acetamide [36]. The same prediction was made by the molecular mechanics modelling of *N,N*-dialkylamides [37]. Furthermore, it was shown that the carbon chemical shifts depend on the degree of pyramidalisation of the nitrogen atom [38]. The ^{13}C NMR chemical shifts calculated by the *ab initio* methods were in excellent agreement (within 2 ppm) with the experimental shifts for the formamide and small peptide model systems with the nonplanar nitrogen atom [38].

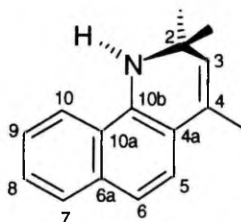
The planar environment of the nitrogen atom has been not confirmed experimentally [39] and, therefore, it is a matter of continuous discussions. Although the various experimental and theoretical studies have come to contradicting conclusions regarding the planarity of formamide, they agree that the force constant for out-of-plane bending at nitrogen is very small [32; 33; 40–42]. The energy difference between the pyramidal and planar nitrogen in the rotational ground state of formamide was predicted as only $0.5 \text{ kcal mol}^{-1}$ [6] compared to approximately 6 kcal mol^{-1} in the transition state. Nevertheless, the different sterical factors such as the strain of the bonds at nitrogen, crowding, but also the electronegative substituents at the nitrogen and the solute-solvent interactions may increase the magnitude of the out-of-plane torsion of amide group and/or lead to the pyramidalisation of nitrogen.

The height of the wagging type inversion barrier ($1.1 \pm 0.1 \text{ kcal mol}^{-1}$) for the formamide has been evaluated from the microwave spectrum [33]. This value is very close to the nitrogen inversion barrier estimated for aniline ($1.5 \text{ kcal mol}^{-1}$) from vapour-phase far-IR spectra [43]. These small values compared to the “usual” nitrogen inversion barriers in ammonia and simple alkyl-substituted amines [44] (approximately 6 kcal mol^{-1} which is equivalent to the energy needed to planarise the nitrogen atom in the rotational transition state of formamide) have been explained as the consequence of the π -conjugation between the nitrogen lone pair and the bonded π -electron system [45], supporting the “resonance model”. However, the authors [45] did not escape the “hybridisation model” [5; 6; 46] since the calculated π -delocalisation in the X-C-N moiety was much more efficiently controlled by the magnitude of nonplanarity of the nitrogen atom than the X-C-N torsion angle “militating against resonance”.

An increased pyramidal character of the nitrogen atom has been predicted for *N*-heteroatom-substituted amides [47] as a consequence of the inductive effect, repulsive lone pair — lone pair interactions, and anomeric effects. In *N*-monoheteroatom-substituted amides, the inversion barriers were less than $0.3 \text{ kcal mol}^{-1}$. However, in *N*-diheteroatom-substituted amides, the inversion barriers ranged between $2\text{--}3 \text{ kcal mol}^{-1}$. A similar effect of the heteroatoms on the nitrogen inversion barriers has been known in amines [48–50]. One of the

recent studies confirmed the high nitrogen inversion barriers in hydroxylamines [51] with the ΔG_{inv}^\ddagger values 11–13 kcal mol⁻¹.

Slow nitrogen inversion has been observed in strained amides such as *N*-carbomethoxyaziridine [52] and *N*-acetylaziridine [53], in which the unfavourable energetics is caused by having a sp² hybridised nitrogen atom in a three-membered ring. In the five- and six-membered rings, the strain is substantially diminished and the nitrogen atom adopts an almost planar structure as observed for the simple piperidine and pyrrolidine compounds [54]. The special cases are the *N*-substituted benzo(*h*)quinolines and their derivatives. Here, the steric interaction between the *N*-substituent and *peri* proton at (10) position (cf. Scheme 2) leads to unusually high nitrogen inversion barrier. In *N*-*p*-tosyl-substituted dihydrobenzo(*h*)quinolones [55], the respective barrier, E_A , has been observed as high as 23 ± 1 kcal mol⁻¹, which is close to the value needed to separate the invertomers at the room temperature.



Scheme 2

The next interesting type of distorted “amides” are the small bridgehead bicyclic lactams which maintain highly pyramidal geometry at nitrogen [56; 57]. However, most of the studies considering these compounds have been focused on the structural properties and reactivity [58; 59] and will be not reviewed here.

3.2. Slow Rotation around the Amide N-C(O) Bond

Unsymmetrically substituted amides may exist as the *cis* and *trans* isomers. By NMR spectroscopy, the separate *cis* and *trans* signals can be observed if the rotation around the C-N bond is slow, i.e., if $k \ll \pi\delta\nu_{AB} / \sqrt{2}$. The relative abundance of the *cis* and *trans* isomers may vary not only from amide to amide, but for a given amide, there may be also a considerable solvent and temperature dependence.

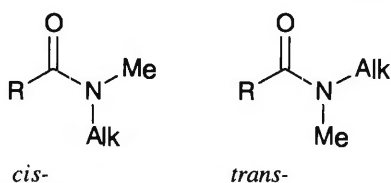
Consequently, both the static and dynamic aspects of the isomerisation at the amide bond should be considered in order to study the dynamics of rotation around this bond. In the following, a short overview will be given about the

gas-phase, liquid-phase and solid state studies of the sterical, inductive and solvent effects on the isomeric distribution and rotational barriers about the amide bond.

Gas-phase studies

The DNMR spectroscopy has been described as one of the main tools for studying the exchange processes. However, the use of DNMR method for the conformational studies of amides in the gas phase is relatively new. The first experiment, which allowed the direct comparison of the gas-phase and solution results for the same molecule, was the study of the internal rotation in *N,N*-dimethyltrifluoroacetamide [60]. Presently, the gas-phase experimental data concerning the simple *N,N*-dialkyl amides are available [61–63]. These data are of particular importance as the primary reference for the quantum chemical calculations, which are frequently applied only to the isolated molecules.

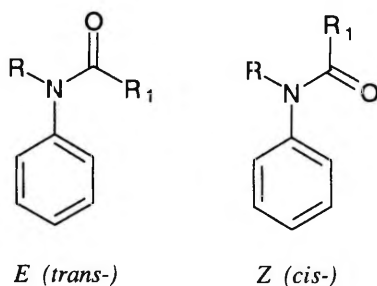
From the quantum-chemical and experimental data, it may be concluded that in the gas phase the amides prevalently adopt a planar structure in the ground state with a following pyramidalisation of the nitrogen atom in the rotational transition state [6; 47]. The restricted amide bond rotation in unsymmetrically substituted amides may give arise to the pair of unequally populated isomers. However, it has been shown that the unsymmetrically substituted *N,N*-dialkylamides do not exhibit a significant conformational preference, i.e., the effect of the size of alkyl groups is negligible. For instance, the population ratios, p_{cis} / p_{trans} , ranged only from 1.06 to 1.16 in *N*-methyl-*N*-alkylformamides [62] (Scheme 3).



Scheme 3

In similar acetamides and trifluoroacetamides, the preference of population is shifted towards the trans isomer as a result of the destabilising sterical interaction between the carbonyl substituent and the *N*-alkyl group. A small increase in the gas-phase conformer stability differences, ΔG_{gas}^0 , 78, 178 and 204 cal mol⁻¹, observed in the order of carbonyl group substituents: H < CH₃ < CF₃, respectively, directly following the substituent size increase, allowed to conclude [62] that the ΔG_{gas}^0 is dominated by the enthalpy rather than the entropy contribution.

As opposite to the *N,N*-dialkylamides, the *N*-arylamides (e.g., anilides) exhibit significant conformational preferences. The gas-phase studies by the electronic spectroscopy together with the *ab initio* calculations revealed [64] that the conformer having the carbonyl oxygen *cis* to the phenyl group is highly preferred in secondary amides, with 94% and 100% population in formanilide and acetanilide, respectively. In *N*-methylformanilide, the reversed ratio, 90/10, was observed preferring the *trans* arrangement (cf. the *E* conformation) (Scheme 4).



Scheme 4

It has been established that the aryl plane tends to be coplanar with the amide plane due to the π -electron delocalisation between nitrogen and the aryl group. Indeed, the amide molecule was found to be planar in the *cis* (*Z*) conformation. It was suggested that the close proximity of oxygen and *ortho* phenyl hydrogen is probably originated from the weak intramolecular O...H-Ar bond [64]. However, a significant out-of-plane torsion of the phenyl group was observed in the *trans* (*E*) conformation, which is consistent with the absence of the above-mentioned stabilising intramolecular hydrogen bond. In addition, a weak attraction between the formyl proton and an aromatic π -electron system may stabilise the nonplanar structure in the *E* conformation. The coplanar *Z* conformation of *N*-methylformanilide is energetically unfavorable as a result of the strained bonds at the nitrogen atom due to the sterical interaction between the methyl group and the *ortho* phenyl hydrogen [64].

The rotational barriers about the N-C(O) bond in the gas phase have been shown to depend from both the substituents at the nitrogen atom and those at the carbonyl group. In *N,N*-dialkylamides, the activation free energy, ΔG^\ddagger , decreases with increasing the "effective" size of the alkyl substituents [63]. However, the effect is rather small, e.g., ΔG^\ddagger ranging from 19.4 kcal mol⁻¹ in *N,N*-dimethylformamide (DMF) [65] to 19.0 kcal mol⁻¹ in *N,N*-diisopropylformamide (DIPF) [66]. The rotational barriers about the amide bond are much more sensitive to the nature of substituents at the carbonyl group. The barrier heights have been found to be related to both the electronegativity and the size of the substituent [62]. Again, the activation free energy decreases with increasing the size of the substituent, e.g., from 19.4 kcal mol⁻¹ in DMF to

15.7 kcal mol⁻¹ in *N,N*-dimethylacetamide (DMA) [67], which can be explained by the sterical destabilisation of the ground state in the latter compound. However, the electronegativity effect destabilises the rotational transition state and, therefore, opposes the effect of the substituent size. For instance, in *N,N*-dimethyltrifluoroacetamide (DMTFA) [60] the ΔG^\ddagger is by 0.7 kcal mol⁻¹ higher from that in DMA.

The electronegativity effects in the isolated heteroatom-substituted amides have been studied by the *ab initio* methods [47]. It appeared that the presence of a single heteroatom on the nitrogen atom reduces the acyl rotation barrier by 1–2 kcal mol⁻¹. The presence of the second heteroatom at the nitrogen atom further lowered the barrier by ca 8 kcal mol⁻¹ as compared to the barriers in the respective single substituted amides. It was shown that the lowering of the acyl C-N rotational barriers is a consequence of the pyramidal stabilisation of the nitrogen atom due to the electronegative heteroatoms, which is accompanied by increased s character (decreased p character) of the n_N orbital and by the lower π conjugation in the group.

Conformational distribution in amides and related compounds in condensed media

The NMR investigations of the stereochemistry of amides in the neat liquids and solutions have been carried out over several decades [1; 68]. The earlier studies about the hindered rotations and inversions together with the principles of NMR applications have been well-reviewed by Kessler [4] and the NMR applications in the amide chemistry by Stewart and Siddall [69].

In the condensed phase, the structural parameters and electronic properties of molecules may be substantially affected by the surrounding solute and/or solvent molecules. For instance, the amide molecule will be polarised in a dielectric medium and, respectively, the C-N bond will be shortened [8]. The effect of environment on the sterical properties of amides may be responsible for the change of conformational distribution as compared to that in the gas phase.

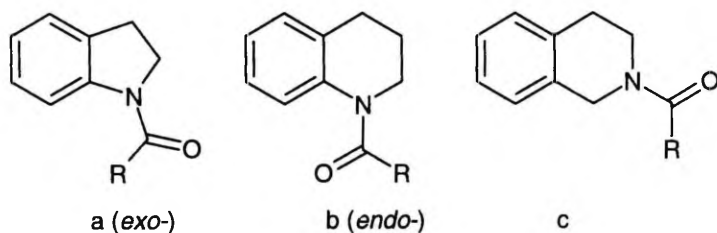
It was mentioned above that the *N,N*-dialkylformamides do not exhibit significant conformational preference in the gas phase [62]. However, in the solution, a clear relationship between the substituent's size and the conformational distribution has been observed [70]. Although the isomer with the bulkier substituent *trans* to carbonyl oxygen is only slightly preferred in the case of formamides (ca 55/45) and the respective *cis/trans* conformer ratio does not depend on the size of alkyl groups in the gas phase [63], this ratio increases from 60/40 to 89/11 in the neat liquids of *N*-ethyl-*N*-methyl- and *N*-*t*-butyl-*N*-methylformamide, respectively. The following trend of the increase of the *cis/trans* ratio on the size of alkyl groups has been observed: Me < Et < ^{*i*}Pr < ^{*t*}Bu. However, the isomeric distribution seems to be almost unaffected by the length of the alkyl

chain and the effective interaction of the alkyl group with the carbonyl group is determined by the branching at the α -carbon. As an example, the percentage of the major isomer (*trans*) was reported as 60% and 61% in the case of *N*-methyl-*N*-ethyl- and *N*-methyl-*N*-butylformamide, respectively, and as 67% and 66% in the case of *N*-methyl-*N*-isopropyl- and *N*-methyl-*N*-cyclohexylformamide, respectively [70].

On the contrary, the non-hydrogen substituents at the carbonyl group force the conformation with the oxygen *cis* to the bigger substituent to be preferred in the gas phase. However, in the polarisable media the increased polarisation of the carbonyl oxygen competes with the size of the carbonyl substituent and therefore leads to the decrease in the relative amount of the *cis* conformer. Indeed, almost equal populations of *cis-trans* isomers were observed in the neat liquids of *N,N*-dialkylacetamides [70] and in the tetrachloroethane solutions of *N,N*-dialkyltrifluoroacetamides [63].

In the *tertiary* anilides, the relative populations of *cis-trans* isomers [71–74] are comparable with those observed in the gas phase [64], i.e., only the *E* conformation is observed in the amides with the non-hydrogen substituent at the carbonyl group. In formamides, the existence of the *Z* conformation has been also detected. The *E/Z* conformer ratio 95/5 in neat *N*-methyl- and *N*-ethylformanilides [72] is comparable with the ratio (90/10) observed in the gas phase. Therefore, the origin of the isomeric distribution is probably similar to that in the gas phase.

The importance of steric factors as a main contributor to the conformational preference has been also discussed in the case of other “amide-like” molecules such as *N*-acylated indolines [75] (cf. Scheme 5a), tetrahydroquinolines [75] (cf. Scheme 5b), tetrahydroisoquinolines [76] (cf. Scheme 5c), etc.



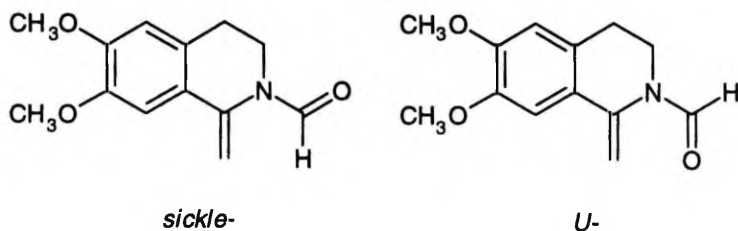
Scheme 5

Furthermore, it is interesting to note that the conformer population preferences are significantly affected by the change of the carbonyl oxygen with the sulphur. For instance, 100% of the *endo* isomer was observed in *N*-acetylindoline whereas *N*-thionacetylindoline has 100% of *exo* isomer [75]. A similar interchange of the conformational preference has been observed in the case of *N*-acylated anilines. For instance, in *N*-methylacetanilide the population of *E* conformer was 95%, whereas in *N*-methyl-*N*-*m*-tolylthionacetamide this con-

former was not detected. The explanation based on the different ability of oxygen and sulphur to form a hydrogen bond could be also considered as plausible.

Furthermore, it has been suggested that several other factors besides the sterical interactions may affect the conformational distribution at the N-C(O) bond in *N*-aryl-substituted amides. Those include the conjugation between the π -electron systems of the amide and aryl groups, the bipolar repulsion between the partially negatively charged oxygen and aromatic ring, and a weak intramolecular attraction between the formyl proton and the phenyl π -electron density. It has been suggested that any of these factors should stabilise the *E* conformation [69], particularly in the polar environments. However, the opposite trend, i.e., the increase of the relative amount of the *Z*-conformer with increasing polarity has been observed in *N*-arylamides (anilides) [77].

The *sickle* and *U* isomers were detected by NMR in the solutions of 2-formyl-1-methylidene-1,2,3,4-tetrahydroisoquinoline (cf. Scheme 6) [76]. The ratio of isomers was found to be dependent on solvent, ranging from 26/1 in chloroform to 13/1 in dimethylsulfoxide. The preference of the sickle form was ascribed to the π - π repulsion between the carbonyl and alkylidene groups. The increased polarity of the medium probably leads to the increase of the electron density on the oxygen, turning thus it more attractive to the methylidene protons.



Scheme 6

The conformational distribution in secondary amides is one of the most affected by the solvent due to the ability of nitrogen to form hydrogen bonded complexes with the hydrogen bonding solvent molecules. The "natural" isomer abundance in neat liquids or 10M DMSO solutions of *N*-alkylformamides and acetamides has been studied using the nitrogen-15 NMR spectroscopy [78]. A large set of secondary amides ranging from *N*-methylamides to *N*-*tert*-pentylamides was examined and it was revealed that the preferred conformer in all cases was the one with the oxygen *trans* to the alkyl group. The acetamides were observed exclusively in the *trans* conformation. In formamides, a small increase in the population of the *cis* isomer was observed with increasing bulk of alkyl group. Still it is interesting to note that even in the bulky *tert*-pentyl compound, the ratio of *trans/cis* isomers was observed as high as 78/22. However, the authors [78] have limited the discussion with only few remarks about

the sterical hindrances. It is obvious that the main factor determining the predominance of the *trans* conformation in formamides is the intermolecular amide-amide interaction since only in the *trans* configuration the maximum number (2 in these amides) of O...H-N hydrogen bonds could be formed. The stabilisation achieved by the hydrogen bonding probably exceeds the sterical repulsion between the carbonyl and alkyl groups.

Both the *N*-alkyl- [79] and *N*-arylamides [14] appear to be prevalently in the *trans* conformation, also in solutions. Besides of the above mentioned stabilising solute-solute hydrogen bonding, other solute-solvent interactions may play an important role. At the low concentration of amides, particularly acetamides, it has been observed that in binary dioxane — water mixtures the amide molecule is bound to three water molecules: two at the amide oxygen and one at the amino-group [80]. The theoretical studies including the *ab initio* [81], density functional theory [82] and molecular mechanics [83] calculations reveal that the hydrogen bonding in *N*-methylacetamide — water complexes is co-operative in the predominant *trans* and not co-operative in the *cis* conformation. Here, the term co-operative means that the solvation energy of multiple-bonded complexes, ΔE_{solv}^m is different from the sum of the solvation energies for the respective single-bonded amide — water complexes, hence the co-operation effect $\Delta\Delta E_{solv}$ is stabilising the *trans* isomers.

$$\Delta\Delta E_{solv} = \Delta E_{solv}^m - \sum_i \Delta E_{solv,i} \quad (19)$$

A strong concentration dependence of the conformer ratio has been observed in *N*-arylformamides [69]. In very diluted low polarity solvents, the *cis* isomer was found to be more abundant, e.g. the *trans/cis* ratio decreased from 73/27 to 45/55 by going from the 52.5 to the 1.5 mole percent CDCl_3 solution of formanilide [14]. Two possible explanations have been offered [14]: (a) the solvated *cis* isomer is thermodynamically more stable than the *trans* isomer or (b) the cyclic hydrogen bonded solute-solute complexes are prevalent even at the low concentrations.

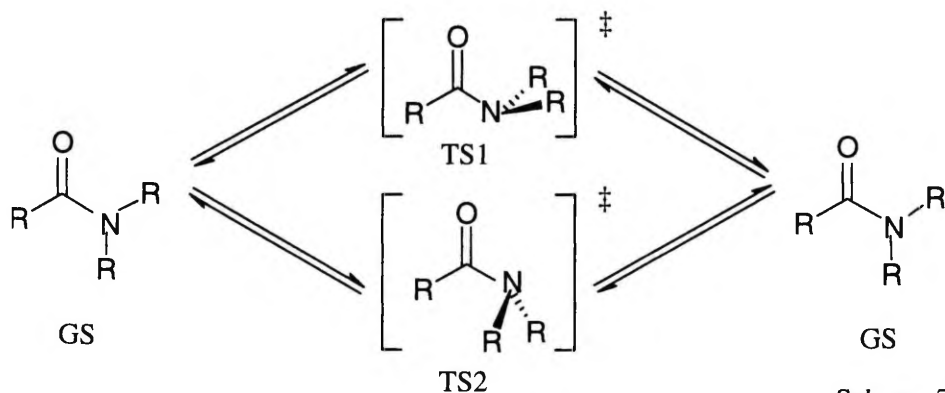
Also, a substantial solvent dependence of the conformer ratio has been observed in the case of secondary amides. The most drastic case is the bulky *N*-*tert*-butylformamide in which the amount of the *cis* isomer increases from 18% in benzene solution to 48% in chloroform solution [79]. This observation is consistent with the suggested increase of the bulk of the carbonyl group in more polar solvents leading to the out-of-plane torsion of the amide group together with a decreased N-C(O) conjugation. This suggestion is also supported by the observed deshielding of the ^{17}O NMR resonance of the *cis* isomer as compared to the *trans* isomer [84]. It has also been shown that the carbonyl oxygen is more strongly solvated in the case of *cis* isomer because of the sterical restrictions to solvation in the *trans* isomer [84].

Molecular structure of amides in crystal. The X-ray diffraction spectroscopy has been widely used to study the molecular structure of *N*-arylamides and bezamides, which in most cases can be easily crystallised from the proper solvents. It has been revealed that a *trans* preference is common in the case of secondary anilides with non-hydrogen substituents at the carbonyl group [85; 86], whereas the respective *N*-alkylanilides exist predominantly in the *cis* conformation [73; 74; 87]. The *cis* preference of *N*-alkylbenzanilides and its derivatives has been explained by the attractive aromatic-aromatic interactions [88]. A similar aromatic-aromatic interaction has been observed in oligomeric cyclic arylamides [89] and the derivatives of *N*-methylated ureas [90].

In conclusion, the previous conformational studies of amides and related compounds have revealed that the factors determining the conformational equilibrium in solutions vary from amide to amide, whereas the conformational distribution may be affected by temperature, concentration, nature of the solvent and geometrical and electronic properties of molecules.

Rotational barriers about the N-C(O) bond. Solvent effects

A classical case for the amide bond rotation is presented on the Scheme 6, where the molecule in the ground state adopts a planar or almost a planar structure with the following pyramidalisation in the rotational transition state. Two possible structures of C_s symmetry, TS1 and TS2 (cf. Scheme 7), have been found for the transition state by the quantum chemical calculations.



The gas-phase calculations predict TS1 to be of lower energy in the unsubstituted formamide due to the favourable hydrogen-oxygen interactions. However, the SCRF calculations have proved TS2 to be the lower energy transition state in the polar media, e.g. in acetone and water [8]. For dimethylformamide and dimethylacetamide, the different rotational transition states TS2 and TS1 have

been predicted both in the gas and liquid phase, respectively [91]. Since TS2 has higher dipole moment than TS1, the polar solvents are expected to support this transition state in all *N*-alkylated amides [91; 92]. In the case of dimethylacetamide, the TS1 and TS2 were found to be of close energy in aqueous solutions [93]. However, in most solvents the TS1 transition state is probably still preferred for the amides with the non-hydrogen substituent at the carbonyl group due to the repulsive interactions between the substituents at the carbonyl and amine groups.

Earlier studies of the amide bond rotation in solutions and the data on amide bond rotational barriers have been reviewed by Stewart and Siddall [69]. A comparison of these data and the more recent experimental results in solutions [94–96] with the gas-phase data [62; 63] and the *ab initio* calculated rotational barriers [91] gives the following overall picture about the amide bond rotations. First, the substituent effects in the solutions are similar to those observed in the gas phase, i.e. the increase in the size of the *N*-alkyl substituents decreases the rotational barrier. Notably, the effect is of greater magnitude in solutions. The replacement of the hydrogen at the carbonyl group with a bigger substituent further decreases the rotational barrier. Some illustrative activation free energy values characterising the rotational barriers are collected in the Table 1.

Table 1. Activation free energies, ΔG^\ddagger , characterising the amide bond rotation of *N,N*-dialkylamides ($R_1C(O)NR_2R_3$) in different media.

R ₁	R ₂	R ₃	ΔG^\ddagger , kcal mol ⁻¹		
			gas ^a	solution ^b	
H	Me	Me	19.4	20.7 (298)	C ₂ Cl ₄
H	Me	Bu	19.3	20.1 (298)	TCE ^c
H	Me	ⁱ Pr	19.1	19.9 (298)	TCE
H	Et	Et	19.2	20.6 (393)	<i>o</i> -DCB ^d
Me	Me	Me	15.3	17.3 (298)	CCl ₄
Me	ⁱ Pr	ⁱ Pr	14.3	15.6 (298)	CCl ₄
Et	Me	Me	–	17.4 (331)	CCl ₄
ⁱ Pr	Me	Me	–	16.2 (299)	<i>o</i> -DCB

^a Rotational barriers at 298 K; ^b rotational barriers at the temperature shown in parentheses (in K); ^c tetrachloroethane; ^d *ortho*-dichlorobenzene.

In principle, all factors destabilising the ground state or stabilising the transition state may reduce the rotational barriers. For instance, the difference in the activation free energies by approximately 4 kcal mol⁻¹ in *N*-formyl- and *N*-acetyl derivatives of tetrahydroquinoline, respectively, has been explained by the stronger steric strain in acetyl derivative [97]. A direct conjugation of the aryl group (or other π -electron system) with the C=O bond stabilises the transition

state and, consequently, reduces the barrier height of the N-C(O) bond rotation [69]. The relatively low barriers as compared to the ordinary amides have been observed also in the amides (and related molecular systems) in which the nitrogen atom is a part of aromatic π -electron system, e.g., *N*-acylated pyrroles [98], in which the carbonyl and the ring π systems compete for the nitrogen lone pair [99].

The rotational barriers in solutions are expected to be somewhat higher than in the gas phase due to the stronger conjugation between the amino- and carbonyl groups. In *N,N*-dialkylamides, the liquid-phase values of the rotation activation free energies, ΔG^\ddagger , are approximately 1...3 kcal mol⁻¹ higher than those in the gas phase [62; 63]. The change in activation parameters on moving from the gas phase to liquids has been also attributed to the change in the dipole moment during the rotation. A polar solvent is expected to stabilise the ground state with the higher dipole moment more than the respective transition state [94].

All previous studies [69; 94] have clearly shown that the rate of amide bond rotation decreases as either the polarity or the hydrogen bond donor ability of the solvent increases. Furthermore, different solvents may affect the amide rotational barrier by different mechanisms (specific and nonspecific interactions), but the nature of these interactions should be similar for the homologous series of amides. An excellent linear correlation has been obtained between the rotational barriers of DMF and DMA in the relatively low-polarity solvents ($1 \leq \epsilon \leq 36.7$) [91] (cf. Fig. 3). The stronger solvent effect in the case of DMA was explained by the larger dipole moment difference between the ground state and TS1 as compared to that between the ground state and TS2 in DMF. A good linear relationship has been obtained between the rotational barriers at the amide bond and Onsager-Kirkwood function, $(\epsilon-1)/(2\epsilon+1)$, in non-hydrogen-bonding solvents [91]. A small deviation from linearity was observed for the aromatic and halogenated solvents, which are known to give larger solvent effects in a variety of reactions [100], and also for the hydrogen-bonding solvents (~ 0.5 – 1.0 kcal mol⁻¹). However, the rotational barriers in all above considered types of solvents (cf. Fig. 3) correlated well ($R^2=0.97$ and 0.93 for DMF and DMA, respectively) with the Reichardt's empirical solvent polarity parameter, E_T [25].

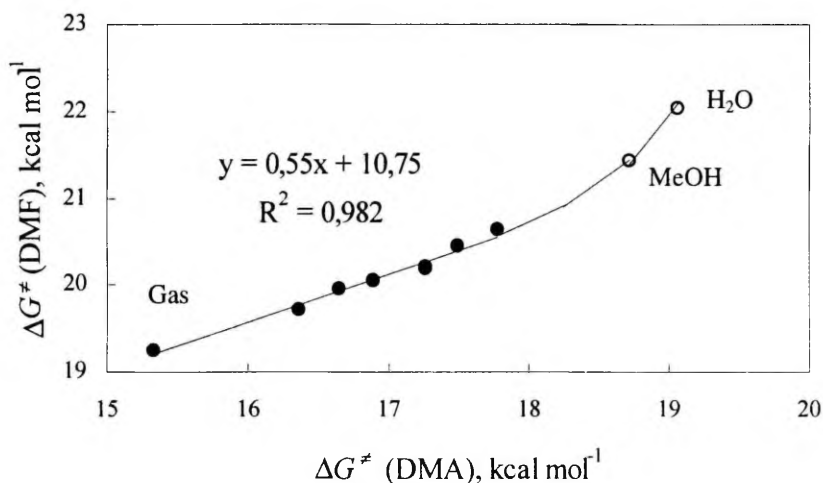


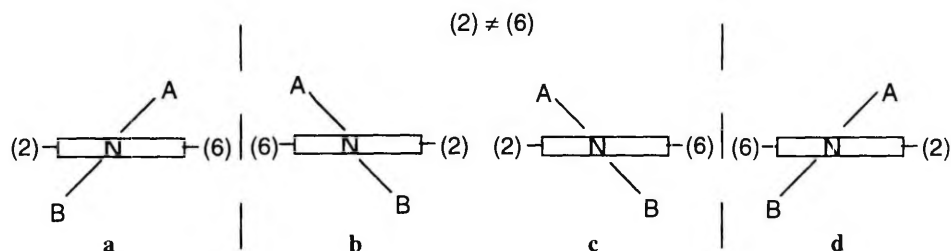
Figure 3. The relationship between the rotational barriers of dimethylformamide (DMF) and dimethylacetamide (DMA) in media of variable polarity. For the non-hydrogen-bonding solvents (solid circles), the slope of the respective linear relationship is 0.55.

Similarly to the hydrogen bonding which supports the electron density shift to the oxygen atom, the complexation of amide molecules with different cations in solutions should also increase the rotational barrier at the amide bond. For instance, the presence of metal perchlorates in propylene carbonate solutions of DMA increased the activation energy, E_A , by $\sim 1\text{--}2$ kcal mol⁻¹ as compared to the 18.3 kcal mol⁻¹ in an electrolyte-free solution [101].

3.3. Dynamic Processes at the Other than Amide Bond

The flat amide group may have substantial rotational barriers around the N-Ar bonds in *N*-aryl-substituted amides. In general, the conjugated π -electron systems tend to be coplanar due to the resonance interactions. For instance, a coplanar or nearly such molecular structure has been suggested for the unstrained *N*-arylimines [102], the secondary [64] and the tertiary anilides [103]. However, the substitution of phenyl ring in *ortho*-position forces the amide plane turn out from the aryl plane. The degree of out-of-plane torsion of the phenyl ring has been estimated by the dipole moment measurements in dioxane [104] and by the dependence of the formyl proton resonance frequencies on the diamagnetic field of aryl ring [22]. In the case of asymmetric aryl group, the rotation around the *N*-aryl bond may give rise to the pair of optical isomers. In

principle, four energy minimums can be distinguished on the potential energy surface of rotation, corresponding to the conformers **a–d** in Scheme 8.



Scheme 8

These conformers are separated from each other by the high-energy transition state at $\sim 0^\circ$ (180°) and the low-energy transition state at $\sim 90^\circ$ (270°). However, the latter is usually too low ($< 5 \text{ kcal mol}^{-1}$) to be detected by the NMR spectroscopy. Therefore, the pairs **a–b** and **c–d** may be considered as the single rotamers. Nevertheless, if the substituents containing the diastereotopic groups are attached to the centre of asymmetry, i.e., to the nitrogen atom in the present case, the protons of diastereotopic groups will be unisochronous under the conditions of slow rotation [105; 106]. In such a case, the rate of the respective rotational process can be determined by dynamic NMR.

It has been shown that the sterical hindrance is primarily responsible for the rotational barriers around the bonds between the *ortho*-substituted phenyl and adjacent to it groups [4]. Therefore, the respective optical isomers can be considered as the atropisomers. Similarly to 2- or 2,6-substituted phenyl compounds, the hindered rotation can be observed in α -naphthyl compounds. Here, the *peri*-hydrogen in (8) position is responsible for the hindrance to the rotation. The respective energy barriers have been determined for several α -naphthylalkanes [107], -alkenes [108], -amines [109; 110], -imines [102; 111], -ketones [112] and -sulphoxides [113]. These data indicate that the barriers are higher at the bonds connecting the α -naphthyl position with a sp^2 -hybridised atom. This is caused by the requirement for the distortion of the planarity of the group at the transition state.

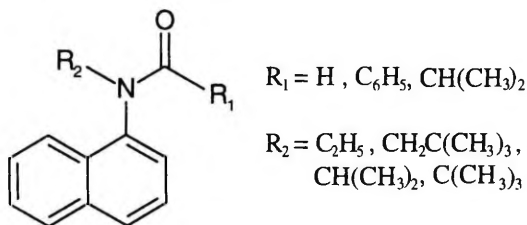
Such generalisation can be well attributed to the N-aryl bond rotational barriers in amides. More precisely, all factors disturbing the planarity of amide group and promoting the nitrogen atom pyramidalisation, should decrease the rotational barrier for the N-aryl bond rotation. Indeed, the rotational barrier in benzanilides is ca $1.5 \text{ kcal mol}^{-1}$ lower than in the analogous acetanilides [114]. The reduced N-C(O) double-bond character in ureas is reflected by the further lowering of rotational barriers about this bond [115] and also by weak solvent and Lewis acid effects on the N-C(O) bond rotation [116].

4. SUMMARY OF ORIGINAL PAPERS

This chapter gives an overview of our original work published in six articles on the conformational equilibria and dynamic processes in the compounds with an amide group. The first part summarises the results of the NMR and quantum chemical studies on the isomeric distribution and rotational dynamics in *N*-alkyl-*N*-1-naphthylamides [I, II], the solvent effects on the *E/Z* conformational equilibria in *N*-alkyl-*N*-1-naphthylformamides [III], and the quantum chemical modelling of the rotational processes in *N,N*-diarylamides [IV]. The second part summarises the studies on the conformationally restricted *N*-acylated 1,2-dihydrobenzo(*h*)quinolines [V, VI] including the synthesis of 1,2-dihydrobenzo(*h*)quinolines [V] as promising objects for the study of the restricted inversion at the nitrogen atom, and the NMR and quantum chemical modelling of the hindered inversion in the respective *N*-acylated compounds [VI].

4.1. *N*-Arylamides

The first two articles [I–II] summarise the study on the stereodynamics in several *N*-alkyl-*N*-1-naphthylamides presented on Scheme 9.



Scheme 9

In these compounds, the two conformational exchange processes can be observed by the NMR spectroscopy. In addition to the slow amide bond rotation, the interaction between the *peri* hydrogen and the amide group results in the hindrance to the nitrogen-aryl bond rotation. The *N*-alkyl substituents were chosen in such a way that they would contain the diastereotopic groups suitable as a probe in the NMR measurements due to their unisochrony under the conditions of slow rotation. Indeed, the separate NMR signals of the diastereotopic groups were observed for all *N*-alkyl-*N*-1-naphthyl-amides studied, witnessing a twisted structure at *N*-naphthyl bonds. The NMR spectra for the respective formamides showed the existence of both the *E* and *Z* conformers in solutions. In the case of benzoyl- and isobutyrylamides, only one conformer was observed.

The conformations in formamides were assigned by using the differential chemical shielding of formyl protons (cf. Table II in [I]) and differential NOE spectroscopy (Table III in [I]). For the isobutyryl- and benzoylamides, the chemical shift difference measurements, i.e. the ASIS analysis were carried out in chloroform and benzene solutions (cf. Tables IV–VI in [I]). According to these studies, the *E* conformer was assigned as the major isomer in formamides. Also, this conformer was shown to be predominant in benzoyl- and isobutyrylamides. It was established that the *E* conformers were characterised by substantial upfield shifts of the *N*-alkyl signals upon changing the solvent from chloroform to benzene. As an opposite, the respective signals for the *Z* conformers were almost unaffected by the change of the solvents.

The results of the NOE analysis (cf. Fig. 1 [I]) were consistent with the amide structure in which the plane defined by the amide group was almost orthogonal to the plane defined by the aryl (naphthyl) group. Also, the large difference between the resonance frequencies for the formyl protons of the *E* and *Z* conformers is apparently a consequence of a substantial shielding of proton in the *E* form by the aromatic π electron system. This observation confirms therefore the conclusion about the more or less orthogonal position of the amide and naphthyl groups.

The X-ray analysis of *N*-neopentyl-*N*-1-naphthylformamide revealed that the *E* conformation of this compound has approximately perpendicular naphthyl and amide planes in the solid state [I]. The respective experimentally observed torsion angles were in an excellent agreement with those calculated by the semiempirical AM1 method for the isolated molecule [II], thus confirming the reliability of the respective semiempirical model for the studies of stereochemistry in *N*-arylamides.

According to the dynamic NMR study, the rotational barriers about N-C(O) bonds of formamides appeared to be somewhat higher than those about the nitrogen-aryl bonds. Also, the barrier heights (ΔG^\ddagger) for the N-Ar bond rotation of *Z* conformers were ca 1–1.5 kcal mol⁻¹ higher than for respective *E* conformers (cf. Table VII in [I]). However, the rotational barrier about N-Ar bonds increased substantially with increasing the size of the *N*-alkyl groups. The opposite trend has been known for the rotation around the N-C(O) bond. Therefore, it is possible that the rotational barriers about both the N-C(O) and N-Ar bonds become similar in the case of voluminous substituents at the nitrogen atom. Such situation was observed for the *N*-isopropyl-*N*-1-naphthylformamide: the two quartets of methyl signals in the dynamic NMR spectra coalesced into one doublet, corresponding to the fast rotation around both the N-Ar and N-C(O) bonds.

The quantum-chemical modelling (AM1 SCF) of the compounds presented in Scheme 9, lead to correct predictions of the conformational barriers and distribution of isomers of *N*-1-naphthylamides in low polarity solvents [II].

However, the single- and multi-cavity SCRF models predicted a substantial increase of the relative population of the *Z* conformer in respective formamides in polarisable media (cf. Table 1 in [II]). These results agreed with the experimentally observed relative populations of the *E* and *Z* conformers of these compounds in the chloroform ($\epsilon = 4.8$) and tetrachloroethane ($\epsilon = 8.2$) solutions [I]. A closer study of solvent effects on the *E/Z* equilibrium of tertiary *N*-1-naphthylformamides was carried out in [III]. The isomeric distribution at the N-C(O) bond, measured as the ratio of integrated peaks of formyl protons of the *E* and *Z* conformers (cf. Table 1 in [III]), was correlated with the dielectric permittivity of solvent in the range of $4.8 < \epsilon < 46.8$. An excellent linear relationship between the free energy of conformational equilibrium, ΔG^0 , and the dielectric permittivity, ϵ , was obtained [cf. Fig. 1 in [III]] for the compounds with the smaller alkyl groups (i.e. R = Et, CH₂-^{*i*}Bu, ^{*i*}Pr) at the nitrogen atom. The following relationships for the respective compounds

$$\Delta G_{R=Et}^0 = -0.017\epsilon + 1.342; R^2 = 0.981 \quad (20)$$

$$\Delta G_{R=CH_2-^iBu}^0 = -0.017\epsilon + 1.176; R^2 = 0.985 \quad (21)$$

$$\Delta G_{R=^iPr}^0 = -0.017\epsilon + 1.032; R^2 = 0.939 \quad (22)$$

revealed the presence of an uniform solvent effect on the *E/Z* equilibria. The experimentally observed trends of ΔG^0 values were qualitatively described by the MCa SCRF model. However, it was evident that the electrostatic reaction field model alone is not sufficient to describe the solvent effect on the *E/Z* equilibria in these amides. The MCa SCRF calculations predicted a substantial out-of-plane torsion within the amide group of the *Z* conformer. Consequently, the electronic properties of the amide group should be quite different in both conformers, which may lead to the different solvation. Differential solvation at the oxygen atom may be also caused by the sterical restrictions for the solvation in *E* conformers. This factor has been suggested to be important in the case of bulky amides, particularly in *N*-*tert*-butyl-substituted amides. Furthermore, the sterically restricted solvation should also depend on the size and shape of the solvent molecules. Indeed, this explains the poor correlation between ΔG^0 and ϵ (cf. Eq. (23)) for the *N*-*tert*-butyl-*N*-1-naphthylformamide.

$$\Delta G_{R=^tBu}^0 = -0.013\epsilon + 0.343; R^2 = 0.658 \quad (23)$$

In conclusion, the solvent effect on the conformational equilibrium in *N*-alkyl-*N*-1-naphthylformamides is determined by the combination of the interaction of the solute molecules with the dielectric medium and the differential solvation of the *E* and *Z* isomers by adjacent solvent molecules.

The fourth article [IV] presents the quantum chemical study of the conformational dynamics in *N,N*-diarylamides. The semiempirical AM1 SCF investi-

gation of the full PES revealed the existence of two pairs of enantiomers for *N,N*-di(2-methylphenyl)-3,3-dimethylbutyrylamide and the eight conformers for the *N*-1-naphthyl-*N*-(2-methylphenyl)-3,3-dimethylbutyrylamide, which, in principle, could be observed in the NMR spectra of respective compounds. According to the calculations, it was predicted that in the former compound, two conformational transitions corresponding to the enantiomerisation and to the single rotation along the N-aryl bond, respectively, can be distinguished in the NMR spectra. The predicted $\Delta G_{\text{liquid}}^*$ values of $\sim 15 \text{ kcal mol}^{-1}$ and $\sim 17 \text{ kcal mol}^{-1}$, respectively, are in a good accordance with the experimentally measured values (13.2 and 17.3 kcal mol^{-1}).

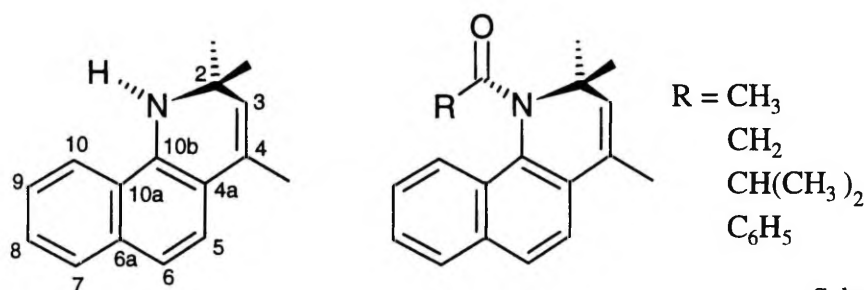
The two conformational transitions were predicted also for the unsymmetrically substituted *N,N*-diarylamides. The first of them corresponds to the concerted rotation around the N-aryl bonds and the other to the concerted rotation along the N-aryl and N-C(O) bonds. Therefore, the existence of an averaged set of NMR signals over the all possible conformers has been predicted for this compound.

4.2. *N*-Acylated 1,2-Dihydrobenzo(*h*)quinolines

The derivatives of 1,2-dihydrobenzo(*h*)quinoline are a compounds with complex stereochemistry. First, as a result of substantial steric repulsion between the H(10) proton and the substituent at the nitrogen atom, the latter is characterised by an unusually high inversion barrier [55]. On the other hand, these compounds are also interesting due to the possibility to model the rotational processes over the H(8) position of the *N*-naphthyl derivatives by the inversion at the nitrogen atom. The steric interactions are expected to be of the similar magnitude in these two structures and, consequently, similar barriers can be expected for both processes.

The slow rates of inversion in 1,2-dihydrobenzo(*h*)quinoline derivatives can be measured by NMR due to the nonequivalence of the geminal protons at the (2) position as demonstrated in the case of the *N*-tosylbenzoquinolone derivatives [55]. However, the geminal protons in these compounds are additionally splitted by the protons at the (3) position, which are, in principle, also diastereotopic and can be nonequivalent. Consequently, the complicated ABXY coupled resonance bands would appear in the proton NMR spectra, which make the measurements of the coalescence temperature much more complicated. Therefore, we have preferred the 2,2-dimethyl derivatives of 1,2-dihydrobenzo(*h*)quinoline, which, in the case of slow inversion, would display the simple AB coupling in the respective NMR spectra.

A simple one-pot method was worked out for the synthesis of 1,2-dihydro-2,2,4-trimethylbenzo(*h*)quinoline [V]. This method is a modification of the Scaup's synthesis [117] and perspective for the synthesis of other stereochemically interesting benzoquinoline derivatives. In the sixth paper [VI] of this thesis, the results of the conformational study of several *N*-acyl-1,2-dihydro-2,2,4-trimethylbenzo(*h*)quinolines (Scheme 9) are reported. The semiempirical AM1 SCF calculations together with the NOE difference analysis (cf. Tables 1 and 3, and Fig. 1 in [6]) revealed that in these molecules, the nitrogen atom is pyramidal with a substantial out-of-plane torsion of the acyl group, and the molecules adopt the *E* conformation in the ground state.



Scheme 9

As expected, the separate NMR signals were observed for the geminal methyl groups in all *N*-acyl derivatives. The large difference (~ 1 ppm) of these signals is caused by the weak intramolecular hydrogen bonding between the oxygen atom and one of the methyl groups. The inversion barriers were found from the temperature dependence of the NMR spectrum of the AB system of the geminal methyl groups. The established coalescence temperatures $T_c = 342$; 363 ; 383.5 and 294 K correspond to the activation free energies $\Delta G_c^* = 15.5$, 16.6 , 17.6 and 13.4 kcal mol⁻¹ for the acetyl, chloroacetyl, isobutyryl and benzoyl derivatives, respectively. In the case of *N*-chloroacetyl- and *N*-isobutyryl derivatives, a second temperature dependent splitting of the NMR signals was also observed. The respective coalescence temperatures 342.4 K and 360.8 K for the isotopic protons of chloromethyl group (cf. Fig. 2 in [VI]) and methyls of isopropyl group correspond to the activation free energies $\Delta G_c^* = 16.5$ and 17.7 kcal mol⁻¹, respectively.

As expected, the AM1 model underestimated substantially the inversion barriers for these compounds. However, an excellent linear relationship was obtained between the AM1 calculated inversion barriers and the experimentally determined activation free energies:

$$\Delta G_{liquid}^* = 0.87E_A(\text{AM1}) + 7.38 \text{ (kcal mol}^{-1}\text{)} \quad (24)$$

$$R^2 = 0.985; s = 0.28$$

According to this relationship, the calculated $E_A = 0.2 \text{ kcal mol}^{-1}$ for the 1,2-dihydro-2,2,4-trimethylbenzo(*h*)quinoline corresponds to the activation free energy of $7.5 \text{ kcal mol}^{-1}$, which is very close to the experimentally known inversion barrier in ammonia (6 kcal mol^{-1}).

The inversion barriers, in 1,2-dihydrobenzo(*h*)quinoline derivatives, are directly correlated with the size of the acyl groups at the nitrogen atom. The exception is the *N*-benzoyl derivative, which is probably destabilised due to the repulsion between the two aromatic rings in the ground state.

REFERENCES

1. Gutowsky, H. S., Holm, C. H. *J. Chem. Phys.* **1956**, 25, 1228.
2. Sandström, J. *Dynamic NMR Spectroscopy*; Academic Press, London, 1982.
3. Orrell, K. G.; Šik, V.; Stephenson, D. *Progress in NMR Spectroscopy* **1990**, 22, 141.
4. Kessler, H. *Angew. Chem.* **1970**, 237.
5. Wiberg, K. B., Laidig, K. E. *J. Am. Chem. Soc.* **1987**, 109, 5935.
6. Wiberg, K. B., Breneman, C. M. *J. Am. Chem. Soc.* **1992**, 114, 831.
7. Bader, R. F. W., Cheeseman, J. R., Laidig, K. E., Wiberg, K. B., Breneman, C. *J. Am. Chem. Soc.* **1990**, 112, 6530.
8. Burton, N. A., Chiu, S. S.-L., Davidson, M. M., Green, D. V. S., Hillier, I. H., McDouall, J. J. W., Vincent, M. A. *J. Chem. Soc., Faraday Trans.* **1993**, 89, 2631.
9. Becker, E. D. *High Resolution NMR. Theory and Chemical Applications*; Academic Press, Inc., 1970.
10. Kemp, W. *NMR in Chemistry. A Multinuclear Introduction*; Macmillan Education Ltd., 1986.
11. Pihlaja, K., Kleinpeter, E. *Carbon-13 NMR Chemical Shifts in Structural and Stereochemical Analysis*; VCH Publishers, Inc., 1994.
12. Karplus, M. *J. Chem. Phys.* **1959**, 30, 11.
13. Bourn, A. J. R., Randall, E. W. *Mol. Phys.* **1964**, 8, 567.
14. Bourn, A. J. R., Gillies, D. G., Randall, E. W. *Tetrahedron*, **1964**, 20, 1811.
15. Fraser, R. R., McGreer, D. E. *Can. J. Chem.* **1961**, 39, 505.
16. Rogers, M. T., Woodbrey, J. C. *J. Phys. Chem.* **1962**, 66, 540.
17. Hatton, J. V., Richards, R. E. *Mol. Phys.* **1960**, 3, 253.
18. Hatton, J. V., Richards, R. E. *Mol. Phys.* **1962**, 5, 139.
19. Solomon, I. *Phys. Rev.* **1955**, 99, 559.
20. Solomon, I. *J. Chem. Phys.* **1956**, 25, 261.
21. Johnson, C. E., Bovey, F. A. *J. Chem. Phys.* **1958**, 29, 1012.
22. Rae, I. D. *Can. J. Chem.* **1966**, 44, 1334.
23. Harris, R. K. *Nuclear Magnetic Resonance Spectroscopy. A Physico-chemical View*; Pitman Publishing Inc., 1983.
24. Levine, I. N. *Quantum Chemistry*, 3rd ed., Allyn and Bacon Inc., Boston, 1983.
25. Reichardt, C. *Solvents and Solvent Effects in Organic Chemistry*, 3rd ed., VCH Publishers: Weinheim, 1990.
26. Tapia, O., Goscinski, O. *Mol. Phys.* **1975**, 29, 1653.
27. Karelson, M. M. *Org. React.* **1980**, 17, 357.
28. Tamm, T., Karelson, M. *Org. React.* **1989**, 26, 211.
29. Karelson, M., Tamm, T., Zerner, M. C. *J. Phys. Chem.* **1993**, 97, 11901.
30. Wiberg, K. B., Rablen, P. R. *J. Am. Chem. Soc.* **1995**, 117, 2201.
31. Laidig, K. E., Cameron, L. M. *J. Am. Chem. Soc.* **1996**, 118, 1737.
32. Kurland, R. J., Wilson, E. B., Jr. *J. Chem. Phys.* **1957**, 27, 585.
33. Costain, C. C., Dowling, J. M. *J. Chem. Phys.* **1960**, 32, 158.
34. Fogarasi, G., Pulay, P., Török, F., Boggs, J. E. *J. Mol. Struct.* **1979**, 57, 259.
35. Fogarasi, G., Balázs, A. *J. Mol. Struct. (Theochem)* **1985**, 133, 105.

36. Jeffrey, G. A., Houk, K. N., Paddon-Row, M. N., Rondan, N. G., Mitra, J. *J. Am. Chem. Soc.* **1985**, *107*, 321.
37. Schnur, D. M., Yuh, Y. H., Dalton, D. R. *J. Org. Chem.* **1989**, *54*, 3779.
38. Sulzbach, H. M., Schleyer, P. v. R.z, Schaefer, H. F., III. *J. Am. Chem. Soc.* **1995**, *117*, 2632.
39. Ventura, O. N., Rama, J. B., Turi, L., Dannenberg, J. J. *J. Phys. Chem.* **1995**, *99*, 131.
40. Hirota, E., Sugisaki, R. *J. Mol. Spectrosc.* **1974**, *49*, 251.
41. Wright, G. M., Simmonds, R. J., Parry, D. E. *J. Comput. Chem.* **1988**, *9*, 601.
42. Kwiatkowski, J. S., Leszczyński, J. *J. Mol. Struct.* **1993**, *279*, 277.
43. Larsen, N. W., Hansen, E. L., Nicolaisen, F. M. *Chem. Phys. Lett.* **1976**, *43*, 584.
44. Lambert, J. B. *Top. Stereochem.* **1971**, *6*, 19.
45. Ferretti, V., Bertolasi, V., Gilli, P., Gilli, G. *J. Phys. Chem.* **1993**, *97*, 13568.
46. Laidig, K. E., Bader, F. W. *J. Am. Chem. Soc.* **1991**, *113*, 6312.
47. Rauk, A., Glover, S. A. *J. Org. Chem.* **1996**, *61*, 2337.
48. Levin, C. C. *J. Am. Chem. Soc.* **1975**, *97*, 5649.
49. Bent, H. A. *Chem. Rev.* **1961**, *61*, 275.
50. Perrin, C. L., Thoburn, J. D., Elsheimer, S. *J. Org. Chem.* **1991**, *56*, 7034.
51. Hassan, A., Wazeer, M. I. M., Perzanowski, H. P., Ali, Sk. A. *J. Chem. Soc., Perkin Trans. 2*, **1997**, 411.
52. Anet, F. A. L., Osyany, J. M. *J. Am. Chem. Soc.* **1967**, *89*, 352.
53. Tarasenko, N. A., Avakyan, V. G., Belik, A. V. *Zh. Strukt. Khim.* **1978**, *19*, 541.
54. Paulsen, H., Todt, K. *Chem. Ber.* **1967**, *100*, 3397.
55. Speckamp, W. N., Pandit, U. K., Korver, P. K., van der Haak, P. J., Huisman, H.O. *Tetrahedron*, **1966**, *22*, 2413.
56. Greenberg, A., Moore, D. T., DuBois, T. D. *J. Am. Chem. Soc.* **1996**, *118*, 8658.
57. Wang, Q.-P., Bennet, A. J., Brown, R. S., Santarsiero, B. D. *J. Am. Chem. Soc.* **1991**, *113*, 5757.
58. Hall, H. K. Jr., El-Shekeil, A. *Chem. Rev.* **1983**, *83*, 549.
59. Greenberg, A. In *Structure and Reactivity*; Liebman, J.F., Greenberg, A., Eds.; Vol. 7, Molecular Structure and Energetics; VCH Publishers: New York, 1988, pp 139–178.
60. Ross, B. D., True, N. S., Decker, D. L. *J. Phys. Chem.* **1983**, *87*, 89.
61. Fiegel, M. *J. Phys. Chem.* **1983**, *87*, 3054.
62. Suarez, C., Tafazzoli, M., True, N. S., Gerrard, S., LeMaster, C. B., LeMaster, C. L. *J. Phys. Chem.* **1995**, *99*, 8170.
63. Taha, A. N., Neugebauer, S. M., True, N. S. *J. Phys. Chem. A*, **1998**, *102*, 1425.
64. Manea, V. P., Wilson, K. J., Cable, J. R. *J. Am. Chem. Soc.* **1997**, *119*, 2033.
65. Ross, B. D., True, N. S. *J. Am. Chem. Soc.* **1984**, *106*, 2451.
66. LeMaster, C. B., True, N. S. *J. Phys. Chem.* **1989**, *93*, 1307.
67. Ross, B. D., True, N. S., Matson, G.B. *J. Phys. Chem.* **1984**, *88*, 2675.
68. Phillips, W. D. *J. Chem. Phys.* **1955**, *23*, 1363.
69. Stewart, W. E., Siddall, T. H., III. *Chem. Rev.* **1970**, *70*, 517.
70. LaPlanche, L. A., Rogers, M. T. *J. Am. Chem. Soc.* **1963**, *85*, 3728.
71. Pedersen, B. F., Pedersen, B. *Tetrahedron Lett.* **1965**, 2995.
72. Bourn, A. J. R., Gillies, D. G., Randall, E. W. *Tetrahedron* **1966**, *22*, 1825.

73. Itai, A., Toriumi, Y., Tomioka, N., Kagechika, H., Azumaya, I., Shudo, K. *Tetrahedron Lett.* **1989**, 30, 6177.
74. Itai, A., Toriumi, Y., Saito, S., Kagechika, H., Shudo, K. *J. Am. Chem. Soc.* **1992**, 114, 10649.
75. Nagarajan, K., Nair, M. D., Pillai, P. M. *Tetrahedron* **1967**, 23, 1683.
76. Kitamura, M., Tsukamoto, M., Takaya, H., Noyori, R. *Bull. Chem. Soc. Jpn.* **1996**, 69, 1695.
77. Chupp, J. P., Olin, J. F. *J. Org. Chem.* **1967**, 32, 2297.
78. Nakanishi, H., Roberts, J. D. *Org. Magn. Res.* **1981**, 15, 7.
79. LaPlanche, L. A., Rogers, M. T. *J. Am. Chem. Soc.* **1964**, 86, 337.
80. Kobayashi, M., Nishioka, K. *J. Phys. Chem.* **1987**, 91, 1247.
81. Guo, H., Karplus, M. *J. Phys. Chem.* **1992**, 96, 7273.
82. Han, W.-G., Suhai, S. *J. Phys. Chem.* **1996**, 100, 3942.
83. Baudry, J., Smith, J. C. *J. Mol. Struct.* **1994**, 308, 103.
84. Gerothanassis, I. P., Troganis, A., Vakka, C. *Tetrahedron Lett.* **1996**, 37, 6569.
85. Brown, C. J. *Acta Cryst.* **1966**, 21, 442.
86. Kashino, S., Ito, K., Haisa, M. *Bull. Chem. Soc. Jpn.* **1979**, 52, 365.
87. Pedersen, B. F. *Acta Chem. Scan.* **1967**, 21, 1415.
88. Azumaya, I., Kagechika, H., Yamaguchi, K., Shudo, K. *Tetrahedron* **1995**, 51, 5277.
89. Azumaya, I., Kagechika, H., Yamaguchi, K., Shudo, K. *Tetrahedron Lett.* **1996**, 37, 5003.
90. Yamaguchi, K., Matsumura, G., Kagechika, H., Azumaya, I., Ito, Y., Itai, A., Shudo, K. *J. Am. Chem. Soc.* **1991**, 113, 5474.
91. Wiberg, K. B., Rablen, P. R., Rush, D. J., Keith, T. A. *J. Am. Chem. Soc.* **1995**, 117, 4261.
92. Gao, J. *J. Am. Chem. Soc.* **1993**, 115, 2930.
93. Duffy, E. M., Severance, D. L., Jorgensen, W. L. *J. Am. Chem. Soc.* **1992**, 114, 7535.
94. Drakenberg, T., Dahlqvist, K.-I., Forsén, S. *J. Phys. Chem.* **1972**, 76, 2178.
95. Berg, U., Blum, Z. *J. Chem. Res. (S)*, **1983**, 206.
96. Gryff-Keller, A., Terpinski, J., Zajaczkowska-Terpinska, E. *J. Chem. Res. (S)*, **1984**, 330.
97. Garner, G., V., Meth-Cohn, O., Suschitzky, H. *J. Chem. Soc. (C)*, **1971**, 1234.
98. Bain, A. D., Duns, G., J., Ternieder, S., Ma, J., Werstiuk, N. H. *J. Phys. Chem.* **1994**, 98, 7458.
99. Fraenkel, G., Kolp, C. J., Chow, A. *J. Am. Chem. Soc.* **1992**, 114, 4307.
100. Abraham, R. J., Bretnschneider, E. In *Internal Rotation in Molecules*; Orville-Thomas, W., Ed.; Wiley: London, 1974; Chapter 13.
101. Waghorne, W. E., Ward, A. J. I., Clune, T. G., Cox, B. G. *J. Chem. Soc., Faraday Trans. II*, **1980**, 76
102. Casarini, D., Lunazzi, L., Macciantelli, D. *J. Chem. Soc., Perkin Trans. 2*, **1992**, 1363.
103. Leis, J. Personal communications.
104. Aroney, M. J., Le Févre, R. J. W., Singh, A. N. *J. Chem. Soc.* **1965**, 3179.
105. Siddall, T. H., III, Prohaska, C. A. *J. Am. Chem. Soc.* **1966**, 88, 1172.
106. Shvo, Y., Taylor, E. C., Mislou, K., Raban, M. *J. Am. Chem. Soc.* **1967**, 89, 4910.

107. Anderson, J. E., Barkel, D. J. D. *J. Chem. Soc., Perkin Trans. 2*, **1984**, 1053.
108. Anderson, J. E., Hazlehurst, C. J. *J. Chem. Soc., Chem. Commun.* **1980**, 1188.
109. Casarini, D., Lunazzi, L., Placucci, G., Macciantelli, D. *J. Org. Chem.* **1987**, 52, 4721.
110. Casarini, D., Foresti, E., Lunazzi, L., Macciantelli, D. *J. Am. Chem. Soc.* **1988**, 110, 4527.
111. Bjørge, J., Boyd, D. R., Watson, C. G. *Tetrahedron Lett.* **1972**, 1747.
112. Casarini, D., Lunazzi, L., Pasquali, F., Gasparrini, F., Villani, C. *J. Am. Chem. Soc.* **1992**, 114, 6521.
113. Casarini, D., Foresti, E., Gasparrini, F., Lunazzi, L., Macciantelli, D., Misiti, D., Villani, C. *J. Org. Chem.* **1993**, 58, 5674.
114. Price, B. J., Eggleston, J. A., Sutherland, I. O. *J. Chem. Soc. B*, **1967**, 922.
115. Martin, M. L., Filleux-Blanchard, M. L., Martin, G. J., Webb, G. A. *Org. Magn. Reson.* **1980**, 13, 396.
116. Haushalter, K. A., Lau, J., Roberts, J. D. *J. Am. Chem. Soc.* **1996**, 118, 8891.
117. Manske, R. H. F., Kulka, M. The Skraup Synthesis of Quinolines. *Organic Reactions* **1953**, 7, 59.

KONFORMATSIOONILISTE ÜLEMINEKUTE DÜNAAMIKA JA TASAKAAL AMIIDIDES

Kokkuvõte

Keemiliste ühendite omadused, kaasa arvatud reaktsioonivõime, on seotud otseselt molekulide struktuuri ja konformatsiooniliste iseärasustega. Seetõttu on sisemolekulaarsete dünaamiliste protsesside ja nendega seotud energeetiliste barjääride tundmaõppimine olulisel kohal nii füüsikalises, orgaanilises kui ka kvantkeemias.

Käesolev väitekiri on kokkuvõte N-C(O) sidet sisaldavates ühendites toimuvate sisemolekulaarsete dünaamiliste protsesside eksperimentaalsetest ja kvantkeemilistest uuringutest. Esimene peatükk käsitleb sisemolekulaarsete inversiooni- ja rotatsiooniprotsesside olemust ja konformatsiooniliste üleminekute barjääre iseloomustavaid kineetilisi ja termodünaamilisi parameetreid. Teine peatükk on pühendatud tuumamagnetresonantsspektroskoopia (TMR) ja kvantmehaanikale kui peamistele uurimismeetoditele konformatsioonanalüüsi ja molekulaarse dünaamika valdkonnas. Kolmas peatükk annab ulatusliku ülevaate amiidide stereokeemiast, käsitledes nii struktuurifragmentide kui ka erinevate keskkondade mõju konformatsioonilistele tasakaaludele ja isomerisatsiooniprotsesside kineetikale. Neljas peatükk sisaldab kokkuvõtet originaaltöödest (I–VI).

Selle uurimistöö esimeses osas käsitletakse tertsiaarsete *N*-arüülamiidide stereokeemiat [I–IV]: nii lämmastikarüül- kui ka lämmastikkarbonüül- (amiid-) sideme juures toimuvaid konformatsioonilisi üleminekuid *N*-1-naftüülamiidides [I, II] ja *N,N*-diarüülamiidides [IV]. Samuti on uuritud keskkonna polaarsuse mõju isomerisatsiooni tasakaalule tertsiaarsetes *N*-1-naftüülformamiidides [III].

Paralleelselt tehtud TMR ja kvantkeemilised (AM1 SCF ja SCRF) uuringud näitasid, et *N*-1-naftüülamiidides on amiidrühm oluliselt välja keerdunud naftüülrühma defineeritud tasapinnast. Samuti leidis kinnitust, et *N*-1-naftüülformamiidide lahustes on kaks tasakaalulist isomeeri, mis vastavad üldlevinud nomenklatuuri järgi *E*- ja *Z*-konformeeridele. Uuringud näitasid, et *E*-isomeer on tunduvalt eelistatud vähepolaarsetes keskkondades (vt. tabel II [I]). Analoogete isobutüül- ja bensoüülamiidide korral oli lahustes ainult üks isomeer, mis aroaatse solvendi indutseeritud keemiliste nihete alusel (vt. tabelid IV–VI [I]) omistati *E*-isomeerile. Spektraalsed uuringud kinnitasid takistatud pöörlemist nii amiid- kui ka *N*-naftüülsideme ümber. Vastavad rotatsioonibarjäärid määrati TMR signaali kuju temperatuur-sõltuvuse abil. Leiti, et *N*-naftüülsideme rotatsiooni aktivatsiooni vabaenergiate väärtused vastavates formamiidides (vt. tabel VII [I]) sõltuvad otseselt *N*-alküülrühma suuruselt.

Poolempiirilised AM1 SCF arvutused [II] olid heas kooskõlas röntgen-spektraalanalüüsi määratud *N*-neopentüül-*N*-1-naftüülformamiidi molekuli geomeetriliste parameetritega [I]. SCRF meetodiga arvatud rotatsioonibarjäärid olid tunduvalt väiksemad vastavatest eksperimentaalsetest suurustest. Samas näidati, et mitmeõõnsuse mudeliga võib kvalitatiivselt ennustada asendusrühmadest ja solvendi polaarsusest tingitud nihkeid *E/Z*-isomeeride suhtelistes populatsioonides.

Solvendi efektide põhjalikum käsitus on kajastatud kolmandas artiklis [III]. Leiti, et *E* ja *Z*-isomeeride tasakaal tertsiaarsete *N*-1-naftüülamiidide lahustes on lineaarses sõltuvuses keskkonna dielektrilisest läbitavusest (vt. joonis 1 [III]). Paralleelsete NMR ja SCRF uuringute tulemuste põhjal oletati, et solvendi efekt käsitletud isomerisatsiooni tasakaalule sisaldab nii amiidi molekuli ja solvendi indutseeritud dielektrilise välja vahelist vastasmõju kui ka spetsiifilist solvatatsiooni hapniku aatomi juures.

AM1 SCF meetodil modelleeriti võimalikke dünaamilisi protsesse mõnedes *N,N*-diarüülamiidides [IV]. Uurimus näitas, et analoogsete ühendite korral võimaldab antud meetod teha korrektseid ennustusi tuumamagnetresonants-spektroskoopias jälgitavate konformatsiooniliste üleminekute ja vastavate aktivatsioonibarjääride kohta.

Uurimuse teises osas on käsitletud 1,2-dihüdrosobenzo(*h*)kinoliinide stereokeemiat. Artikkel [V] on pühendatud 1-naftüülamiini ja metüülalküülketoonide vahelise reaktsiooni uurimisele. Uurimuse tulemusena töötati välja lihtne meetod 1,2-dihüdro-2,2,4-trimetüülbenso(*h*)kinoliini sünteesiks. Samuti võib saadud tulemuste põhjal järeldada, et optimaalsete tingimuste väljatöötamise korral võib käsitletud keemilist reaktsiooni rakendada edukalt ka mitmete teiste stereokeemilisteks uuringuteks sobivate 1,2-dihüdrosobenzo(*h*)kinoliini derivaatide valmistamiseks.

Artiklis [VI] käsitletakse enantiomerisatsiooni dünaamikat *N*-atsüül-1,2-dihüdro-2,2,4-trimetüülbenso(*h*)kinoliinides. Uuringu tulemuste põhjal näidati, et *N*-atsüül-1,2-dihüdro-2,2,4-trimetüülbenso(*h*)kinoliinides on lämmastiku aatom püramiidse sidemete paigutusega, mis vastab sp^3 hübridisatsiooni astmele. Nii spektraalsed uuringud kui ka AM1 arvutused näitasid amiidsideme puudumist neis molekulides. Eelpool kirjeldatud meetodiga määrati enantiomerisatsiooni (ehk antud juhul inversiooni) aktivatsiooni vabaenergiad mitmetes *N*-atsüül derivaatides ja leiti, et analoogselt eelpool käsitletud *N*-1-naftüülamiididega suureneb vastava dünaamilise protsessi aktivatsiooni vabaenergia lämmastikuga seotud asendusrühma suurenedes. AM1 SCF meetodil arvatud inversioonibarjäärid olid väga heas lineaarses sõltuvuses vastavatest eksperimentaalsetest suurustest. Leitud korrelatsioonivõrrandi abil ennustati inversioonibarjääri suurus 1,2-dihüdro-2,2,4-trimetüülbenso(*h*)kinoliinis. Saadud väärtus ($7,5 \text{ kcal mol}^{-1}$) on heas korrelatsioonis inversioonibarjääriga ammoniaagi derivaatides.

ACKNOWLEDGMENTS

I wish to express my deep and sincere gratitude to my doctoral advisor Professor Mati Karelson for a professional guidance and support during the years of our collaboration.

I am grateful to Professor Kalevi Pihlaja (University of Turku) for fruitful collaboration and for the opportunity to work at the University of Turku in the friendly atmosphere at his group.

I would also like to thank all the people at the Instrumental Centre of the Department of Chemistry at the University of Turku, especially Dr. Karel Klika, Ms Kirsti Wiinamäki and Dr. Vladimir Ovcharenko.

I am also very grateful to Dr. Aino Pihl for fruitful cooperation.

I would like to thank Dr. Svante Axelsson for a friendship and introducing me in the amazing ^{11}C chemistry.

I am grateful to Professor Günther Paulus Schiemenz for the guidance and fruitful discussions on the amide-chemistry and, also, for the opportunity to work at the University of Kiel.

I would also like to thank all my friends and members of the chair of theoretical chemistry (University of Tartu) for the good company and continuous support during the preparation of this thesis.

PUBLICATIONS

Stereochemistry of Arylamides,
1. NMR Spectra of Some *N*-(1-Naphthyl)amides,
J. Leis, M. Karelson and G.-P. Schiemenz,
ACH-Models in Chemistry, 135 (1–2), pp 157–171,
Copyright © 1998, Akademiai Kiado, Budapest.

Stereochemistry of arylamides, 1. NMR spectra of some *N*-(1-naphthyl)amides

JAAN LEIS¹, MATI KARELSON^{1*} and GÜNTER PAULUS SCHIEMENZ²

¹Department of Chemistry, University of Tartu, 2 Jakobi St., Tartu, EE2400, Estonia

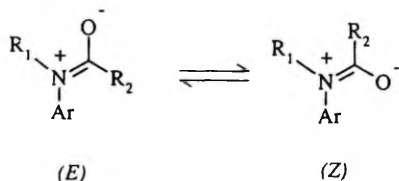
²Institute of Organic Chemistry, University of Kiel, Olshausenstrasse 40/60, Kiel, Germany

Received October 21, 1997

The results of the NMR study of the conformational equilibria and dynamics at the amide group of a series of *N*-(1-naphthyl)amides are reported. In the case of *N*-(1-naphthyl) formamides, the presence of two conformers, corresponding to the *E*- (carbonyl group *trans* to the naphthyl ring) and *Z*-form (carbonyl group *cis* to the naphthyl ring) of the amide, has been detected. In the case of isobutyryl and benzoyl amides, only one conformer (the *E*-form) was observed in solution.

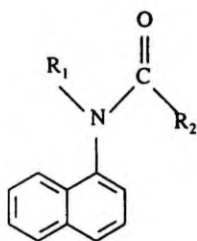
Introduction

The investigation of the stereochemistry and potential surface of amides is of fundamental importance because the tertiary structure of polyamides and many natural proteins is predetermined by the conformational dynamics and equilibria at the amide group. It is well-known that the mesomeric interaction within the amide group leads to a partial double-bond character and a substantial rotational barrier of the carbon-nitrogen bond [1, 2]. As a result, the *N*-substituted amides can, in principle, exist in two planar conformations with respect to the relative position of the *N*-substituents and the acid residue. In the present paper, the respective conformers are denoted as the *E* (carbonyl group *trans* to the naphthyl ring) and *Z* (carbonyl group *cis* to the naphthyl ring) forms of amides (Scheme 1).



Scheme 1

* To whom correspondence should be addressed



R ₁	R ₂	Compound
Et	H	1
<i>i</i> Pr	H	2
<i>t</i> Bu	H	3
CH ₂ - <i>t</i> Bu	H	4
<i>i</i> Pr	<i>i</i> Pr	5
<i>i</i> Pr	Ph	6
CH ₂ - <i>t</i> Bu	<i>i</i> Pr	7
CH ₂ - <i>t</i> Bu	Ph	8

Scheme 2

The relative stability of different amide conformers and the height of the respective rotational barrier are directly influenced by both the steric and electronic interactions between the groups adjacent to the amide bond. These interactions may significantly be affected by the surrounding medium, i.e., by the solvent. In the present work, the assignments about the conformations of a series of *N*-(1-naphthyl)amides (Scheme 2), studied both experimentally and theoretically, have been done. Also, the different factors affecting the relative stability and conformational dynamics have been discussed.

Nuclear magnetic resonance (NMR) spectroscopy has been extensively used for the study of conformational equilibria and dynamics arising from the hindered rotation along the N–C bond in amides (cf. [2–8]). The height of the rotational barriers is estimated either from the coalescence temperature of the NMR spectrum [9] or calculated more precisely from the lineshape of the NMR spectra at different temperatures (dynamic NMR) [10, 11].

The conformations of numerous amides including various *N*-aryl substituted amides, have been thoroughly investigated using NMR technique (cf. [2, 3]). However, to our best knowledge, adequate studies on the respective naphthyl compounds are missing.

In particular, the 1-naphthyl amides chosen for the present study involve additional interesting sterical effects arising between the atoms on groups at the *peri* positions of the naphthyl ring (for an overview of these effects, cf. [12–23]). It is well-known that, in general, 1-naphthyl substituted compounds have a nonplanar structure [18–23], with the plane of the 1-substituent revolved with respect to that of the naphthyl group. Depending on the size of the 1-substituent, the rotation around the

corresponding substituent-ring bond can also be substantially hindered due to the steric interaction with the *peri*-hydrogen. Therefore, the respective twisted enantiomeric conformations may become distinguishable in the NMR spectra of the respective 1-substituted naphthalenes [2] in the case of substituents with a prochiral centre (e.g., alkyl groups such as ethyl, isopropyl, neopentyl and their analogues) and therefore possessing anisochrony of diastereotopic groups [3].

The height of the rotational barrier along the ring-substituent bond in 1-naphthyl substituted compounds determines whether the twisted rotamers could be experimentally separable. It has been suggested that the barrier should be at least ~ 23 kcal/mol [2, 3] to allow the separation of rotamers at room temperature. For instance, the *S* and *R* conformational enantiomers of several 1-naphthylimines with high rotation barriers have been recently separated using common chromatographic methods [22]. The structure and steric properties of 1-naphthylamides is expected to be similar to those of 1-naphthylimines. Consequently, it is of considerable interest to search for the amides with high intramolecular rotation barriers and, possibly, with separable rotamers.

Experimental

All melting points were measured by the apparatus of Tottoli (Büchi Factory, Flawil, Switzerland), and are uncorrected. The mass spectra of compounds were recorded on a Finnigan MAR 8230 Mass spectrometer, the IR-spectra were recorded on a Perkin Elmer Infrared Spectrometer 283B in the range of $500\text{--}4000\text{ cm}^{-1}$. The elemental analyses were performed using the commercial microanalytical laboratory Pascher, Remagen, Germany.

The NMR spectra were recorded on AC200 or AM300 (Bruker-Physik, Karlsruhe) instruments. The ^1H -NMR spectra at room temperature were measured in CDCl_3 or $\text{C}_2\text{D}_2\text{Cl}_4$. The ASIS measurements were performed in C_6D_6 solutions. The ^{13}C -NMR spectra were recorded in CDCl_3 solutions. The chemical shifts were calculated in ppm relative to the solvent or tetramethylsilane as internal standard. The variable temperature measurements were performed by the AM300 or JEOL LAMBDA 400 instruments in $\text{C}_2\text{D}_2\text{Cl}_4$ solutions, whereby the temperature was calibrated with ethylene glycol.

Table I

Structure determination summary for compound 4

<i>Crystal data</i>	
Empirical formula	C ₁₆ H ₁₉ NO
Crystal size (mm)	2.00×2.00×2.00
Crystal system	Orthorhombic
Space group	<i>P</i> 2 ₁ 2 ₁
Unit cell dimensions	<i>a</i> = 6,493(8); <i>b</i> = 8,161(14); <i>c</i> = 25,64(6)
Volume	1358(4) Å ³
<i>Z</i>	4
Formula weight	241.32
Density (calc.) (Mg/m ³)	1.180
Absorption coefficient (mm ⁻¹)	0.073
<i>F</i> (000)	520
<i>Data collection</i>	
Diffractometer used	Siemens (Nicolet-Syntex) R3m/V
Radiation	MoK _α (λ = 0.71073 Å)
Temperature (K)	200
Monochromator	Highly oriented graphite crystal
θ range for data collection (°)	1.59–22.08
Scan type	ω
Scan speed	Variable; 5.0 to 29.3° min ⁻¹ in ω
Scan range ω (°)	0.6
Index ranges	–6 ≤ <i>h</i> ≤ 0; –8 ≤ <i>k</i> ≤ 8; –27 ≤ <i>l</i> ≤ 27
Reflections collected	3750
Independent reflections	1677 (<i>R</i> _{int} = 0.0303)
Observed reflections (<i>I</i> > 2σ(<i>I</i>))	1533
Absorption correction	ψ – scan, Δψ = 10°
<i>Solution and refinement</i>	
System used	SHELXL93, SHELXTL PLUS
Solution	Direct methods
Refinement method	Full-matrix least-squares on <i>F</i> ²
No. of parameters refined	239
Final <i>R</i> -indices (obs. data)	<i>R</i> = 0.0293, <i>wR</i> = 0.0698
<i>R</i> -indices (all data)	<i>R</i> = 0.0347, <i>wR</i> = 0.0734
Goodness of fit on <i>F</i> ²	1.029
Absolute structure parameter	3(2)
Largest difference peak (e/Å ³)	0.132
Largest difference hole (e/Å ³)	–0.136

The Nuclear Overhauser Effect (NOE)

Experiments were carried out on a JEOL LAMBDA 400 instrument using nitrogen saturated CDCl_3 solutions at 25 °C. The NOE values were produced as enhancements compared to the signal intensities of the original non-irradiated control spectra.

X-ray diffraction

The crystal system of compound **4** is orthorhombic with space group $P2(1)2(1)$, $a = 6.493(8) \text{ \AA}$, $b = 8.161(14) \text{ \AA}$, $c = 25.64(6) \text{ \AA}$, $\alpha = \beta = \gamma = 90^\circ$, $V = 1358(4) \text{ \AA}^3$, $z = 4$, $D_c = 1.180 \text{ g/cm}^3$. $\text{MoK}\alpha$ radiation $\lambda = 0.71073 \text{ \AA}$, $F(000) = 520$, absorption coefficient 0.073 mm^{-1} . The intensity data were collected by Siemens (Nicolet Syntex) R3m/V diffractometer. The structure of **4** was resolved using direct methods and refined by full-matrix least-squares analysis using the SHELX program packages [24, 25]. The summary of structure determination data is presented in Table I.

Quantum-chemical calculations

The fully optimised geometry of compound **4** was calculated using the semiempirical AM1 SCF method [26] within the MOPAC 6.0 program package [27].

Synthesis of N-(1-naphthyl)-N-alkylamines

The secondary *N*-aryl amines were synthesised using the general reaction between *N*-aryl amines and alkyl halides [28] with subsequent treatment of the arylammonium halide with 50% potassium hydroxide. All the synthesised compounds were tested for purity on TLC and by the ^1H -NMR spectra.

Synthesis of N-(1-naphthyl)-N-alkylformamides

The *N*-(1-naphthyl)-*N*-alkylformamides were prepared by refluxing the secondary amines with formic acid [29, 30]. In some cases, a water-separator was used to remove the water formed in the course of the reaction, in order to reduce the possibility of side reactions. The products were purified chromatographically (LC) and, if possible, recrystallised.

1: m.p. 53–54.5 °C, IR (cm^{-1}): 1680, 1670.2 ($\text{C}=\text{O}$), ^1H -NMR (300 MHz, $\text{C}_2\text{D}_2\text{Cl}_4$): 8.50 (s, 1H, $\text{C}(\text{O})\text{H}$, min), 8.19 (s, maj), 8.0–7.3 (m, 7H, Ar), 4.18 (br s, 1H, CH_2 , maj), 3.85 (m, min), 3.70 (m, 1H, CH_2 , min), 3.58 (br s, maj), 1.16

(t, $J = 14.4$ Hz, 3H, CH₃, min), 1.11 (t, $J = 14.4$ Hz, maj), MS (70 eV, m/z): 199 (M^+ , [C₁₃H₁₃NO]⁺, 56.8%).

2: oily liquid, IR (cm⁻¹): 1681.1 (C=O), ¹H-NMR (300 MHz, C₂D₂Cl₄): 8.58 (s, 1H, C(O)H, min), 8.10 (s, maj), 8.0–7.5 (m, 6H, Ar), 7.36 (dd, $J = 1.2$ Hz/7.3 Hz, 1H, H(2), maj), 7.29 (dd, $J = 1.2$ Hz/7.2 Hz, min), 4.85 (qq, $J = 6.8$ Hz/6.8 Hz, 1H, CH, maj), 4.20 (qq, $J = 6.8$ Hz/6.8 Hz, min), 1.45 (d, $J = 6.8$ Hz, 3H, CH₃, min), 1.37 (d, $J = 6.8$ Hz, maj), 1.15 (d, $J = 6.8$ Hz, 3H, CH₃, min), 1.01 (d, $J = 6.8$ Hz, 3H, CH₃, maj), MS (70 eV, m/z): 213 (M^+ , [C₁₄H₁₅NO]⁺, 65.8%).

3: m.p. 128.5–130 °C, IR (cm⁻¹): 1660 (C=O), ¹H-NMR (200 MHz, CDCl₃, TMS): 8.97 (s, 1H, C(O)H, min), 8.27 (s, maj), 8.0–7.3 (m, 7H, Ar), 1.48 (s, 9H, 3xCH₃, maj), 1.47 (s, min), MS (70 eV, m/z): 227 (M^+ , [C₁₅H₁₇NO]⁺, 20.7%).

4: m.p. 50–51.5 °C, IR (cm⁻¹): 1678.3 (C=O), ¹H-NMR (300 MHz, CDCl₃, TMS): 8.52 (s, 1H, C(O)H, min), 8.36 (s, maj), 7.9–7.4 (m, 7H, Ar), 3.98 (d, $J = 13.5$ Hz, 1H, CH₂, maj), 3.72 (d, $J = 14.5$ Hz, min), 3.68 (d, $J = 13.5$ Hz, 1H, CH₂, maj), 3.60 (d, $J = 14.5$ Hz, min), 0.89 (s, 9H, 3xCH₃, min), 0.88 (s, maj), MS (70 eV, m/z): 241 (M^+ , [C₁₆H₁₉NO]⁺, 69.2%), calcd. (C₁₆H₁₉NO) C 79.63, H 7.94, N 5.80, found C 78.71, H 7.94, N 5.84.

Synthesis of N-(1-naphthyl)-N-alkylisobutyrylamides and N-(1-naphthyl)-N-alkylbenzoylamides

The *N*-(1-naphthyl)-*N*-alkyl substituted isobutyryl- and benzoylamides were prepared using the reaction between the corresponding secondary amine and acyl chloride [31, 32] at room temperature. A twofold excess of the starting amine was used to bind the hydrogen chloride arising in the course of the reaction. Purification was achieved as described above. The yield of the reactions varied from 10% to 80%.

5: m.p. 72–73 °C, IR (cm⁻¹): 1645.7 (C=O), ¹H-NMR (200 MHz, CDCl₃, TMS): 7.9–7.8 (m, 3H, Ar), 7.6–7.5 (m, 3H, Ar), 7.30 (dd, 1H, H(2)), 5.08 (qq, $J = 7.4$ Hz/7.4 Hz, 1H, NCH), 2.00 (qq, $J = 7.4$ Hz/7.4 Hz, 1H, CCH), 1.30 (d, $J = 7.4$ Hz, 3H, NCCH₃), 0.95 (d, $J = 7.4$ Hz, 3H, CCCH₃), 0.94 (d, $J = 7.4$ Hz, 3H, CCCH₃), 0.85 (d, $J = 7.4$ Hz, 3H, NCCH₃), MS (70 eV, m/z): 255 (M^+ , [C₁₇H₂₁NO]⁺, 29.8%), calcd. (C₁₇H₂₁NO) C 79.96, H 8.29, N 5.49, found C 79.82, H 8.29, N 5.53.

6: m.p. 146–147 °C, IR (cm⁻¹): 1622; 1632.4 (C=O), ¹H-NMR (200 MHz, CDCl₃, TMS): 8.0–6.9 (m, 12H, Ar), 5.03 (br s, 1H, CH), 1.50 (d, $J = 6.7$ Hz, 3H, CH₃),

1.08 (d, $J = 6.85$ Hz, 3H, CH₃), MS (70 eV, m/z): 289 (M^+ , [C₂₀H₁₉NO]⁺, 10.79%), calcd. (C₂₀H₁₉NO) C 83.01, H 6.62, N 4.84, found C 82.23, H 6.60, N 4.93.

7: m.p. 67–68 °C, IR (cm⁻¹): 1662.2 (C=O), ¹H-NMR (300 MHz, CDCl₃, TMS): 7.9–7.4 (m, 7H, Ar), 4.35 (d, $J = 13.5$ Hz, 1H, CH₂), 3.80 (d, $J = 13.5$ Hz, 1H, CH₂), 2.27 (qq, $J = 6.7$ Hz/6.7 Hz, 1H, CH), 1.06 (d, $J = 6.8$ Hz, 3H, CH₃), 0.91 (s, 9H, 3xCH₃), 0.86 (d, $J = 6.8$ Hz, 3H, CH₃), MS (70 eV, m/z): 283 (M^+ , [C₁₉H₂₅NO]⁺, 6.6%).

8: IR (cm⁻¹): 1648.8 (C=O), ¹H-NMR (400 MHz, CDCl₃, TMS): 8.0–6.9 (m, 12H, Ar), 4.62 (d, $J = 13.5$ Hz, 1H, CH₂), 3.42 (d, $J = 13.5$ Hz, 1H, CH₂), 0.98 (s, 9H, 3xCH₃), MS (70 eV, m/z): 317 (M^+ , [C₂₂H₂₃NO]⁺, 10.5%), calcd. (C₂₂H₂₃NO) C 83.24, H 7.30, N 4.41, found C 83.24, H 7.34, N 4.62.

The experimental rotation barriers (ΔG^\ddagger) were calculated at the coalescence point of the NMR signals of diastereotopic groups using the following equations for the equally populated AB systems [9]:

$$\Delta G^\ddagger = aT [9.972 + \log (T/\delta\nu)], \quad (1a)$$

$$\Delta G^\ddagger = aT [9.972 + \log (T/\sqrt{\delta\nu^2 + 6J_{AB}^2})], \quad (1b)$$

where $a = 4.575 \times 10^{-3}$ kcal/mol K, T is the coalescence temperature in K, and $\delta\nu$ is the difference between the resonance frequencies (ν [Hz]) of the A and B protons.

Results and discussion

Two sets of NMR signals were obtained for each of the *N*-(1-naphthyl)formamides and only one set of signals in the case of the *N*-(1-naphthyl)amides of isobutyric and benzoic acids. The two sets of ¹H-NMR signals were assigned to belong to the *E* and *Z* conformers of *N*-(1-naphthyl)formamides, respectively (Table II). Due to the influence by the diamagnetic field of an aromatic ring, the ¹H-NMR signal of the formyl hydrogen in the *E* form is expected to be shifted to the higher field as compared to the corresponding signal of the *Z* form. Accordingly, the *E* form was observed as the major conformation and the *Z* form being the minor conformation in these amides.

This assignment was confirmed by the NOE difference measurements. The NOE values for the compound **1** are presented in Table III and the typical spectrum recorded in the NOE experiment in Fig. 1. These results clearly indicate that the formyl proton is *cis* to the naphthyl ring in the major conformer and *cis* to the alkyl group in the minor conformer.

Table II

The formyl proton chemical shifts (δ [ppm]) at room temperature and the ratio of the *E* and *Z* conformers of *N*-(1-naphthyl)formamides calculated from the intensities of NMR signals

Compound	CDCl ₃			C ₂ D ₂ Cl ₄		
	(<i>E</i>)	(<i>Z</i>)	Ratio	(<i>E</i>)	(<i>Z</i>)	Ratio
1	8.23	8.58	1:0.12	8.19	8.50	1:0.14
2	8.16	8.67	1:0.18	8.10	8.58	1:0.29
3	8.27	8.97	1:0.57	8.13	8.88	0.88:1
4	8.36	8.52	1:0.15	8.32	8.47	1:0.18

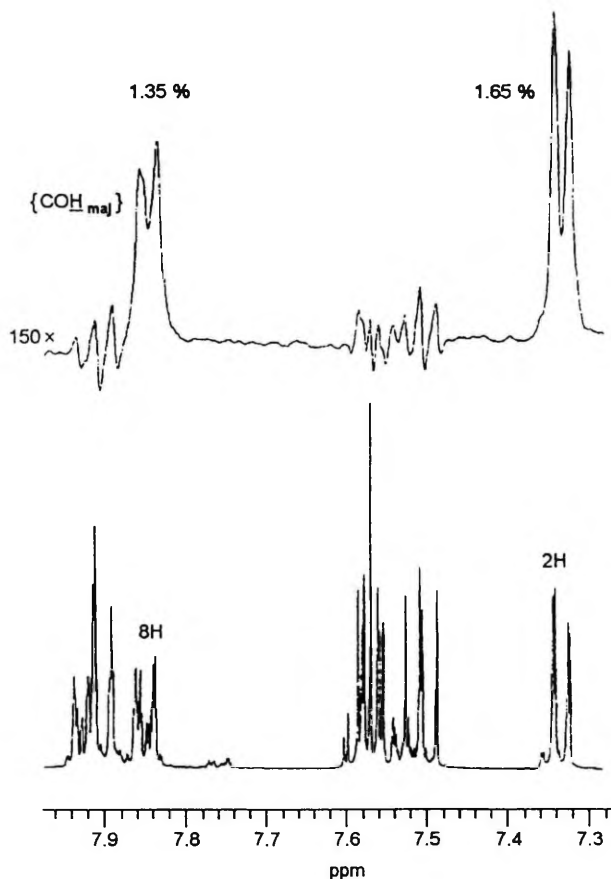


Fig. 1. Aromatic region of the 400 MHz differential NOE spectrum (vertically amplified 150 times with respect to the control spectrum) obtained on irradiation of the formyl proton of the major conformer of compound 1. The signals of the hydrogens in positions 8 and 2 of naphthalene display enhancements of 1.35 and 1.65%, respectively

Table III

The NOE values for compound 1 (expressed as a percentage from the original signals) observed for the given protons, on irradiation of the formyl proton of the major and minor conformers. H(8) and H(2) express the hydrogens at the respective positions of the naphthyl ring

Observed	Irradiated	NOE
H(8)	COH _{maj}	1.35
	COH _{min}	—
H(2)	COH _{maj}	1.65
	COH _{min}	—
CH ₂	COH _{maj}	0.19 ^a ; 0.08 ^b
	COH _{min}	4.17 ^a ; 2.52 ^b
CH ₃	COH _{maj}	0.48
	COH _{min}	0.04

^a Enhancement of the upfield multiplet;

^b Enhancement of the downfield multiplet

Furthermore, the bipolar repulsion between the carbonyl group and π -system of the naphthyl ring in the compounds **1–4** forces these molecules to the *E* conformation. Notably, the compound **3** has the smallest *E/Z* ratio, caused by the largest steric repulsion between the respective alkyl (tertiary butyl) group and the carbonyl group. The other alkyl groups (ethyl, isopropyl and neopentyl in **1**, **2** and **4**, respectively) are less demanding sterically and, as a result, these compounds have very similar experimentally measured ratios of *E* and *Z* forms. However, the enhancement of the polarity of the solvent (from chloroform to tetrachloroethane) increases the relative population of the *Z* form.

Previous studies [2] have revealed that in the crystalline state, the anilides are predominantly in the *E* configuration. Our present results on the X-ray diffraction analysis of the crystalline *N*-(1-naphthyl)-*N*-neopentylformamide (**4**) indicate also the presence of only a single conformer of this compound in solid state. However, it was established (Fig. 2) that the arrangement of bonds at nitrogen atom is planar and that the amide plane is almost perpendicular to the naphthyl plane in this compound. The bond angles $\angle C_f-N-C_p$, $\angle C_f-N-C_n$ and $\angle C_n-N-C_p$ (where C_f , C_p , and C_n are the formyl carbon atom, the 1-carbon atom of the neopentyl group and the 1-carbon atom of the naphthyl group, respectively) are close to 120° (119.5°, 118.8° and 121.4°, respectively). The respective AM1 SCF calculated bond angles (120.4°, 118.4° and 121.0°, respectively) are in a good agreement with the experimental data. The bond

between the amide nitrogen and formyl carbon atom is shortened and, correspondingly, has a partial double-bond character ($R_{\text{N-C(O)}} = 1.346 \text{ \AA}$, whereas a typical length of a N-C single bond is about 1.45 \AA). For the comparison, in compound 4, the X-ray measured N-C_p single bond length is 1.469 \AA and the N-C_n single bond length 1.436 \AA . The AM1 SCF quantum-chemically calculated bond lengths (1.388 \AA for N-C_f bond; 1.447 \AA for N-C_n bond and 1.421 \AA for N-C_p bond) are in a satisfactory agreement with the experiment. The measured torsion angles (-69.0° for $\angle \text{C}_f\text{-N-C}_n\text{-C}_{n2}$, and 106.7° for $\angle \text{C}_f\text{-N-C}_n\text{-C}_{n6}$) correspond to approximate perpendicularity of the naphthyl and amide planes, with the formyl group shifted slightly more apart from the naphthyl ring. Once more, an excellent agreement between the experimental and AM1 calculated (-68.3° and 107.1° , respectively) torsion angles was obtained.

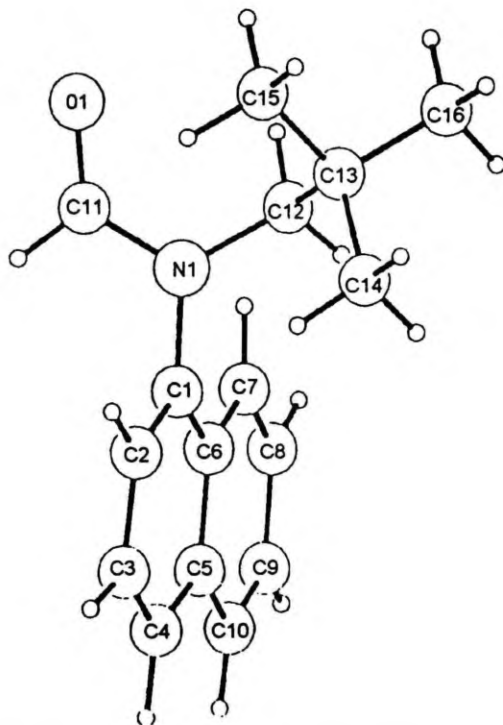


Fig. 2. Structure of the crystalline compound 4 as obtained by the X-ray diffraction analysis

Unlike the formyl compounds discussed above, the isobutyryl and benzoyl amides possess only one set of ^1H -NMR signals even at -70°C . Therefore, if the accidental line degeneracy of the NMR signals excepted, only one of the possible conformers has to be populated in these compounds. Unfortunately, the NOE analysis could not give unambiguous results regarding the conformational structure of these molecules. However, it was reasonable to expect that the change of solvent from chloroform- d_1 to benzene- d_6 should shift the NMR signals of the different conformers to different extents (aromatic-solvent-induced shift, ASIS) [33–35], depending on the position (*s-cis* vs. *s-trans*) of the nuclei. Several *N*-naphthyl amides were thus examined by ^1H -NMR in chloroform- d_1 and benzene- d_6 solutions. The respective spectral data are presented in Tables IV and V.

Table IV

*The NMR spectral data of some N-(1-naphthyl)amides at room temperature
(^1H -NMR, 300 MHz, CDCl_3 , TMS)*

Comp.	Ar	R ₁	R ₂	$\delta(\text{CH}_3)$ [ppm]	$J(\text{CH}_3)$ [Hz]	$\Delta\nu_{\text{AB}}(\text{CH}_3)$ [Hz]
1 (<i>E</i>)	Nap	Et	H	1.13	7.2	–
1 (<i>Z</i>)	Nap	Et	H	1.17	7.1	–
2 (<i>E</i>)	Nap	^iPr	H	1.19	6.8	108
2 (<i>Z</i>)	Nap	^iPr	H	1.30	6.8	90
4 (<i>E</i>)	Nap	$\text{CH}_2\text{-}^i\text{Bu}$	H	0.885	–	–
4 (<i>Z</i>)	Nap	$\text{CH}_2\text{-}^i\text{Bu}$	H	0.89	–	–
6 ^b	Nap	^iPr	Ph	1.29	6.7	84
7	Nap	$\text{CH}_2\text{-}^i\text{Bu}$	^iPr	0.92	–	–
8	Nap	$\text{CH}_2\text{-}^i\text{Bu}$	Ph	0.96	–	–

Comp.	$\delta(\text{CH}_2)$ [ppm]	$J(\text{CH}_2)$ [Hz]	$\Delta\nu_{\text{AB}}(\text{CH}_2)$ [Hz]	$\delta(\text{CH})$ [ppm]	$J(\text{CH})$ [Hz]
1 (<i>E</i>)	3.88 ^a	–	180	–	–
1 (<i>Z</i>)	3.78 ^a	–	45	–	–
2 (<i>E</i>)	–	–	–	4.85	6.8
2 (<i>Z</i>)	–	–	–	4.20	6.8
4 (<i>E</i>)	3.84	13.6	89	–	–
4 (<i>Z</i>)	3.67	14.6	39	–	–
6 ^b	–	–	–	5.03 ^a	–
7	3.72	13.5	382	–	–
8	4.01	13.5	360	–	–

^a Broadened signals; ^b ν_{NMR} is 200 MHz

Table V

The NMR spectral data of some *N*-(1-naphthyl)amides at room temperature
(¹H-NMR, 300 MHz, C₆D₆, TMS)

Comp.	Ar	R ₁	R ₂	δ(CH ₃) [ppm]	<i>J</i> (CH ₃) [Hz]	Δ <i>ν</i> _{AB} (CH ₃) [Hz]
1 (<i>E</i>)	Nap	Et	H	0.87	7.1	–
1 (<i>Z</i>)	Nap	Et	H	0.59	7.0	–
2 (<i>E</i>)	Nap	ⁱ Pr	H	1.06	6.9	118.3
2 (<i>Z</i>)	Nap	ⁱ Pr	H	0.83	6.9	74.1
4 (<i>E</i>)	Nap	CH ₂ - ^t Bu	H	0.88	–	–
4 (<i>Z</i>)	Nap	CH ₂ - ^t Bu	H	0.63	–	–
6	Nap	ⁱ Pr	Ph	1.30	6.8	121.8
7	Nap	CH ₂ - ^t Bu	ⁱ Pr	0.94	–	–
8	Nap	CH ₂ - ^t Bu	Ph	1.04	–	–

Comp.	δ(CH ₂) [ppm]	<i>J</i> (CH ₂) [Hz]	Δ <i>ν</i> _{AB} (CH ₂) [Hz]	δ(CH) [ppm]	<i>J</i> (CH) [Hz]
1 (<i>E</i>)	3.67 ^a	–	~234	–	–
1 (<i>Z</i>)	– ^b	–	–	–	–
2 (<i>E</i>)	–	–	–	4.92	6.8
2 (<i>Z</i>)	–	–	–	3.53	6.8
4 (<i>E</i>)	3.85	13.5	81.7	–	–
4 (<i>Z</i>)	3.14	14.5	25.5	–	–
6	–	–	–	5.03	6.7
7	3.82	13.4	427.9	–	–
8	4.16	13.3	410.2	–	–

^a Broadened signals; ^b The signals are not observable due to the coalescence of the signals of a major isomer (*E*)

The ASIS values (Δ) were calculated as follows:

$$\Delta = [\delta(\text{CDCl}_3) - \delta(\text{C}_6\text{D}_6)] \text{ [ppm]}. \quad (2)$$

Since the isomeric composition of formamides had been established as described above, their respective ASIS data were used as the reference to assign the configuration of isobutyryl and benzoyl amides.

In the case of formamides, a large upfield solvent shift of alkyl protons was observed in *Z* conformation, in contrast to a very small or even downfield shift of the same protons in *E* conformation (Table VI). The isobutyryl and benzoyl amides were characterised by downfield or small upfield shifts. Therefore, it can be concluded that these compounds exist in solution predominantly in *E* conformation.

Table VI

The ASIS values (Δ)^a of some N-(1-naphthyl)amides calculated by the Eq. (2)

Comp.	$\Delta(\text{CH}_3)^b$	$\Delta(\text{CH}_2)^b$	$\Delta(\text{CH})$
1 (<i>E</i>)	5.2	–	–
1 (<i>Z</i>)	11.6	–	–
2 (<i>E</i>)	2.6	–	–1.4
2 (<i>Z</i>)	9.4	–	13.4
4 (<i>E</i>)	0.1	–0.2	–
4 (<i>Z</i>)	5.2	10.6	–
6	–0.2	–	0
7	–0.4	–2.0	–
8	–1.6	–3.0	–

^a The ASIS values (Δ) are given in [ppm]×20, "+" shows the upfield shift and "–" downfield shift of the corresponding signals upon changing the solvent from chloroform to benzene; ^b in the AB case the reference is made to the centre of the AB system

At room temperature, amides having hindered rotation about the N–Ar bond displayed anisochronous NMR signals for prochiral substituents at the nitrogen atom. However, in the variable temperature measurements, the coalescence of these signals are only present in *N*-(1-naphthyl)formamides. Evidently, the large steric effects to the rotation along nitrogen-naphthyl bond in isobutyryl and benzoyl amides lead to the anisochrony of the NMR signals for the protons of diastereotopic groups even above 100 °C. Consequently, in the case of these compounds the pairs of enantiomers should be potentially separable.

A summary on activation energies (ΔG^\ddagger), calculated from the coalescence temperatures according to Eq. (1) are presented in Table VII. Notably, the calculation of the activation energies of the rotation about the N–Ar bond is complicated due to the existence of two conformers (*E* and *Z*) of amides in solution. In the case of higher activation barriers of rotation around the N–Ar bond (e.g., in 2), the respective coalescence of the anisochronous NMR signals of the diastereotopic groups becomes overshadowed by the coalescence of the NMR signals due to the fast exchange between the *E* and *Z* conformers.

Table VII

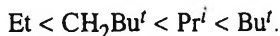
The activation energies (ΔG^\ddagger) of rotation about the nitrogen-aryl bond of some *N*-(1-naphthyl)amides, calculated at the coalescence temperature (T_c). The difference of the resonance frequencies ($\Delta\nu_{AB}$) of A and B sites, and the frequency of the NMR is indicated

Compound	ΔG^\ddagger (kcal/mol)	T_c (°C)	$\delta\nu_{AB}^a$ (Hz)	ν_{NMR} (Hz)
1 (<i>E</i>)	14.5	38	180 (25 °C)	300
1 (<i>Z</i>)	16.0	50	45 (25 °C)	300
2 (<i>E</i>)	19.1	127	138 (46 °C)	400
4 (<i>E</i>)	16.1	61	87 (19 °C)	300
			(J 13.5)	
4 (<i>Z</i>)	17.2	75	36 (19 °C)	300
			(J 14.5)	

^a In parentheses the temperature, at which the $\delta\nu_{AB}$ is measured, is indicated

Furthermore, *N*-(1-naphthyl)-*N*-*tert*-butylformamide (3), which has no prochiral carbon at the amide nitrogen atom displayed two sets of NMR signals at room temperature which were typical for the mixture of *E* and *Z* conformers. At about 50 °C, the signals started to broaden and eventually became coalescent into one set of signals at 80 °C. The calculated rotational barrier for N-C(O) bond was approximately 19.0 kcal/mol. In latter case, the difference in exchange rates was ignored because of the approximately equal populations (0.9:1) of both conformers.

Our results also indicate that, if applicable, the activation energies of rotation about the N-Ar bond are about 1 kcal/mol higher for the *Z* conformers than those for the corresponding *E* conformers of *N*-(1-naphthyl)formamides. Also, this rotation barrier depends on the size of alkyl substituents bound to the amide nitrogen, with the following increasing order:



In order to confirm the interpretation of the conformational dynamics and equilibria of *N*-(1-naphthyl)amides, the complementary quantum-chemical calculations were carried out. The results of this theoretical modelling and the overall discussion of results is presented in the next communication of this series [36].

*

The authors wish to acknowledge Volkswagen Stiftung (Hannover, Germany) for their generous support of this work.

References

- [1] NASIPURI, D.: *Stereochemistry of Organic Compounds, Principles and Applications*, J. Wiley & Sons, New York, 1991
- [2] STEWART, W. E., SIDDALL, T. H.: *Chem. Rev.*, **70**, 517 (1970)
- [3] KESSLER, H.: *Angew. Chem.*, 237 (1970)
- [4] SIDDALL, T. H.: *J. Phys. Chem.*, **70**, 2249 (1966)
- [5] SIDDALL, T. H., STEWART, W. E., KNIGHT, F. D.: *J. Phys. Chem.*, **74**, 3580 (1970)
- [6] SIDDALL, T. H., STEWART, W. E.: *J. Chem. Soc. Chem. Commun.*, 617 (1968)
- [7] SIDDALL, T. H., STEWART, W. E.: *J. Phys. Chem.*, **73**, 40 (1969)
- [8] BEDFORD, G. R., GREATBANKS, D., ROGERS, D. B.: *Chem. Commun.*, 330 (1966)
- [9] BINCH, G.: In *Topics in Stereochemistry*, Vol. 3 (Eds ELIAL, E. L., ALLINGER, N. L.), Interscience, New York, 1968, p. 97
- [10] KAPLAN, J. I., FRAENKEL, G.: *NMR of Chemically Exchanging Systems*, Academic Press, New York, 1980
- [11] SANDSTROM, J.: *Dynamic NMR Spectroscopy*, Academic Press, London, 1982
- [12] HARRIS, M. M., COOKE, A. S.: *J. Chem. Soc., C*, 2575 (1967)
- [13] ALDER, R., ANDERSON, J. E.: *J. Chem. Soc. Perkin Trans. 2*, 2086 (1973)
- [14] ANDERSON, J. E., FRANCK, R. W., MANDELLA, W. L.: *J. Am. Chem. Soc.*, **94**, 4608 (1972)
- [15] ANDERSON, J. E., COOKSEY, C. J.: *J. Chem. Soc. Chem. Commun.*, 942 (1975)
- [16] CLOUGH, R. L., ROBERTS, J. D.: *J. Am. Chem. Soc.*, **98**, 1018 (1976)
- [17] ANDERSON, J. E., HAZLEHURST, C. J.: *J. Chem. Soc. Chem. Commun.*, 1188 (1980)
- [18] CASARINI, D., FORESTI, E., LUNAZZI, L., MACCIANTELLI, D.: *J. Am. Chem. Soc.*, **110**, 4527 (1988)
- [19] CASARINI, D., DAVALLI, S., LUNAZZI, L., MACCIANTELLI, D.: *J. Org. Chem.*, **54**, 4616 (1989)
- [20] DAVALLI, S., LUNAZZI, L., MACCIANTELLI, D.: *J. Org. Chem.*, **56**, 1739 (1991)
- [21] CASARINI, D., LUNAZZI, L., PASQUALI, F., GASPARRINI, F., VILLANI, C.: *J. Am. Chem. Soc.*, **114**, 6521 (1992)
- [22] CASARINI, D., LUNAZZI, L., MACCIANTELLI, D.: *J. Chem. Soc. Perkin Trans. 2*, 1363 (1992)
- [23] CASARINI, D., FORESTI, E., GASPARRINI, F., LUNAZZI, L., MACCIANTELLI, D., MISITI, D., VILLANI, C.: *J. Org. Chem.*, **58**, 5674 (1993)
- [24] SHELDRICK, G. M.: *SHELX93*, University of Gottingen, 1988
- [25] SHELDRICK, G. M.: *SHELX93*, University of Gottingen, 1993
- [26] DEWAR, M. J. S., ZOEBSCH, E. G., HEALY, E. F., STEWART, J. J. P.: *J. Am. Chem. Soc.*, **107**, 3902 (1985)
- [27] STEWART, J. J. P.: *MOPAC 6.0*, QCPE No. 455, 1989
- [28] CASARINI, D., LUNAZZI, L., PLACUCCI, G., MACCIANTELLI, D.: *J. Org. Chem.*, **52**, 4721 (1987)
- [29] FIESER, L. F., JONES, J. E.: In *Organic Syntheses*, Coll. Vol. 3, pp. 590–591
- [30] ROBSON, J. H., REINHART, J.: *J. Am. Chem. Soc.*, **77**, 498 (1955)
- [31] Autorenkollektiv: *Organikum*, 17. Aufl., VEB Deutscher Verlag der Wissenschaften, Berlin, 1988, p. 412
- [32] GRYFF-KELLER, A., TERPINSKI, J., ZAJACZKOWSKA-TERPINSKA, E.: *J. Chem. Res. S*, 330 (1984)
- [33] HATTON, J. V., RICHARDS, R. E.: *Mol. Phys.*, **3**, 253 (1960)
- [34] HATTON, J. V., RICHARDS, R. E.: *Mol. Phys.*, **5**, 139 (1962)
- [35] SHVO, Y., TAYLOR, E. C., MISLOW, K., RABAN, M.: *J. Am. Chem. Soc.*, **89**, 4910 (1967)
- [36] LEIS, J., MARAN, U., SCHIEMENZ, G. P., KARELSON, M.: *ACH - Models in Chem.*, **135**, 173 (1998)

Stereochemistry of Arylamides,
2. AM1 SCF and SCRF Quantum-Chemical
Modelling of Some *N*-(1-Naphthyl)amides,
J. Leis, U. Maran, G.-P. Schiemenz and M. Karelson,
ACH-Models in Chemistry, 135 (1–2), pp 173–181,
Copyright © 1998, Akademiai Kiado, Budapest.

Stereochemistry of arylamides, 2. AM1 SCF and SCRF quantum-chemical modelling of some *N*-(1-naphthyl)amides

JAAN LEIS¹, UKO MARAN¹, GÜNTER PAULUS SCHIEMENZ² and MATI KARELSON^{1*}

¹*Department of Chemistry, University of Tartu, 2 Jakobi St., Tartu, EE2400, Estonia*

²*Institute of Organic Chemistry, University of Kiel, Olshausenstrasse 40/60, Kiel, Germany*

Received October 21, 1997

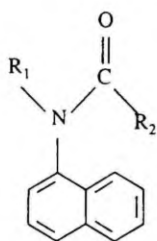
The results of AM1 self-consistent field (SCF) and self-consistent reaction field (SCRF) quantum-chemical calculations of the conformational equilibria and dynamics at the amide group of a series of *N*-(1-naphthyl)amides are reported. In accordance with the experimental observation, the presence of two conformers, corresponding to the *E*- and *Z*-form of the amide, has been predicted by the calculations. The AM1 multi-cavity self-consistent reaction field calculation results predict the change in the relative population of these two conformers due to the change in the dielectric medium. The isobutyryl and benzoyl amides are predicted to have one conformer (the *E*-form) strongly predominant in solutions.

Introduction

In this paper, the results of the quantum-chemical calculations of the stationary points on the intramolecular rotational potential surfaces of a series of *N*-(1-naphthyl)amides are presented. This study represents a complementary part to the experimental investigation reported in the previous communication of this series [1]. The conformational properties of the *N*-(1-naphthyl)amides listed in Scheme 1 were calculated for the molecules in different dielectric media using the AM1 self-consistent field (SCF) [2] and self-consistent reaction field (SCRF) [3-8] quantum-chemical methods.

For the sake of comprehensiveness, two compounds were studied in addition to those investigated in [1], the unsubstituted *N*-(1-naphthyl)formamide (**9**) and *N*-methyl-*N*-(1-naphthyl)formamide (**10**).

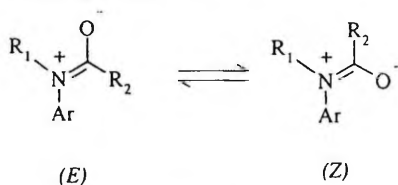
* To whom correspondence should be addressed



R ₁	R ₂	Compound
Et	H	1
<i>i</i> Pr	H	2
<i>t</i> Bu	H	3
CH ₂ - <i>t</i> Bu	H	4
<i>i</i> Pr	<i>i</i> Pr	5
CH ₂ - <i>t</i> Bu	<i>i</i> Pr	6
<i>i</i> Pr	Ph	7
CH ₂ - <i>t</i> Bu	Ph	8
H	H	9
Me	H	10

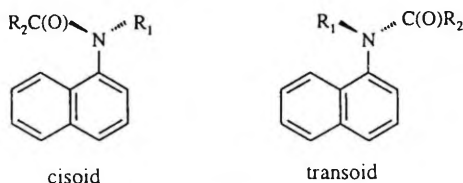
Scheme 1

Throughout this paper, we follow the notations and conventions used in [1]. Because of the mesomeric interaction within the amide group and corresponding partial double-bond character of the carbon-nitrogen bond, the *N*-substituted amides can, in principle, exist in two planar conformations with respect to the relative position of the *N*-substituents and the acid radical. The respective conformers are distinguished as the *E* and *Z* forms of amides (Scheme 2).



Scheme 2

The rotation about the N-Ar bond in *N*-(1-naphthyl)amides may give the rise to two additional conformational minima (Scheme 3) which can be designated as the *cisoid*- and *transoid*-conformations with respect to the relative position of the naphthyl and C(O)R groups.



Scheme 3

Different theoretical methods of molecular modelling including molecular mechanics [9, 10], quantum chemical methods [11–13] and molecular dynamics [14, 15] have been used for the study of the structure of different amide conformers and the respective conformational barriers. In the present study, we have selected the quantum-chemical self-consistent reaction field (SCRF) method for the calculation of relative stability of different conformers of amides and conformational barriers in polarizable dielectric media. The choice of the semiempirical approach (AM1) was essentially directed by the relatively large size of the molecules studied to pursue accurate *ab initio* calculations with extended basis sets and with the inclusion of the post-Hartree–Fock corrections. The good quality *ab initio* calculations of rotational transition barriers for systems of this size would require very large computer time and hardware resources. However, a satisfactory correlation has been found between the AM1 and *ab initio* calculated rotation barriers of amides [16] which allows to make quantitative predictions for larger molecular systems proceeding from the semiempirical results. Also, the computer software to perform the calculations for molecules in liquid media was readily available. The respective extension of the MOPAC 6.0 program package [19] had been developed by us earlier [6, 17, 18].

Methodology

All quantum-chemical calculations were performed at the semiempirical level using Austin Model 1 (AM1) [2] parameterization. Considerable solvent effects on the rotational barriers of various substituted amides have been reported in many cases [20–23] and therefore it was important to account for the influence of the surrounding medium on the calculated rotational equilibria and barriers. The non-specific solvation effects were described quantum-chemically using the reaction field approach. Two models were employed, one of which corresponds to the single spherical cavity self-consistent reaction field (SCa SCRF) [3–5] and another to the multi-cavity self-consistent reaction field (MCa SCRF) representation of the solute-solvent electrostatic interaction [6–8]. The calculations were also performed for the isolated molecules, corresponding to the gas phase at low temperature and pressure. In SCRF calculations, the polarizable medium with high dielectric permittivity, corresponding to the aqueous solution ($\epsilon = 80$) was modelled. It has been also shown that the AM1 calculated rotation barriers for different ureas, thioureas, amides and thioamides are in a good linear relationship with the experimental data [16]. The respective correction was accounted for in the further discussion of the absolute values of the barriers.

In the framework of the SCa SCRF method, the molecular Hamiltonian of the solute is modified by the addition of a term accounting for the dipolar interaction between the solute charge distribution and the polarizable dielectric medium [4]:

$$\hat{\mathbf{H}} = \hat{\mathbf{H}}^0 + \frac{\Gamma \langle \phi | \hat{\mu} | \phi \rangle \hat{\mu}}{2}, \quad (1)$$

where ϕ is the electronic wave function of the molecule, $\hat{\mu}$ is the dipole moment operator and $\hat{\mathbf{H}}^0$ – the Hamiltonian for the isolated molecule. The factor Γ in the perturbation term (the reaction field tensor) is a function of both the dielectric properties of the solvent and the size of the solute molecule. In the case of the SCa SCRF method when the solute is embedded into a single spherical cavity in dielectric medium, the electronic energy of the solute molecule E_{el} is calculated by solving the following one-electron Fock equations using the self-consistent reaction field (SCRF) procedure [4, 5]

$$(\mathbf{f}_0 - 1/2 \Gamma \langle \phi | \hat{\mu} | \phi \rangle \hat{\mu}) \psi_i = \epsilon_i \psi_i, \quad (2)$$

where \mathbf{f}_0 is the unperturbed one-electron Fock operator and ψ_i – the molecular orbitals. The total energy of the solute molecule includes also the interaction of nuclear charges with the solvent reaction field.

The MCa SCRF method has been described in detail elsewhere [6] and therefore we present only the essentials here. This method proceeds from the observation that the interaction of the charge and higher electrical moments of a charge distribution in a spherical cavity with the corresponding reaction field does not depend on the position of the charge or (point) multipole centres in this cavity [24]. By partitioning the solute molecule into rotationally flexible fragments, which are embedded into the respective spherical cavities with characteristic radii for these fragments, a closed expansion for the electrostatic solvation energy of a solute in the dielectric medium can be obtained. Proceeding from this expansion, it is possible to build a variational functional for the total energy E and to derive the corresponding Hartree-Fock-type equations to be solved iteratively using the self-consistent reaction field (MCa SCRF) procedure [6].

Results and discussion

The results of the AM1 calculations of heats of formation of the series of *N*-(1-naphthyl)amides are presented in Table I. The data for four conformations are

given, corresponding to the *transoid-E* (a), *cisoid-E* (b), *transoid-Z* (c) and *cisoid-Z* (d) configuration of the substituents at the amide group (cf. Schemes 2 and 3). The results of calculation confirm the experimental observation of two conformers of these compounds in low dielectric constant media (CDCl_3 , $\text{C}_2\text{D}_2\text{Cl}_4$) [1]. The calculated energy difference between the more stable (either *cisoid* or *transoid*) *Z*- and *E*-form of a given molecule is small, with the *E*-form slightly more stabilised. In the case of unsubstituted *N*-(1-naphthyl)formamide (9), the *transoid*-conformation with respect to the relative position of the naphthyl group and the amide carbonyl oxygen (form a in Tables), is dominant. In the case of some *N*-(1-naphthyl)-*N*-alkylformamides (1–2, 10), the *cisoid*-conformation with respect to the relative position of these groups (form b in Tables) becomes more stabilised, apparently because of the steric repulsion between the alkyl group at the amide nitrogen and the *peri*-hydrogen of the naphthyl group. In compounds 3 and 4, with more bulky *tert*-butyl and neopentyl groups at the amide nitrogen, the amide plane becomes perpendicular to the naphthyl ring plane and therefore only two forms, corresponding to the *E*- and *Z*-conformation of the amide group, are present. Accordingly, the final optimised geometries starting from either the *cisoid*- or *transoid*-conformation with respect to the relative position of the acid radical and *N*-substituent to the naphthyl ring are identical and the calculated heats of formation of the respective pairs of the conformers (a and b, and c and d) are the same (cf. Table I). This is in agreement with the experimental observation of only one conformer for both the *E* and *Z* forms in the solution according to the NMR spectra of the respective compounds [1].

The results of the AM1 SCa SCRf calculations of conformational minima in high dielectric constant media ($\epsilon = 80$) are very similar to the results for the isolated molecules. For all conformers studied, the calculated solvent stabilisation was less than 1 kcal/mol which is by far too small for a realistic estimate of the solvation energy of amides in aqueous solutions. It has been shown by us earlier [6, 8] that in such systems the total reaction field has to be represented as a superposition of the reaction fields of individual, conformationally flexible, molecular fragments. The respective AM1 MCa SCRf calculations gave more reasonable values for the solvation energy of different conformational forms of the amides studied (5–10 kcal/mol, cf. the data in Table I). Also, the solvation energy was found to depend significantly on the conformation of the compound. For instance, the *cisoid-E* form of compound 1 is stabilised by 6.16 kcal/mol by high dielectric constant medium whereas the *transoid-Z* form of the same compound has the calculated solvent stabilisation energy 10.05 kcal/mol. As a result of this differentiation, the *Z*-form of the *N*-(1-naphthyl)formamides is predicted

to have the heat of formation similar or even lower than that of the *E*-form in high polarity media, leading to the higher relative population of this form in these media. This tendency has been also observed experimentally. For instance, the relative population of the *Z*-form has increased from 36% in CDCl_3 ($\epsilon = 4.8$) to 53% in $\text{C}_2\text{D}_2\text{Cl}_4$ ($\epsilon = 8.2$) [1].

The AM1 calculations of the isobutyryl and benzoyl amides (compounds 5–8) confirm the experimental observation of only one conformer of these compounds in the solution. The *E*-form is significantly more stabilised (by up to 5 kcal/mol) in comparison with the *Z*-form. The optimised molecular geometry is identical if obtained either from the *transoid-E* or *cisoid-E* (or *transoid-Z* or *cisoid-Z*) starting conformation. Accordingly, the calculated energies of these minima are pairwise equal (cf. Table I) and correspond to a single *E*- and *Z*-form of the amide, respectively. In each of these forms, the amide plane is calculated to be perpendicular to the plane of the naphthyl ring. As opposite to the *N*-(1-naphthyl)formamides, the *E*-form of the isobutyryl and benzoyl amides is predicted to be the most stable form in all media studied.

Table I

AM1 SCF and AM1 MCa SCRF calculated heats of formation ΔH_f° (kcal/mol) of different conformers of compounds 1–10

Conformer	ϵ	Method	1	2	Compound		
					3	4	5
a	1	SCF	12.257	8.659	8.855	-9.182	-4.657
	80	MCa SCRF	8.238	2.664	2.868	-15.519	-9.516
b	1	SCF	11.630	8.291	8.841	-9.176	-4.647
	80	MCa SCRF	6.606	1.728	3.417	-14.044	-9.034
c	1	SCF	13.797	9.998	10.638	-7.472	-0.234
	80	MCa SCRF	3.218	0.208	1.116	-17.424	-5.792
d	1	SCF	14.850	12.370	10.630	-7.470	-0.232
	80	MCa SCRF	6.433	4.265	0.703	-17.499	-5.721

Conformer	ϵ	Method	6	7	Compound		
					8	9	10
a	1	SCF	-22.732	41.473	25.782	8.891	17.255
	80	MCa SCRF	-28.162	35.799	18.328	1.038	11.610
b	1	SCF	-22.899	41.478	24.356	10.728	16.833
	80	MCa SCRF	-28.007	35.954	18.114	4.562	11.451
c	1	SCF	-19.996	45.281	25.761	10.181	19.300
	80	MCa SCRF	-26.674	39.895	19.396	0.138	8.896
d	1	SCF	-19.494	45.286	24.797	13.813	20.123
	80	MCa SCRF	-27.370	40.222	18.472	5.625	11.322

Table II

AM1 SCF and AM1 MCa SCRF calculated rotation barriers ΔE (kcal/mol) about the N-C(O) bond of compounds 1, 9 and 10. The data $\Delta E'$ are corrected for the deficiency of the AM1 parameterization according to the formula $\Delta E' = 4.5 + 1.6 \Delta E(\text{AM1})$ [16]

Compound	ϵ	Method	ΔE	$\Delta E'$
9	1	SCF	11.88	23.05
	80	SCa SCRF	12.72	24.85
	80	MCa SCRF	10.93	21.99
10	1	SCF	11.03	22.15
	80	SCa SCRF	11.43	22.79
	80	MCa SCRF	10.45	21.22
1	1	SCF	10.00	20.50
	80	SCa SCRF	10.60	21.46
	80	MCa SCRF	10.88	21.91

Because of the computational limitations, the comprehensive quantum-chemical calculations of rotation barriers were performed only for compounds 1, 9, and 10. The results given in Table II indicate that the calculated rotation barrier about the N-C(O) bond is approximately constant regardless of the substituents involved at the amide group and of the dielectric medium involved. The absolute values of the barrier (10–12 kcal/mol) are underestimated because of the known deficiency of the AM1 parameterization. By applying the correction suggested in [16], a rather good quantitative agreement can be achieved between the calculated and experimental rotation barriers [25].

Table III

AM1 SCF and MCa SCRF calculated rotation barriers ΔE_n^E and ΔE_n^Z (kcal/mol) about the N-Ar bond for the respective E- and Z-forms of compounds 1, 9 and 10^a

Compound	ϵ	Method	ΔE_n^E	ΔE_n^Z
9	1	SCF	5.57	6.34
	80	SCa SCRF	5.40	6.69
	80	MCa SCRF	6.47	12.97
10	1	SCF	7.79	8.96
	80	SCa SCRF	8.05	8.94
	80	MCa SCRF	8.12	9.33
1	1	SCF	10.05	11.94
	80	SCa SCRF	9.20	10.15
	80	MCa SCRF	8.53	11.51

^a The rotation barriers for compound 9 correspond to the passage of alkyl group over the C(2) and for 10 and 1 over the C(8)

The rotation around the nitrogen-naphthyl bond may be achieved by two possible pathways. The alkyl group at nitrogen atom can pass over the atom at position 2 or, alternatively, over the atom at position 8 of the naphthalene ring. The calculations show that the difference of the calculated rotation barriers for these two pathways is about 4–6 kcal/mol (e.g., 15.50 and 11.94 kcal/mol for the compound 1Z, $\epsilon = 1$). In both of the *E* and *Z* configurations, the lower barrier corresponds to the passage of the alkyl groups over C(8). The compound 9 (unsubstituted amide) does not have any significant steric repulsion between the NH group and the naphthalene ring. Therefore, as expected, this compound has almost planar structure in conformational minimum and a very low barrier (0.5 kcal/mol) for the rotation about the *N*-naphthalene bond. Notably, the AM1 calculated barriers along the N-C_n bond are significantly (4–5 kcal) lower (cf. Table III) than the experimental ΔG^\ddagger [1]. However, the trend in the computed barriers, showing the increase of the rotational barrier with increasing volume of the alkyl group, is parallel to the trend observed experimentally [1]. Also, the difference of the calculated rotational barriers ($\Delta E_a^Z - \Delta E_a^E$) in *E* and *Z* conformers of 1 is in a good accordance with the respective experimental data (1.9 and 1.5 kcal/mol, respectively).

In conclusion, the results presented in this work demonstrate that the AM1 MCa SCRF calculations give correct predictions of the predominant conformers and conformational barriers of 1-naphthylamides in solution.

*

The authors wish to acknowledge Volkswagen Stiftung (Hannover, Germany) for their generous support of this work.

References

- [1] LEIS, J., KARELSON, M., SCHIEMENZ, G. P.: *ACH – Mod. Chem.*, **135**, 157 (1998)
- [2] DEWAR, M. J. S., ZOEBISCH, E. G., HEALY, E. F., STEWART, J. J. P.: *J Am. Chem. Soc.*, **107**, 3902 (1985)
- [3] HYLTON, J., CHRISTOFFERSEN, R. E., HALL, G. G.: *Chem. Phys. Lett.*, **26**, 501 (1974)
- [4] TAPIA, O., GOSCINSKI, O.: *Mol. Phys.*, **29**, 1653 (1975)
- [5] KARELSON, M.M.: *Organic Reactivity (Tartu)*, **17**, 357 (1980)
- [6] KARELSON, M., TAMM, T., ZERNER, M. C.: *J. Phys. Chem.*, **97**, 11901 (1993)
- [7] MARAN, U., PAKKANEN, T. A., KARELSON, M.: *J. Chem. Soc. Perkin Trans. 2*, 2445 (1994)
- [8] DIERCKSEN, G. H. F., KARELSON, M., TAMM, T., ZERNER, M. C.: *Int. J. Quant. Chem.*, **S28**, 339 (1994)
- [9] COLEBROOK, L. D.: *Can. J. Chem.*, **69**, 1957 (1991)

- [10] YU, H. A., PETTITT, B. M., KARPLUS, M.: *J. Am. Chem. Soc.*, **113**, 2425 (1991)
- [11] SAUVAITRE, H., TYSSEYRE, J., ELGUERO, J.: *Bull. Soc. Chim. Fr.*, 635 (1976)
- [12] FRAENKEL, G., KOLP, C. J., CHOW, A.: *J. Am. Chem. Soc.*, **114**, 4307 (1992)
- [13] SHUSTOV, G. V., KADORKINA, G. K., VARLAMOV, S. V., KACHANOV, A. V., KOSTYANOVSKY, R. G., RAUK, A.: *J. Am. Chem. Soc.*, **114**, 1616 (1992)
- [14] VAN GUNSTEREN, W. F., BERENDSEN, J. H. C.: *Angew. Chem. Int. Ed. Engl.*, **29**, 992 (1990)
- [15] VAN GUNSTEREN, W. F., BRÜCHSWEILER, R., ERNST, R. R.: *J. Am. Chem. Soc.*, **115**, 4764 (1993)
- [16] FEIGEL, M., STRASSNER, T.: *THEOCHEM*, **102**, 33 (1993)
- [17] KARELSON, M., TAMM, T., KATRITZKY, A. R., CATO, S., ZERNER, M. C.: *Tetrahedron Comp. Methodol.*, **2**, 295 (1989)
- [18] KARELSON, M., ZERNER, M. C.: *J. Phys. Chem.*, **96**, 6949 (1992)
- [19] STEWART, J. J. P.: *MOPAC 6.0*, QCPE No. 455, 1989
- [20] PETTITT, B. M., KARPLUS, M., ROSSKY, P. J.: *J. Phys. Chem.*, **90**, 6365 (1986)
- [21] JORGENSEN, W. L., GAO, J.: *J. Am. Chem. Soc.*, **110**, 4212 (1988)
- [22] RADOM, L., RIGGS, N. V.: *Aust. J. Chem.*, **35**, 1071 (1982)
- [23] WIBERG, K. B., WONG, M. W.: *J. Am. Chem. Soc.*, **115**, 1078 (1993)
- [24] BÖTTCHER, C. J. F., BORDEWIJK, P.: *Theory of Electric Polarization*, 2nd ed., vol. II, Elsevier Co, Amsterdam, 1978
- [25] STEWART, W. E., SIDDALL, T. H.: *Chem. Rev.*, **70**, 517 (1970)

Reprinted from the Tetrahedron, Vol. 54,
J. Leis, K. D. Klika and M. Karelson,
Solvent Polarity Effects on the *E/Z* Conformational Equilibrium of
N-1-naphthylamides, pages 7497–7504,
Copyright 1998, with permission from Elsevier Science.

Solvent Polarity Effects on the *E/Z* Conformational Equilibrium of *N*-1-naphthylamides

Jaan Leis^a, Karel D. Klika^b and Mati Karelson^{a*}

^aDepartment of Chemistry, University of Tartu, 2 Jakobi St., Tartu, EE2400, Estonia

^bDepartment of Chemistry, University of Turku, FIN-20014, Turku, Finland

Received 7 April 1998; accepted 20 April 1998

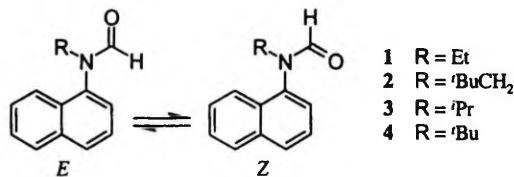
Abstract: The ratio of the *E* and *Z* conformers of *N*-alkyl-*N*-1-naphthylformamides has been measured in a series of solvents using NMR spectroscopy. A linear relationship was found between the free energy of the conformational equilibrium, ΔG° , and the relative dielectric permittivity of the solvent. The comparison of NMR data with quantum-chemically calculated SCRF heats of equilibria reveals that the solvent effect is a combination of both the electrostatic and specific solute-solvent interactions, the latter being directly connected to the solvent-induced steric deformations of the solute molecule.
© 1998 Elsevier Science Ltd. All rights reserved.

INTRODUCTION

The importance of the amide bond isomerisation caused by the hindered rotation around this bond, is recognised in many processes that require alternation of peptide structure. Also, the isomeric composition of synthetic polyamides, products of the retro synthesis¹⁻³ and the rate of polymerisation processes may be affected by the conformational distribution of the monoamides. Since most of these processes occur in solution, the solvent effects may, in principle, affect the conformational dynamics and equilibria at amide bond. The NMR spectroscopy is perhaps the most widely used method in determining the ratio of *cis/trans* (or *E/Z*) conformers in amides⁴. Applicable in different solvents, it also allows direct measurement of the solvent effects on the conformational equilibria. Although the influence of the solvent through its polarity on the conformational equilibrium has been discussed in the case of several amides⁴⁻⁸, the detailed mechanism of these effects is still not well understood. For instance, it has been found that in the case of secondary amides the specific solvation plays an important role through the inter- and intramolecular hydrogen bonding^{4,5,9,10}. However, the specific solvent effects should be less significant in the case of tertiary amides and the conformational equilibria should be predetermined by the nonspecific interactions arising from the polarity of the environment.

In this work, the solvent effect on the conformational equilibrium of the series of *N*-alkyl substituted *N*-1-naphthylformamides was investigated using the nuclear magnetic resonance spectroscopy (NMR). This

equilibrium is defined between the *E* (oxygen atom *cis* to the alkyl group) and *Z* (oxygen atom *trans* to the alkyl group) conformers (Scheme 1) of amides^{11,12}. In addition, the influence of the solvent polarity on the equilibrium was modelled quantum chemically using AM1 semiempirical parameterisation¹³ within the MOPAC 6.0 SCF¹⁴ and SCRF¹⁵ program packages. Both the single-cavity (SCa SCRF)¹⁵ and multi-cavity (MCa SCRF)^{16,17} reaction field models were applied.



Scheme 1

RESULTS AND DISCUSSION

The Nuclear Magnetic Resonance (NMR) spectroscopy.

The ratio of *E* and *Z* conformers of *N*-1-naphthylamides was determined from the integrated NMR signals of formyl proton recorded in solvents of varying polarity. The respective experimental results are presented in Table 1. All measurements were carried out at 298 K.

Table 1. The Ratio ($X_Z = [Z]/[E]$) of the *Z* and *E* Conformations of *N*-alkyl-*N*-1-naphthylformamides (1–4) in the Solvents of Different Relative Permittivity (ϵ).

Solvent	ϵ (25°C) ¹⁸	1	2	3	4
CDCl ₃	4,7	0,11	0,15	0,18	0,57
C ₂ D ₂ Cl ₄	8,2	0,14	0,18	0,26	0,95
(CD ₃) ₂ CO	20,5	0,19	0,27	0,28	0,58
CD ₃ OD	32,6	0,29	0,33	0,48	1,23
DMSO- <i>d</i> ₆	46,8	0,38	0,53	0,62	1,72

It has been shown that in formanilide the chemical shift of the formyl proton is independent of the solute concentration⁵. The data presented in Table 2 demonstrate that the chemical shifts of formyl proton in both conformers are also almost independent of solvent and only very small upfield shift can be observed with the increase of solvent polarity. Also, as the molecules examined differed only by the alkyl substituents at the

carbonyl group, the electronic effects within these compounds should be similar and the variance in chemical shifts would be caused mainly by the steric effects. Accordingly, the difference in the chemical shifts of the *E* conformers of the studied compounds can be attributed to the differences in the torsion angle between the amide and the naphthyl groups. Thus, the formyl proton of the sterically bulky *N*-isopropyl- (3) and *N*-*tert*-butyl-*N*-1-naphthylformamide (4) is more shielded due to the diamagnetic field of the naphthyl ring as compared to the sterically less restricted compounds 1 and 2. This observance is well supported by the AM1 MCa SCRf calculated torsion angles between the formyl proton and the N-C1-C9 plane. In the case of the polarisable medium with the relative dielectric permittivity $\epsilon = 4.7$, the calculated angle was 97.6, 101.3, 75.5 and 77.4° in *E* conformers of 1-4, respectively. The shielding of the formyl proton by the naphthyl ring is negligible in the *Z* conformation, however, other factors may affect the respective proton NMR shift. For instance, the shift of the formyl proton signal to the low field in compound 4 (Table 2) can be attributed to the weak intramolecular interaction between formyl proton and *tert*-butyl group.

Table 2. Chemical Shifts (δ , ppm) of Formyl Proton Relative to Tetramethylsilane (TMS).

Compound	CDCl ₃	C ₂ D ₂ Cl ₄	CD ₃ C(O)CD ₃	CD ₃ OD	DMSO-d ₆
1 <i>E</i>	8.23	8.19	8.18	8.17	8.17
1 <i>Z</i>	8.58	8.50	8.56	8.53	8.52
2 <i>E</i>	8.36	8.32	8.31	8.31	8.30
2 <i>Z</i>	8.52	8.47	8.53	8.51	8.48
3 <i>E</i>	8.16	8.10	8.10	8.10	8.06
3 <i>Z</i>	8.67	8.58	8.64	8.62	8.58
4 <i>E</i>	8.18	8.13	8.10	8.10	8.05
4 <i>Z</i>	8.96	8.88	8.94	8.92	8.88

From the data presented in Table 1, the Gibbs energies of equilibria were calculated as follows:

$$\Delta G^0 = -RT \ln X_Z \quad (1)$$

The graphical representation of the results (Figure 1) witnesses the existence of an approximately linear relationship between ΔG^0 and ϵ . This is somewhat unusual as a linear relationship between ΔG^0 and the Kirkwood function $(\epsilon-1)/(2\epsilon+1)$ would be expected from the theoretical considerations¹⁹. The slopes (*a*) of the linear relationship $\Delta G^0 = a\epsilon + b$ appear to be constant for different compounds, indicating the presence of a uniform solvent effect on the equilibria. The intercept (*b*) is characteristic to the solute molecule. The decrease in the population of the *E* isomer with the increase of the polarity of the solvent may be attributed to the increase in the steric interaction between oxygen atom and the alkyl substituent. Notably, the dimensions of

oxygen atom depend on the state of ionization, e.g., the van der Waals radii are 1.40 Å for O^0 and 1.76 Å for O^- , respectively¹⁸. The SCRf calculations indicate that in the polar media the amide group is more polarized with increased partial negative charge on the oxygen atom²⁰. For instance, the MCa SCRf calculated Mulliken charge in carbonyl oxygen of formamide is -0.418 in $CHCl_3$ ($\epsilon = 4.7$) and -0.437 in DMSO ($\epsilon = 46.8$). Hence, this atom is expected to have larger van der Waals radius in high dielectric constant media and, correspondingly, stronger sterical interaction with the rest of the molecule.

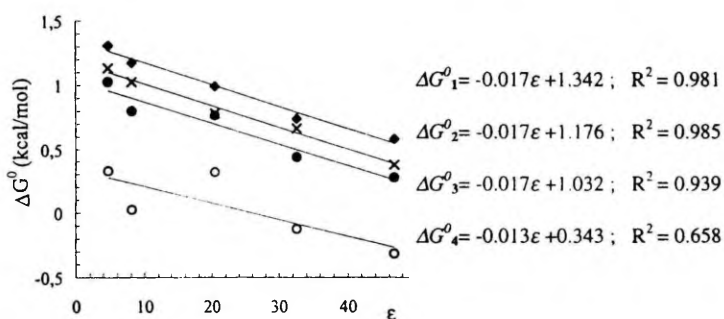


Fig. 1. The relationship between the free energy of conformational equilibrium (1), ΔG^0 , and the relative permittivity of the solvent, ϵ .

The poorer correlation for the compound 4 shows that additional factors besides of the solvent dielectric properties may become important for sterically more restricted compounds. Gerothanassis *et al.*²¹ have recently demonstrated using the heteronuclear Overhauser effect spectroscopy (HOESY) that *E/Z* isomers of *tert*-butylformamide are differently hydrated in aqueous solution. They concluded that significant decrease in the population of the *Z* isomer as compared to the *E* isomer should be attributed to the combined effect of reduced hydration of the *Z* amide CO group and out-of-plane deformation of the amide group due to the bulky *tert*-butyl group.

These conclusions are also applicable in the case of *N*-1-naphthylformamides. The AM1 MCa SCRf calculations predict a more substantial out-of-plane torsion of the carbonyl group from amide plane in the *E* conformation as compared to the *Z* conformation. For instance, the respective torsion angle is 26.9, 22.3, 26.8 and 27.5° in *E* forms, and 0.03, 4.60, 1.23 and 0.87° in *Z* forms of 1-4, respectively.

The HOESY studies by Gerothanassis²¹ were carried out in aqueous solutions and, therefore, it is difficult to predict how the differential solvation would be affected by the size or shape of the solvent molecules. The difference in the size and shape of solvent molecules could be the additional factor leading to the poor correlation between ΔG^0 and ϵ for the compound 4.

We have also examined the dependence of the X_Z on the temperature. The observed trend is consistent with the dependence of ϵ on temperature. In dimethylsulfoxide (DMSO), the Z/E ratio of compound **4** was found to be 1.49, 1.43 and 1.32 at 35, 50 and 75°C, respectively. Thus, the decrease of ϵ with increase of temperature is accompanied with the shift of the conformational equilibrium in favour of the *E* form.

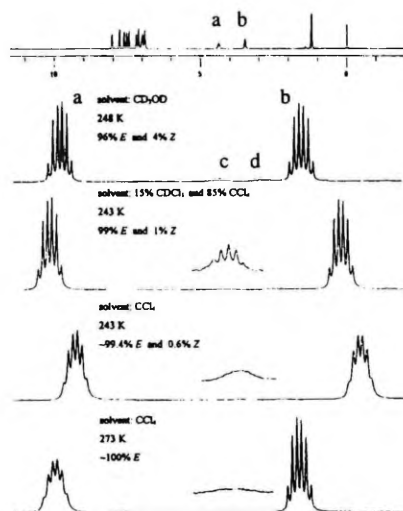


Fig. 2. The NMR signals (a,b,c and d) of the methylene protons of the ethyl group of compound **5** in different solvents. The increased image of the down-field band of minor conformer (c) is shown additionally.

The full spectrum of compound **5** (recorded in tetrachloromethane at 273K) is presented on the top.

Therefore, our results suggest that the variation of temperature and solvent could enable to observe experimentally the minor conformers at amide bonds (cf. Figure 2). For instance, in the case of *N*-ethyl-*N*-1-naphthylbenzamide (**5**), only one conformer (*E*) is experimentally observable in low polarity solvents. However, significant population (4%) of the minor conformer (*Z*) was recorded in methanol at low temperatures.

Semiempirical calculations.

The quantum-chemical calculations were carried out at the semiempirical level using Austin Model 1 (AM1)¹³ parameterisation. The non-specific solvation effects were described using the self-consistent reaction field (SCRF) approach^{14-16,22-23}. The single-cavity self-consistent reaction field (SCa SCRF) model performed poorly due to the relatively large size and flexibility of the title compounds. The calculated solvation energies were too small and as a result the calculated ratio of amide conformers was very little dependent on the solvent polarity. The more realistic estimate of the solvation energy of *N*-1-naphthylamides was obtained using the

multi-cavity self-consistent reaction field (MCa SCRf) model. Indeed, this method described the observed conformational equilibria changes better, but still only qualitatively (cf. Fig. 3).

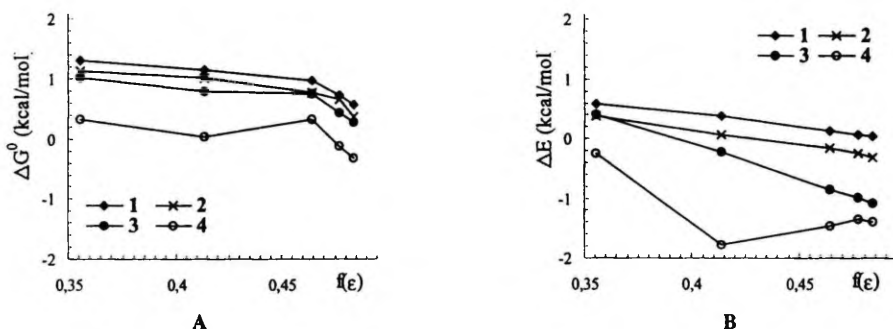


Fig. 3. The relationship of experimental ΔG° (Eq. (1)), A, and AM1 MCa SCRf calculated ΔE (kcal/mol), B, on the Kirkwood-Onsager function, $f(\epsilon) = (\epsilon - 1)/(2\epsilon + 1)$.

Consequently, our results indicate that the electrostatic reaction field model alone is not sufficient to describe the solvent effect on the conformational equilibria at the amide bond. The methods that reflect the molecular dynamics and the specific solvent-solute interactions should be applied and will be considered by us in further studies.

CONCLUSIONS

The present study reveals that the solvent effect on the conformational equilibria of amides involves a simultaneous influence of the non-specific and specific solute-solvent interactions. In the sterically hindered *N*-1-naphthylamides, the relative stability of the *Z* isomer increases with the increase of polarity of the solvent. The free energy of the respective *E/Z* conformational equilibrium is linearly related to the relative dielectric permittivity of the solvent. The discrepancy between the experimental data and the results of self-consistent reaction field calculations indicates that this dielectric effect cannot be explained within the simple Kirkwood-Onsager electrostatic model. However, the quantum-chemical calculations revealed a substantial out-of-plane deformation of the carbonyl group in the *E* isomers. Such deformation leads to the different solvation in *E* and *Z* isomers, similar to that observed in the case of *tert*-butylformamide. Thus, the solvent effect upon the conformational equilibrium in *N*-alkyl-*N*-1-naphthylformamides is determined by the combination of the nonspecific interaction of the solute molecules with the dielectric medium and the differential solvation of the *E* and *Z* isomers by adjacent solvent molecules.

EXPERIMENTAL

Compounds **1–4** were synthesised by formylation of respective *N*-alkyl-*N*-1-naphthylamines with the formic acid. The detailed description of the syntheses and the spectral characteristics of compounds obtained have been reported elsewhere¹¹. *N*-ethyl-*N*-1-naphthylbenzamide (**5**) was prepared by reacting of benzoyl chloride with *N*-ethyl-1-naphthylamine for 48 h at room temperature. Compound **5** was identified as follows: ¹H NMR (CD₃OD, TMS, 248 K, 400 MHz, δ (ppm)) 1.086 (t, 3H, CH₃(min), J 7.1), 1.235 (t, 3H, CH₃(maj), J 7.1), 3.559 (m, 1H, CH₂(maj)), 3.702 (m, 1H, CH₂(min)), 3.870 (m, 1H, CH₂(min)), 4.452 (m, 1H, CH₂(maj)), 6.99–8.05 (m, 12H, ArH) (cf. Fig. 2).

¹H NMR spectra were recorded on JEOL LAMBDA 400 and ALPHA 500 instruments in the deuterated solvents at 25°C. The variable temperature measurements were performed on the ALPHA 500 spectrometer.

ACKNOWLEDGEMENT

We are grateful to Professor Kalevi Pihlaja of Turku University for providing the NMR equipment and his help during these experiments.

REFERENCES

1. Yamaguchi, K., Matsumura, G., Kagechika, H., Azumaya, I., Ito, Y., Itai, A., Shudo, K. *J. Am. Chem. Soc.* **1991**, *113*, 5474.
2. Azumaya, I., Kagechika, H., Yamaguchi, K., Shudo, K. *Tetrahedron* **1995**, *51*, 5277.
3. Azumaya, I., Kagechika, H., Yamaguchi, K., Shudo, K. *Tetrahedron Lett.* **1996**, *37*, 5003.
4. Stewart, W.E., Siddall, T.H. *Chem. Rev.* **1970**, *70*, 517.
5. Bourn, A.J.R., Gillies, D.G., Randall, E.W. *Tetrahedron* **1964**, *20*, 1811.
6. Bourn, A.J.R., Gillies, D.G., Randall, E.W. *Tetrahedron* **1966**, *22*, 1825.
7. Weil, J.A., Blum, A., Heiss, A.H., Kinnaird, J.K. *J. Chem. Phys.* **1967**, *46*, 3132.
8. Drakenberg, T., Dahlqvist, K.-J., Forsen, S. *J. Phys. Chem.* **1972**, *76*, 2178.
9. Rae, I.D. *Can. J. Chem.* **1966**, *44*, 1334.
10. Manea, V.P., Wilson, K.J., Cable, J.R. *J. Am. Chem. Soc.* **1997**, *119*, 2033.
11. Leis, J., Karelson, M., Schiemenz, G.P. *ACH-Models in Chemistry* **1998**, *00*, (in press).
12. Leis, J., Maran, U., Schiemenz, G.P., Karelson, M. *ACH-Models in Chemistry* **1998**, *00*, (in press).

13. Dewar, M.J.S., Zoebisch, E.G., Healy, E.F., Stewart, J.J.P. *J Am. Chem. Soc.* **1985**, *107*, 3902.
14. Stewart, J.J.P. *MOPAC 6.0*, QCPE No. 455, **1989**.
15. Karelson, M., Tamm, T., Katritzky, A.R., Cato, S.J., Zerner, M.C. *Tetrahedron Comp. Methodol.* **1989**, *2*, 295.
16. Karelson, M., Tamm, T., Zerner, M.C. *J. Phys. Chem.* **1993**, *97*, 11901.
17. Karelson, M., Maran, U., Katritzky, A.R. *Tetrahedron* **1996**, *52*, 11325.
18. *CRC Handbook of Chemistry and Physics*; CRC Press Inc., **1994**.
19. Reichardt, C. *Solvents and Solvent Effects in Organic Chemistry*; VCH: Weinheim, **1990**.
20. Burton, N., Chiu, S., Davidson, M., Green, D., Hillier, I., McDouall, J., Vincent, M. *J. Chem. Soc. Faraday Trans.* **1993**, *89*, 2631.
21. Gerothanassis, I.P., Troganis, A., Vakka, C. *Tetrahedron Lett.* **1996**, *37*, 6569.
22. Tapia, O., Goscinski, O. *Mol. Phys.* **1975**, *29*, 1653.
23. Karelson, M. *Organic Reactivity (Tartu)* **1980**, *17*, 357.

J. Leis and M. Karelson.
Quantum-Chemical Study of The Stereochemistry of
Some *N,N*-Diarylamides, Proceedings of the Estonian Academy of
Sciences (Chem.), 000, 000–000, 1998 (submitted).

QUANTUM-CHEMICAL STUDY OF THE STEREOCHEMISTRY OF SOME *N,N*-DIARYLAMIDES

Mati Karelson* and Jaan Leis

Department of Chemistry, University of Tartu, 2 Jakobi St.,
Tartu 51014, Estonia

*e-mail: mati@chem.ut.ee; Fax: +27+375264

Abstract

Conformational distribution and rotational dynamics of some *N,N*-diarylamides, *i.e.*, *N,N*-di(2-methylphenyl)-3',3'-dimethylbutyrylamide (1) and *N*-(2-methylphenyl)-*N*-(1-naphthyl)-3',3'-dimethylbutyrylamide (2) was modelled using the semiempirical AM1 SCF method. The results were used to predict the possible origin of the energy barriers estimated by dynamic NMR spectroscopy.

Key words: amide, rotation, modelling

Introduction

Conformational preferences and dynamic processes in sterically crowded amides have been the subjects of numerous studies over the decades. The most common experimental tool in these investigations has been the NMR spectroscopy. However, depending on the chemical structure of the amide, the unambiguous interpretation of these spectra may be difficult due to the complicated NMR spectra arising from the more than one conformational species in the measured sample. The *N*-arylamides represent a typical example of such situation. The relatively high rotational barriers about both the amide N-C(O) bond and nitrogen-aryl bond(s) may lead to the presence of several equilibril atropisomers in the solution and, correspondingly, to a complicated overall NMR spectrum of the compound. The quantum chemical modelling of the possible conformers and the potential surfaces of the respective conformational transformations may assist to clarify the above mentioned problems.

Quantum-chemical calculations

The quantum-chemical calculations were performed at the semiempirical level using Austin Model 1 (AM1) [Dewar *et al.*, 1985; Stewart, 1989] parameterization. The semiempirical approach was chosen on the basis of the size of the molecules considered in this work. Good-quality *ab initio* calculations of the potential surfaces for rotational transition barriers in the systems of this size

would require very large computer time and hardware resources. Notably, extensive quantum-chemical *ab initio* studies at various levels of theory (SCF LCAO MO, MP2-MP4, G2(MP2)) have been reported only for simple amides including formamide, *N*-methylacetamide, *N,N*-dimethylformamide and *N,N*-dimethylacetamide [Harrison & Stein, 1992; Wiberg & Breneman, 1992; Wiberg *et al.*, 1992; Wiberg & Rablen, 1993; Wong & Wiberg, 1992; Wiberg *et al.*, 1995; Luque & Orozco, 1993]. It is well known that the AM1 method substantially underestimates the rotation barrier along the amide bond [Cieplak, 1994; Feigel & Strassner, 1993], however, a good linear correlation has been found between the experimental and AM1 calculated barriers [Feigel & Strassner, 1993].

Substantial solvent effects on the amide bond rotation barriers have been reported on the basis of the experimental dynamic NMR spectra measurements [Lilley, 1994; Stewart & Siddall, 1970; Feigel, 1983; Ross & True, 1984; Ross *et al.*, 1985]. However, for large systems involving aryl substituents at the amide nitrogen atom, the calculated solvent effects have been found to be nearly constant for a series of similar molecules [Leis *et al.*, 1998]. Therefore, only isolated molecules have been studied in this work.

It has been shown that most rotational activation free energies, particularly the rotational barriers along the amide bond, are predominantly of enthalpic nature [Wiberg *et al.*, 1995]. Consequently, the quantum-chemically calculated relative energies of the conformers and transition states can be used to estimate of the relative populations of different conformers and the activation free energies of the rotational transformations.

Two compounds were considered in the present work, *i.e.* the *N,N*-di(2-methylphenyl)-3',3'-dimethylbutyrylamide (**1**) and *N*-(2-methylphenyl)-*N*-(1-naphthyl)-3',3'-dimethylbutyryl-amide (**2**).

(Scheme 1)

In both cases, the conformational minima and transition barriers were found by the grid search of the multidimensional potential surface contrived from all possible rotations along the N-C_{aryl} bonds and along the C(O)-C(neopentyl) bond.

Results and discussion

N,N-di(2-methylphenyl)-3',3'-dimethylbutyrylamide (**1**)

Four conformers (**1a–1d**) were established for *N,N*-di(2-methylphenyl)-3',3'-dimethylbutyrylamide. The AM1 calculated heats of formation, $\Delta H_{f,298}^{\circ}$, relative energies and relative populations of different conformers at room temperature are given in Table 1.

(Scheme 2)

Notably, the rotation along the C(O)-C(neopentyl) bond is characterised by a low barrier. The following AM1 calculated activation energies were obtained for this rotation: $E_A = 1.05, 0.51, 0.26$ and 0.92 kcal/mol for **1a**, **1b**, **1c** and **1d**, respectively. Consequently, the neopentyl group undergoes rapid rotation and no splitting of the methyl group signals in the NMR spectra is expected to arise from this process even at very low temperature. Therefore, the respective possible rotamers along the C(O)-C(neopentyl) bond can be assumed to correspond to a single structure. The populations p_i of different conformers arising from the rotation along the N-aryl bond were calculated according to the Boltzmann distribution law

$$p_i = \exp(-E_i / RT) / \sum_i \exp(-E_i / RT) \quad (1)$$

where R is the universal gas constant and E_i denote the energies of individual conformers. Two main conformers (**1a** and **1d**) account for the 74% of the population whereas the minor conformers (**1b** and **1c**) account totally for the 26%. For the convenience, only the most stable conformers related to the torsion angle between the *tert*-butyl group and the amide plane have been considered in the calculation of relative populations. However, it should be kept in mind that the precision of the quantum-chemical calculations does not exclude the conformers arising from the rotation around the C(O)-C(neopentyl) bond that must be still considered in the further discussion of the dynamic NMR spectra of this compound.

All possible four rotation paths on the multidimensional molecular potential surface, each corresponding to a single N-C_{aryl} bond rotation were calculated, corresponding to the transitions **1a** \rightleftharpoons **1b**, **1a** \rightleftharpoons **1c**, **1b** \rightleftharpoons **1d** and **1c** \rightleftharpoons **1d**. As an example, the results of the grid search of the potential surface for the transition **1b** \rightarrow **1a** with the rotation step of 10 degrees are presented in Table 2. The AM1 SCF calculated transition energies are summarised in Table 3. Rotational barriers calculated as the difference between the transition state and the most stable conformer (*i.e.* **1a** from the pair **1a**–**1d** and **1b** from **1b**–**1c**) ranges from 7.38 kcal/mol for **1c** \rightarrow **1a** to 8.17 kcal/mol for **1b** \rightarrow **1d**. The similarity of these barriers suggests that only one coalescence process corresponding to the equilibration of the isomers with the tolyl methyl groups on the one side of the amide plane (**1a** and **1d**) and the isomers with the methyls on different sides of the amide plane (**1b** and **1c**), should be observable in dynamic NMR spectra of this compound. The calculated activation energies also indicate that the rate of the conformational transition **1a** (**1d**) to **1b** (**1c**) is somewhat slower than that the reverse process. A closer study of the structure of rotational transition states along the N-C_{aryl} bonds, however, reveals that the NC_{tolyl1}C_{tolyl2} plane has been turned to nearly orthogonal to the plane defined by the carbonyl group, with the

nitrogen atom diverted essentially pyramidal. In other words, these transition states correspond simultaneously to the transition state of the rotation along the amide bond. As mentioned above, the AM1 method underestimates significantly the rotational barriers of these bonds. Still, a satisfactory correlation has been found between the AM1 calculated transition barriers and experimentally measured activation energies for a series of amides, thioamides, ureas and thioureas. Using the corresponding linear relationship [Feigel & Strassner, 1993]

$$\Delta G_{\text{liquid}}^* = 1.6E_A(\text{AM1}) + 4.5 \text{ kcal/mol} \quad (2)$$

the barrier for the most probable rotational transition (**1a** \rightleftharpoons **1c**) is estimated as 17.40 kcal/mol for **1c** \rightarrow **1a** and 16.31 kcal/mol for the reverse process, in excellent accordance with the experimentally measured value $\Delta G_{\text{liquid}}^* = 17.27 \text{ kcal/mol}$ [Lill & Schiemenz, unpublished] (for a comparison, in less crowded *N*-isopropyl-*N*-(2-tolyl)formamide-*Z*, the respective rotational barrier about N-C_{aryl} bond $\Delta G_{\text{liquid}}^* = 16.2 \text{ kcal/mol}$ has been determined at coalescence temperature [Leis, unpublished].) As mentioned above, this rotational barrier corresponds also to the transition state for the amide bond rotation and therefore both methyls of the tolyl groups become equivalent at the coalescence temperature.

However, an experimentally observed further splitting of the NMR spectra of the methyl groups as well as the methylene hydrogens of the neopentyl group at low temperatures indicates the presence of another conformational separation (with an experimental $\Delta G_{\text{liquid}}^* = 13.19 \text{ kcal/mol}$) [Lill & Schiemenz, unpublished]. This can be assigned to the concerted hindered rotation of tolyl groups, corresponding to the transformation of the conformers **1a** to **1d** and **1b** to **1c**, respectively. The latter are essentially the pairs of enantiomers. The respective AM1 calculated transition barriers are $E_A(\text{AM1}) = 6.79$ and 6.44 kcal/mol . Also in this case, the calculated structure of the transition states is similar to those for the amide bond rotation. The predicted (according to the Eq. (2) for the amide bond rotation) $\Delta G_{\text{liquid}}^* = 15.36$ and 14.80 kcal/mol for the two enantiomerisation processes (**1a** \rightarrow **1d**; **1b** \rightarrow **1c**) are somewhat higher than the experimentally observed rotational barrier for this compound (13.19 kcal/mol [Lill & Schiemenz, unpublished]). However, the latter value, estimated from the coalescence temperature of the dynamic NMR spectra, represents obviously the average of two rotational barriers (**1a** \rightarrow **1d**; **1b** \rightarrow **1c**) and would be underestimated due to the chemical exchange between **1a** and **1c**.

N-(2-methylphenyl)-*N*-(1-naphthyl)-3',3'-dimethylbutyrylamide (2)

The conformational space of this compound is more complicated because one of the N-substituents (e.g., the naphthyl group) can be either in *cis*- or *trans*-

position to the carbonyl oxygen of the amide group. The corresponding structures will be referred in the further discussion as the *E* and *Z* conformations.

(Scheme 3)

Similarly to the compound **1**, it was found that the rotation of the *tert*-butyl group along the C(O)-C(neopentyl) bond is characterised by a very low barrier (< 1 kcal/mol). Therefore, only the conformers corresponding to the lowest minimum for this rotation (altogether eight different conformers) were considered in the further discussion. The definition of the conformers, their AM1 calculated heats of formation $\Delta H_{f,298}^o$, relative energies $\delta\Delta H_{f,298}^o$ and populations are given in Table 4. The *Z* conformers seem to be more preferred (by about 1 kcal/mol) over the *E* conformers. However, within the precision of the theoretical method applied (AM1), this is not significant. Moreover, it has been noticed that the *E/Z* conformational preference may be substantially shifted by solvents [Luque & Orozco, 1993; Leis & Klika & Karelson, 1998]. The calculated transition barriers between different conformers are given in Table 5. Importantly, in most cases (except of the transformation **2e**→**2g**), the rotation along the N-C_{aryl} bond leads to the concerted rotation along the amide bond with the respective interchange between the *Z* and *E* conformation. Therefore, the exchange between the conformers **2a**→**2g**, **2c**→**2g**, or **2c**→**2f** will lead to the equalisation of different positions of the methyl at the tolyl group and of the methylene hydrogens at the neopentyl group. The predicted activation free energy for these transitions (according to the Equation (2)) is ranging from $\Delta G_{\text{liquid}}^* = 17.75$ kcal/mol to $\Delta G_{\text{liquid}}^* = 18.45$ kcal/mol.

A lower energy transition state between two twisted conformers **2b**→**2c** has been also found for this compound. The respective AM1 calculated $E_A = 6.35$ kcal/mol corresponds to the theoretically predicted $\Delta G_{\text{liquid}}^* = 14.66$ kcal/mol in the solution. The smaller value as compared to the respective barrier of compound **1** agrees with the observation that the amide bond rotational barrier decreases at a more crowded nitrogen atom [LeMaster & True, 1989].

Conclusions

The dynamic NMR spectra of *N,N*-diaryl-3',3'-dimethylbutyrylamides can be quantitatively interpreted on the basis of the semiempirical quantum-chemical AM1 SCF investigation of the full conformational potential surface of these compounds. Notably, it has been found that the rotational transition states about the N-C_{aryl} bonds coincide with the transition states of the rotation around the amide (N-C(O)) bond, with the plane defined by the amide nitrogen atom and two aryl carbon atoms connected to it turned almost perpendicular to the NCO

plane and nitrogen atom itself substantially pyramidalised. In the case of *N*-(2-methylphenyl)-*N*-(1-naphthyl)-3',3'-dimethylbutyryl-amide (**2**), the rotation along the N-C_{aryl} bond forces also a concerted rotation along the amide bond, leading to the interchange between the *E* and *Z* conformations at this bond. In the case of compound **1**, the AM1 estimated $\Delta G_{\text{liquid}}^*$ (17 ... 18 kcal/mol) for the respective conformational transition is in an excellent agreement with the corresponding experimental value, calculated from the coalescence temperature of the dynamic NMR spectra. Another, lower-temperature splitting of the signals of isotopic groups has been detected in NMR spectra of both compounds, corresponding to the rotational barrier about the amide bond. The respective theoretically predicted $\Delta G_{\text{liquid}}^*$ (14 ... 15 kcal/mol) values compare favourably with the experimental value for the compound **1**.

Mõnede *N,N*-diarüülamiidide stereookeemia kvantkeemilised uuringud

Mati Karelson* ja Jaan Leis

Käesolevas töös rakendati poolempiirilist kvantkeemilist AM1 SCF meetodit ja näidati, et *N,N*-diarüül-3',3'-dimetüülbutürüülamiidide dünaamilise TMR-i spektreid võib nii kvalitatiivselt kui ka kvantitatiivselt interpreteerida nende ühendite potentsiaalipindade modelleerimise kaudu. Täpsemalt käsitleti *N,N*-di(2-metüülfenüül)- (**1**) ja *N*-(2-metüülfenüül)-*N*-(1-naftüül)-3',3'-dimetüülbutürüül-amiidi (**2**). Arvutatud konformatsiooniliste üleminekute potentsiaali pindade põhjal ennustati reaalselt võimalike ja TMR spektrites kajastuvate dünaamiliste protsesside parameetrid. Samuti leiti, et kvantkeemiliselt (AM1 SCF) arvutatud rotatsioonibarjäärid on heas korrelatsioonis eksperimentaalsete aktivatsiooni vabaenergiatega.

References

1. Dewar, M.J.S., Zoebisch, E.G., Healy, E.F. & Stewart, J.J.P. AM1: a new general purpose quantum mechanical molecular model. *J Am. Chem. Soc.*, 1985, **107**, 3902–3909.
2. Feigel, M. Rotation barriers of amides in the gas phase. *J. Phys. Chem.*, 1983, **87**, 3054–3058.
3. Feigel, M. & Strassner, T. A semiempirical AM1, MNDO and PM3 study of the rotational barriers of various ureas, thioureas, amides and thioamides. *THEOCHEM*, 1993, **102**, 33–48.

4. Harrison, R.K. & Stein, R.I. Mechanistic studies of enzymic and nonenzymic prolyl cis-trans isomerization. *J. Am. Chem. Soc.*, 1992, **114**, 3464–3471.
5. Leis, J., Maran, U., Karelson, M. & Schiemenz, G.P. Stereochemistry of arylamides, 2. AM1 SCF and SCRF quantum-chemical modelling of some N-(1-naphthyl)amides. *ACH-Mod. Chem.*, 1998, **135**, 173–181.
6. Leis, J. Personal communications.
7. Leis, J., Klika, K.D. & Karelson, M. Solvent polarity effects on the E/Z conformational equilibrium of N-1-naphthylamides. *Tetrahedron*, 1998, **54**, 7497–7504.
8. LeMaster, C.B. & True, N.S. Gas-phase NMR study of torsional barriers in N,N-diethyl- and N,N-diisopropylformamide. Medium effects on kinetic parameters. *J. Phys. Chem.*, 1989, **93**, 1307–1311.
9. Lill, J. & Schiemenz, G.-P. *Personal communications*.
10. Luque, F.J. & Orozco, M. Theoretical study of N-methylacetamide in vacuum and aqueous solution: implications for the peptide bond isomerization. *J. Org. Chem.*, 1993, **58**, 6397–6405.
11. Ross, B.D. & True, N.S. Gas-phase ^{13}C NMR spectra and exchange kinetics of N,N-dimethylformamide. *J. Am. Chem. Soc.*, 1984, **106**, 2451–2452.
12. Ross, B.D., Wong, L.T. & True, N.S. Gas-phase NMR studies of N,N-dimethylamides. Inter- and intramolecular contributions to internal rotation activation energies. *J. Phys. Chem.*, 1985, **89**, 836–839.
13. Stewart, J.J.P., *MOPAC 6.0*, QCPE No. 455, 1989.
14. Stewart, W.E. & Siddall, T.H. Nuclear magnetic resonance studies of amides. *Chem. Rev.*, 1970, **70**, 517–551.
15. Wiberg, K.B. & Breneman, C.B. Resonance interactions in acyclic systems. 3. Formamide internal rotation revisited. Charge and energy redistribution along the C-N bond rotational pathway. *J. Am. Chem. Soc.*, 1992, **114**, 831–840.
16. Wiberg, K.B., Hadad, C.M., Rablen, P.R. & Cioslowski, J. Substituent effects. 4. Nature of substituent effects at carbonyl groups. *J. Am. Chem. Soc.*, 1992, **114**, 8644–8654.
17. Wiberg, K.B. & Rablen, P.R. Substituent effects. 5. Vinyl and ethynyl derivatives. An examination of the interaction of amino and hydroxy groups with C-C double and triple bonds. *J. Am. Chem. Soc.*, 1993, **115**, 9234–9242.
18. Wiberg, K.B., Rablen, P.R., Rush, D.J. & Keith, T.A. Amides. 3. Experimental and theoretical studies of the effect of the medium on the rotational barriers for N,N-dimethylformamide and N,N-dimethylacetamide. *J. Am. Chem. Soc.*, 1995, **117**, 4261–4270.
19. Wong, M.W. & Wiberg, K.B. Structure of acetamide: planar or nonplanar? *J. Phys. Chem.*, 1992, **96**, 668–671.

Table 1

The AM1 calculated heats of formation, $\Delta H_{f,298}^o$ (kcal/mol), the relative energies (kcal/mol), and the relative population of different conformers of the *N,N*-di(2-methylphenyl)-3',3'-dimethylbutyryl amide (1) at room temperature

Conformer	^t Bu ^a	$\Delta H_{f,298}^o$	$\delta\Delta H_{f,298}^o$ ^b	P(%) ^c
1a	–	–2.51	(0)	48
	+	–1.98	0.53	
	↑	–2.07	0.44	
1b	–	–2.00	(0)	20
	+	–1.67	0.33	
	↑	–1.19	0.81	
1c	–	–1.32	(0)	6
	+	–1.16	0.16	
	↑	–1.22	0.10	
1d	–	–1.18	0.97	26
	+	–0.62	1.53	
	↑	–2.15	(0)	

^a Position of the ^tBu group relative to the amide plane: + in front, – behind and ↑ in plane (*cis* to the oxygen atom); ^b relative energy to the most stable conformer with respect to the position of ^tBu group; ^c calculated relative population of different conformers at room temperature (298 K).

Table 2

The AM1 calculated heats of formation, $\Delta H_{f,298}^o$ (kcal/mol), and the relative energies, $\delta\Delta H_{f,298}^o$ (kcal/mol), for the points at the potential surface, corresponding to the conformational change 1b→1a

Angle ^a	Relative angle	$\Delta H_{f,298}^o$	$\delta\Delta H_{f,298}^o$ ^b
65.36 ^c	(0)	-2.00	(0)
	10	-1.62	0.38
	20	-1.15	0.85
	30	1.00	3.00
	40	0.68	2.68
	50	2.09	4.09
	60	3.67	5.67
	70	5.21	7.21
	80 ^d	6.17	8.17
	90	2.47	4.47
	100	1.26	3.26
	110	0.42	2.42
	120	-0.12	1.88
	130	-0.35	1.65
	140	-0.49	1.51
	150	-1.40	0.60
	160	-1.94	0.06
	170	-2.22	-0.22
	180	-2.40	-0.40
	185 ^e	-2.51	-0.51

^a Dihedral angle $\angle \text{C}(\text{O})\text{-N-C1}_{\text{tolyl}}\text{-C2}_{\text{tolyl}}$, where C2_{tolyl} has the methyl substituent; ^b calculated relative energy of the conformer; ^c conformer 1b; ^d transition state; ^e conformer 1a.

Table 3

The AM1 calculated heats of formation, $\Delta H_{f,298}^o$, of the molecule in the transition state and the respective rotational barriers, E_A (kcal/mol), for different conformational changes of *N,N*-di(2-methylphenyl)-3',3'-dimethylbutyrylamide (1)

Rotation	$\Delta H_{f,298}^o$	E_A
1a→1b	5.64	8.15
1a→1c	5.55	8.06
1b→1a	6.17	8.17
1b→1d	6.17	8.17
1c→1a	5.38	7.38
1c→1d	5.73	7.73

Table 4

The AM1 calculated heats of formation, $\Delta H_{f,298}^o$ (kcal/mol), the relative energies, $\delta\Delta H_{f,298}^o$ (kcal/mol), of the conformers of *N*-(2-methylphenyl)-*N*-(1-naphthyl)-3',3'-dimethylbutyrylamide (2), and their relative population at room temperature

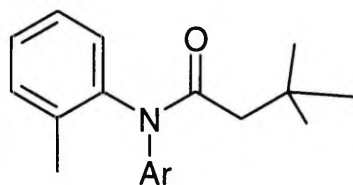
Conformer	<i>E-Z</i> ^a	T ^b	N ^c	$\Delta H_{f,298}^o$	$\delta\Delta H_{f,298}^o$ ^d	P(%) ^e
2a	<i>Z</i>	+	+	25.04	0.41	20
2b	<i>Z</i>	–	+	24.63	(0)	40
2c	<i>Z</i>	+	–	25.19	0.56	16
2d	<i>Z</i>	–	–	25.55	0.92	9
2e	<i>E</i>	+	+	25.69	1.05	7
2f	<i>E</i>	–	+	26.00	1.47	3
2g	<i>E</i>	+	–	26.02	1.49	3
2h	<i>E</i>	–	–	26.20	1.67	2

^a *E* or *Z* conformation considering the position of the naphthyl group with respect of the amide oxygen; ^b relative position of the tolyl group (+ means turned to the same side of the amide plane as the neopentyl group, – means that it is turned to the opposite side); ^c relative position of the naphthyl group (+ means turned to the same side of the amide plane as the neopentyl group, – means that it is turned to the opposite side); ^d relative energy to the most stable conformer (**2b**); ^e calculated relative population of different conformers at room temperature (298 K).

Table 5

The AM1 calculated activation barriers, E_A (kcal/mol), for different conformational transitions of *N*-(2-methylphenyl)-*N*-(1-naphthyl)-3',3'-dimethylbutyrylamide (2)

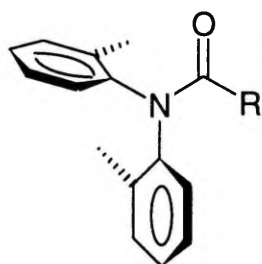
Rotation	E_A
2a → 2f	11.30
2a → 2g	8.72
2b → 2e	16.41
2b → 2f	11.60
2c → 2g	8.28
2c → 2f	8.60
2d → 2g	9.42
2d → 2h	7.17
2e → 2g	8.48



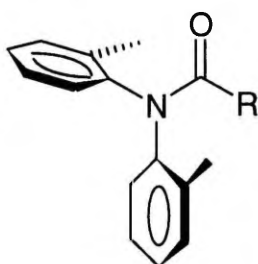
Ar = 2-Tolyl (1)

1-Naphthyl (2)

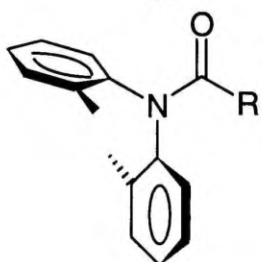
Scheme 1



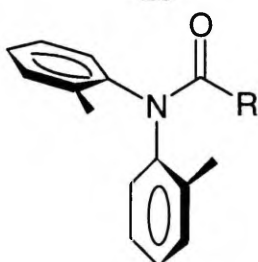
1a



1b

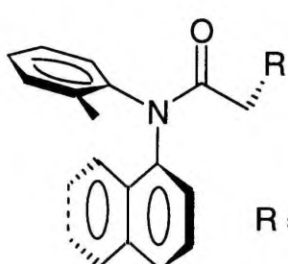


1c



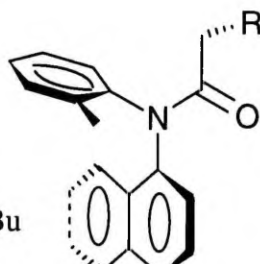
1d

Scheme 2



2b (*E*)

R = *t*Bu



2f (*Z*)

Scheme 3

V

Reaction of 1-Naphthyl Amine with Methyl Ketones: A Possible Route to
The One-Pot Syntheses of Substituted 1,2-Dihydrobenzo(*h*)quinolines,
J. Leis, A. Pihl, K. Pihlaja and M. Karelson,
ACH-Models in Chemistry, 135 (4), pp 573–581,
Copyright © 1998, Akademiai Kiado, Budapest.

Reaction of 1-naphthyl amine with methyl ketones: A possible route to the one-pot syntheses of substituted 1,2-dihydrobenzo(h)quinolines⁺

JAAN LEIS¹, AINO PIHL¹, KALEVI PIHLAJA^{2*} and MATI KARELSON¹

¹Department of Chemistry, University of Tartu, 2 Jakobi St., EE-2400, Tartu, Estonia

²Department of Chemistry, University of Turku, FIN-20014, Turku, Finland

Received March 31, 1998

The *p*-toluenesulfonic acid catalysed reaction between 1-naphthyl amine and several methyl ketones was studied. Under certain conditions this reaction can be used as a one-pot method for the syntheses of substituted 1,2-dihydroquinolines. The reaction mechanism and identification of compounds are discussed.

Introduction

Monohydrate of *p*-toluenesulfonic acid (*p*-TOS) catalyzed the reaction between α -naphthylamine and ethyl 4-acetylbutanoate. The main product was a substituted 1,2-dihydrobenzo(h)quinoline, quite unexpectedly. The same procedure without catalyst or in the presence of a catalytic amount of acetic acid has been effectively used for preparation of a variety of *N*-aryl iminoesters [1]. The reaction of primary amines with the compounds owing carbonyl function is widely used in the synthesis of imines. Therefore, it was reasonable to carry out a more detailed study to reveal the possible reasons of the above mentioned discrepancy. To that end, several methylalkyl ketones, including acetone which is known to give 1,2-dihydro-2,2,4-trimethylbenzo(h)quinoline (1) in the presence of catalysators [2], were reacted with 1-naphthylamine in the presence of *p*-TOS. The results of this study are described in the present paper. Furthermore, as some of the substituted benzoquinolines isolated during this study have not been published before, the short description of the structural confirmation and the full set of the spectral characteristics are presented.

Only for the comparison, the similar reaction between aniline and acetone was applied to the synthesis of 1,2-dihydro-2,2,4-trimethylquinoline, (6), which is an

⁺ Dedicated to Professor Gábor Bernáth on the occasion of his 65th birthday

* To whom correspondence should be addressed

important antioxidant [3-6] in chemical industry. Otherwise we have limited this study to the reaction between methyl ketones and 1-naphthyl amine which, due to the steric and electronic properties, possess a quite different reactivity compared to the substituted anilines, as also revealed by comparing the yields in the 1st and 7th entries of Table I.

Results and discussion

Five methyl ketones: propan-2-one (acetone), butan-2-one, 2-methylbutan-3-one, 2-methylpentan-4-one and ethyl-4-acetylbutanoate were reacted with 1-naphthylamine in the presence of a catalytic amount of *p*-TOS. After prolonged heating (reflux) at $\sim 110^\circ\text{C}$, the reaction mixture was concentrated and without any treatment fractionated by liquid chromatography in silica gel column. From the results presented in Table I it appeared that the rate of the amine conversion under the conditions applied is quite low due to the almost equilibrium reaction conditions (insufficient removal of the condensation product - water). However, the main attention was paid to the composition and the possible identification of the products formed in the reaction.

Table I

Summary of the conditions and the yields of the p-TOS catalysed reaction of methyl ketones with 1-naphthyl amine at $\sim 110^\circ\text{C}$. The yields based on the amine converted in the reaction are shown (in the parentheses the real yields of the syntheses are given)

Entry	$\text{CH}_3\text{C(O)R};$ R-	Molar ratio. of ketone to amine	Duration of the reaction, h	"Imine"	Products "Benzoquinoline"	
1	Methyl	2 : 1	6 + 5 ^a	$\sim 0\%$ (trace)	$\sim 100\%$ (26.9%)	(1)
2		3 : 1	20	$\sim 0\%$ (trace)	$\sim 100\%$ (27.0%)	(1)
3	Ethyl	3 : 1	20 ^f	$\sim 0\%$ (trace)	$\sim 100\%$ (10.1%)	(2a, 2b)
4	2-methylethyl	3 : 1	20 ^f	$\sim 80\%$ ^c (31%)	$\sim 0\%$ (trace)	(3) ^d
5	2-methylpropyl	2 : 1	6.5 + 5	$\sim 92\%$ (53%)	$\sim 0\%$ (trace)	(4)
6	Ethyl-4-butanoate	$\sim 1 : 1$	3.5 ^b	$\sim 0\%$ (trace)	$\sim 100\%$ (34.6%)	(5)
7 ^e	Methyl	2 : 1	120	-	(3.2%)	(6)

^aReflux + the azeotropic removal of water

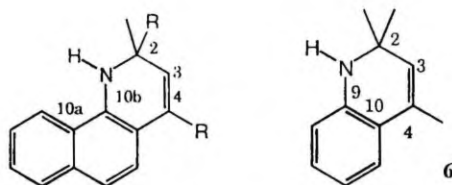
^bHeating at 140°C with the azeotropic removal of water

^c $\sim 20\%$ was the probably polymerized by-product (insoluble in the hot hexane)

^dOnly observed on the TLC plate

^eReacted with aniline

^fIn the cases of 2 and 3 the simple reflux was used instead of azeotropic distillation



Scheme 1. R = CH₃ (1), C₂H₅ (2), CH(CH₃)₂ (3), CH₂CH(CH₃)₂ (4), (CH₂)₃COOC₂H₅ (5)

As a result, it was found that in most cases, except when the sterically more hindered ketones were used (entries 4 and 5 in Table I), the respective substituted 1,2-dihydrobenzoquinoline was almost the only product of the amine conversion. This is based on the fact that the unconverted and/or backproduced amine was almost completely separated by the silica gel column. In the case of 2-methylbutan-3-one and 2-methylpentan-4-one the main products were the respective 1-naphthyl imines, which stability may be explained by the bulkier alkyl groups at the C–N double bond avoiding the further aldol type condensation. Indeed, in both reactions the trace of the cyclized condensation product was observed by the thin layer chromatography (TLC). In the case of butan-3-one the mixture of two tautomers, 1,2-dihydro-2-methyl-2,4-diethylbenzo(*h*)quinoline (2a) and 1,2,3,4-tetrahydro-2-methyl-2-ethyl-4-ethenylbenzo(*h*)quinoline (2b) with the ratio 5/2, was produced with a 10% yield. Identification and the possible mechanisms of formation of the cyclic condensation products (Scheme 1) is discussed in the following sections.

Identification of substituted 1,2-dihydroquinolines

Infrared spectra of all isolated 1,2-dihydrobenzo(*h*)quinolines (1, 2 and 5) contained a single slightly broadened peak at about 3420 cm⁻¹, that is characteristic of the secondary arylamines. The exact molecular weights were established by high resolution mass spectrometry (HR MS). In the electron ionization (EI) at 70 eV, the main fragment was the ion [M–C₃H₆COOC₂H₅]⁺ for compound 5, [M–C₂H₅]⁺ for 2 and that for 1 and 6 the ion [M–CH₃]⁺. The exact constitutions of the molecules were established by ¹H- and ¹³C-NMR spectra. The ¹³C chemical shifts for 1 and 5 are presented in Fig. 1 and those for 2 and 6, and the ¹H data in *Experimental*. The sequence of the carbon atoms in the molecules was determined by COSY technique, the locations of the substituents in the benzoquinoline ring by NOESY, and that of the double bond by the NOE differential measurements.

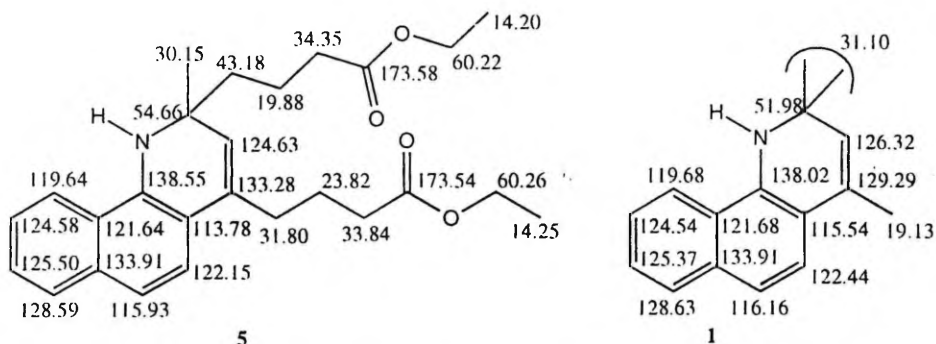
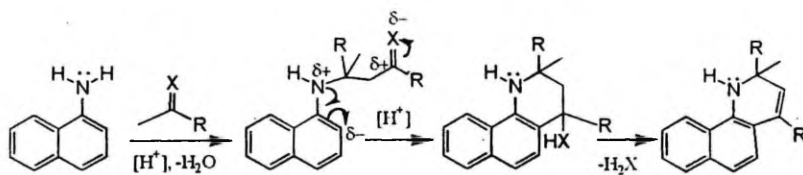


Fig. 1. Carbon-13 chemical shifts, δ (ppm), of the compounds 1 and 5 measured at 125.65 MHz in CDCl₃

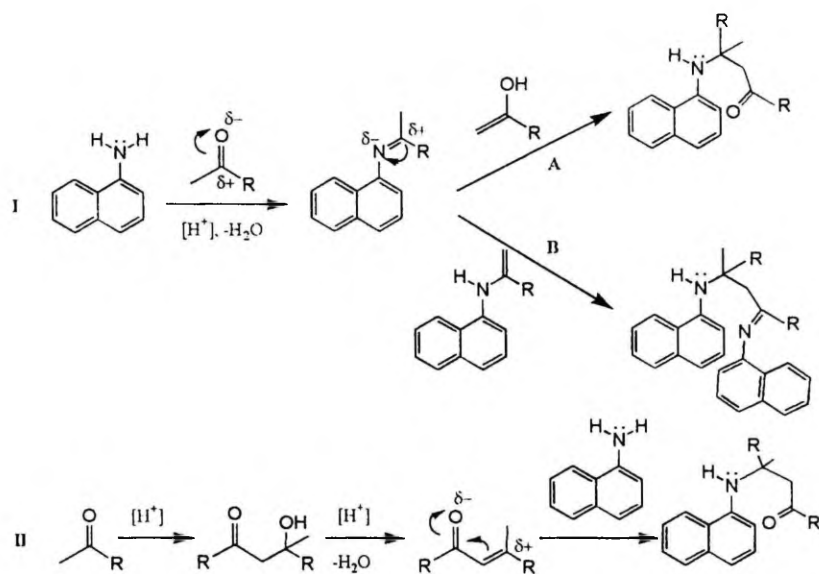
Reaction mechanism

Evidently, the reaction occurs at least in two steps: the formation of an intermediate product, which due to the intramolecular migration of the partial charges, is cyclized by an electrophilic attack to the aryl ring as shown in Scheme 2. Such a ring closure followed by a removal of the water molecule is well-known as a part of the so-called Scaup's reaction [8] and its Doebner von Miller modifications [9]. It is of more interest to find a reasonable mechanism for the formation of the noncyclic intermediate product.

Scheme 3 lists three options deserving more attention: i) The second ketone molecule attacks as a nucleophile to the imine double bond (IA), ii) two imine molecules condense with each other (IB) or iii) naphthylamine binds to the unsaturated ketone formed after condensation of two ketone molecules (II), which is typical for the Doebner von Miller synthesis [9]. To solve the mechanism, all chromatographically separated fractions of the reaction mixture obtained from the synthesis of 1 were analysed by MS. It has to be mentioned that only few weak spots, besides those of the naphthyl amine and the product (1), were observed on a TLC plate.



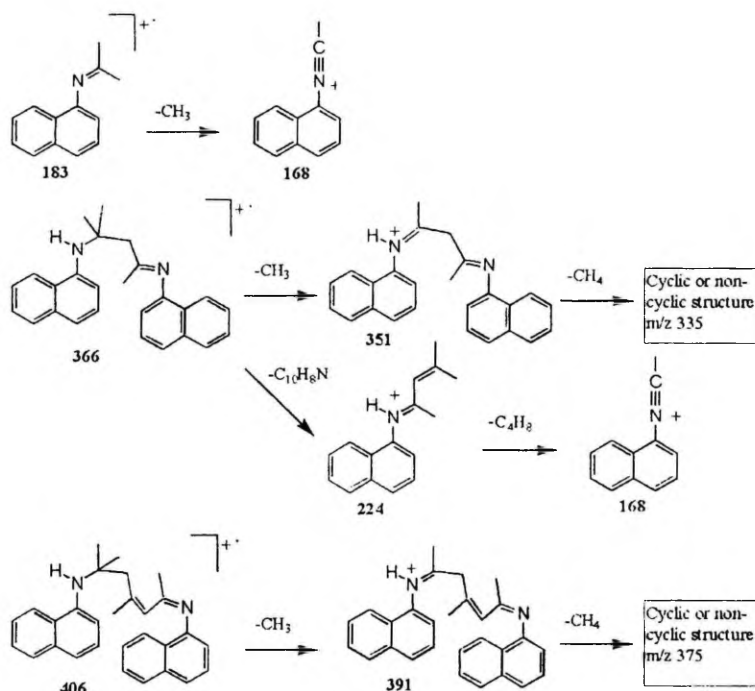
Scheme 2. X=O or C₁₀H₇N



Scheme 3

Nevertheless, the mass-spectra showed clearly the presence of traces of *N*-isopropyl-1-naphthylimine (M^+ , 183) and a couple of its condensation products (M^+ , 366 and 406). The possible fragmentations are described in Scheme 4.

Furthermore, no condensation product of the ketone molecules, that could support the mechanisms **IA** or **II** (see Scheme 3), was revealed by the mass-spectra. From the latter results one may conclude, that in the reactions discussed, the main effect of *p*-TOS is a good catalytic behavior upon the aldol condensation between the imine molecules rather than ketone molecules.



Scheme 4

Conclusion

The results of this study confirm that the derivate of 1,2-substituted dihydrobenzo(*h*)quinoline as the condensation product of two molecules of 1-naphthyl imines is not accidental and should always be considered when the acidic conditions at the moderate temperature are applied in the synthesis of the latter compounds. Furthermore, the *p*-TOS catalysed reaction discussed in this paper, in the case of the efficient removal of water, could be successfully used in moderate yields for the synthesis of several new 1,2-dihydrobenzo(*h*)quinolines which, for example, are interesting objects from the stereochemical point of view.

Experimental

General

Commercially available reactants were used without purification. Melting points were measured by the Electrothermal digital melting point apparatus, and are uncorrected. The infrared (IR) spectra were recorded by GALAXY Series FT-IR 6030 (Mattson Instruments). The electron ionization mass-spectra were recorded on a VG 7070E (VG Analytical, Manchester, UK) spectrometer with direct inlet and the electron impact energy 70 eV. The accurate mass measurements were made by VG ZabSpec spectrometer using peak matching technique (PFK as a reference compound) at a resolution of 8000-9000. ^1H - and ^{13}C -NMR spectra were recorded on a JEOL LAMBDA 400 and ALPHA 500 spectrometers in CDCl_3 containing tetramethylsilane (TMS) as the internal standard. Elemental analysis of **5** was performed at the commercial microanalytical laboratory E. Pascher, Remagen, Germany.

Synthesis of 1,2-dihydro-2-methyl-2,4-di-(ethyl-4-butanoate)benzo(h)quinoline, (5), described as a general procedure

Ethyl 4-acetylbutanoate (31.2 mmol) and 1-naphthylamine (37.7 mmol) were mixed in 20 ml of toluene at room temperature. After the temperature of the magnetically stirred reaction mixture was increased up to 100°C , a few crystals of *p*-TOS were added. Thereupon a slow distillation was carried out during 3.5 h at about 140°C and the stirred mixture was left overnight at room temperature. Then, the reaction mixture was concentrated at reduced pressure and the residual dark oil was fractionated by dichloromethane in the silica gel column. The fraction with $R_f = 0.15$ (CH_2Cl_2) was collected and gave 2.3 g (5.4 mmol) of compound **5** with a 34.6% yield based on the ketoester. The product was recrystallised from methanol (water) as yellow crystals (m.p. $80\text{--}81.5^\circ\text{C}$). Anal. Calculated for $\text{C}_{26}\text{H}_{33}\text{NO}_4$: C 73.73%, H 7.85% and N 3.31%. Found: C 73.7%, H 7.9% and N 3.6%. IR (cm^{-1}) 3416 (N-H), 3055, 2976, 1728 (C=O), 1620, 1520, 1371, 1188, 1030, 802, 742; MS (*EI*, 70eV, m/z) 423 (M^+ , $[\text{C}_{26}\text{H}_{33}\text{NO}_4]^+$), 408 ($[\text{M}-\text{CH}_3]^+$), 378 ($[\text{M}-\text{OC}_2\text{H}_5]^+$), 308 ($[\text{M}-\text{C}_3\text{H}_6\text{COOC}_2\text{H}_5]^+$, 100%), 220, 207; ^1H -NMR (500 MHz, CDCl_3 , TMS, δ (ppm), J (Hz)) 1.21 (t, 3H, CH_3 , J 7.13), 1.26 (t, 3H, CH_3' , J 7.13), 1.33 (s, 3H, CH_3), 1.56–1.64 (m, 2H, $\gamma\text{-CH}_2$), 1.67–1.75 (m, 1H, $\beta\text{-CH}_2$), 1.76–1.85 (m, 1H, $\beta\text{-CH}_2$), 1.92 (~qn, 2H, $\beta'\text{-CH}_2$, J 7.52), 2.29 (t, 2H, $\alpha\text{-CH}_2$, J 7.27), 2.39 (t, 2H, $\alpha'\text{-CH}_2$, J 7.37), 2.51 (br t, 2H, $\gamma'\text{-CH}_2$, J 7.60), 4.09 (q, 2H, OCH_2 , J 7.14), 4.15 (q, 2H, OCH_2' , J 7.12), 4.39 (br s, 1H, NH), 5.24

(s, 1H, H(3)), 7.11 (d, 1H, H(6), J 8.50), 7.31 (d, 1H, H(5), J 8.55), 7.35–7.41 (m, 2H, H(8) & H(9)), 7.67–7.74 (m, 2H, H(7) & H(10)); (Found: M^+ , 423.241 10. Calc. for $C_{26}H_{33}NO_4$: M , 423.240 96).

1,2-dihydro-2,2,4-trimethylbenzo(h)quinoline, (1)

Pale yellow crystals, m.p. 50.3–52.3 °C (Ref. [2]: m.p. 46.8–47.2 °C); IR (cm^{-1}) 3422 (N–H), 2967, 1618, 1518, 1398, 1258 & 1163 ($C(CH_3)_2$), 812, 739; MS (EI , 70eV, m/z) 223 (M^+ , $C_{16}H_{17}N^+$), 208 ($[M-CH_3]^+$, 100%), 165, 104; 1H -NMR (500 MHz, $CDCl_3$, TMS, δ (ppm), J (Hz)) 1.36 (s, 6H, $2CH_3$), 2.09 (d, 3H, CH_3 , J 1.44), 4.44 (br s, 1H, NH), 5.34 (br q, 1H, H(3), J 1.39), 7.15 (br d, 1H, H(6), J 8.44), 7.31 (d, 1H, H(5), J 8.44), 7.35–7.40 (m, 2H, H(8) & H(9)), 7.68–7.73 (m, 2H, H(7) & H(10)); (Found: M^+ , 223.136 12. Calc. for $C_{16}H_{17}N$: M , 223.136 10).

1,2-dihydro-2-methyl-2,4-diethylbenzo(h)quinoline, (2a)

IR (cm^{-1}) 3424 (N–H), 3057, 2965, 1470, 1171, 801, 737, 569; MS (EI , 70eV, m/z) 251 (M^+ , $[C_{18}H_{21}N]^+$), 236 ($[M-CH_3]^+$), 222 ($[M-C_2H_5]^+$, 100%), 207 ($[M-C_2H_5-CH_3]^+$); 1H -NMR (400 MHz, $CDCl_3$, TMS, δ (ppm), J (Hz)) 0.94 (t, 3H, CH_2CH_3 , J 7.4), 1.21 (t, 3H, CH_2CH_3 , J 7.4), 1.31 (s, 3H, CH_3), 1.58 (m, 2H, CH_2), 2.49 (br q, 2H, CH_2 , J 7.3), 4.36 (br s, 1H, NH), 5.23 (br s, 1H, H(3)), 7.12 (d, 1H, H(6), J 8.4), 7.34 (d, 1H, H(5), J 8.5), 7.35 (m, 2H, H(8) & H(9)), 7.68 (m, 1H, H(10)), 7.70 (m, 1H, H(7)); ^{13}C -NMR (100.4 MHz, $CDCl_3$, δ (ppm)) 8.35 (CH_3), 13.16 (CH_3 '), 25.13 (CH_2), 29.54 (CH_3), 36.40 (CH_2 '), 54.82 (C(2)), 114.57 (C(4a)), 115.74 (C(6)), 119.62 (C(10)), 121.66 (C(6a)), 122.14 (C(5)), 123.20 (C(3)), 124.44 (C(9)), 125.32 (C(8)), 128.61 (C(7)), 133.87 (C(10a)), 135.52 (C(4)), 138.61 (C(10b)); (Found: M^+ , 251.167 40. Calc. for $C_{16}H_{17}N$: M , 251.167 65).

1,2-dihydro-2-methyl-2-ethyl-4-ethenylbenzo(h)quinoline, (2b)

1H -NMR (400 MHz, $CDCl_3$, TMS, δ (ppm), J (Hz)) 0.95 (t, 3H, CH_2CH_3 , J 7.4), 1.22 (s, 3H, CH_3), 1.57 (m, 2H, CH_2CH_3), 1.85 (br d, 3H, $=CCH_3$, J 7.0), 2.5 (m, 2H, C(3) H_2), 4.36 (br s, NH), 6.16 (br q, 1H, $=CH$, J 7.0), 7.16 (d, 1H, H(6), J 9.1), 7.37 (m, 2H, H(8) & H(9)), 7.60 (d, 1H, H(5), J 8.8), 7.72 (m, 2H, H(7) & H(10)); ^{13}C -NMR (100.4 MHz, $CDCl_3$, δ (ppm)) 8.24 (CH_2CH_3), 13.44 ($=CCH_3$), 25.72 (CH_3), 33.11 (CH_2CH_3), 35.06 (C(3)), 52.42 (C(2)), 115.19

(C(4a)), 116.47 (C(3)), 116.85 (C(6)), 119.82 (C(10)), 122.60 (C(5)), 123.27 (C(6a)), 124.81 (C(9)), 125.28 (C(8)), 128.52 (C(7)), 131.57 (C(4)), 133.63 (C(10a)), 136.95 (C(10b)).

1,2-dihydro-2,2,4-trimethylquinoline, (6)

Oil (Ref. [7]: m.p. 25–26 °C); IR (cm⁻¹) 3371 (N-H), 3027, 2967, 2857, 1651, 1605, 1480, 1381, 1316, 1259 & 1163 (C(CH₃)₂), 1040, 745; MS (EI, 70eV, *m/z*) 173 (M⁺, [C₁₂H₁₅N]⁺), 158 ([M-CH₃]⁺, 100%), 115 ([C₉H₇]⁺), 77 ([C₆H₅]⁺); ¹H-NMR (400 MHz, CDCl₃, TMS, δ (ppm), *J* (Hz)) 1.27 (s, 6H, 2CH₃), 1.98 (d, 3H, CH₃, *J* 1.5), 3.67 (br s, 1H, NH), 5.30 (q, 1H, H(3), *J* 1.4), 6.43 (dd, 1H, H(8), *J*³ 7.9, *J*⁴ 1.2), 6.63 (dt, 1H, H(6), *J*³ 7.5, *J*⁴ 1.2), 6.98 (dt, 1H, H(7), *J*³ 7.6, *J*⁴ 1.5), 7.05 (dd, 1H, H(5), *J*³ 7.6, *J*⁴ 1.5); ¹³C-NMR (100 MHz, CDCl₃, δ (ppm)) 18.57 (CH₃), 31.02 (2CH₃), 51.78 (C(2)), 112.89 (C(8)), 117.12 (C(10)), 121.52 (C(10b)), 123.60 (C(5)), 128.33 & 128.34 (C(7) & C(9)), 128.53 (C(6)), 143.26 (C(10a)); (Found: M⁺, 173.120 50. Calc. for C₁₂H₁₅N: M, 173.120 45).

*

We thank dr. Karel Klika (University of Turku) for recording the NMR spectra and for helpful discussions and Ms Kirsti Wiinamäki for the MS measurements.

References

- [1] LEIS, J.: Unpublished observations
- [2] VON SCHEURER, H., ZSINDELY, J., SCHMID, H.: *Helv. Chim. Acta*, **56**, 478 (1973)
- [3] KONING, A.J., VAN DER MERVE, G.: *Fett / Lipid*, **98**, 14 (1996)
- [4] BECKER, R., KNORR, A.: *Tribol. Schmierungstechn.*, **42**, 272 (1995)
- [5] BECKER, R., KNORR, A.: *Lubr. Sci.*, **8**, 95 (1996)
- [6] ISHIAKU, U.S., POH, B. T., MOHD ISHAK, Z. A., NG, D.: *Polym. Int.*, **39**, 67 (1996)
- [7] REDDELIEN, G., THURM, A.: *Ber.*, **65**, 1511 (1932)
- [8] MANSKE, R.H.F., KULKA, M.: *Organic Reactions*, **7**, 59 (1953)
- [9] MILLS, W.H., HARRIS, J.E.G., LAMBOURNE, H.: *J. Chem. Soc.*, **119**, 1294 (1921)

J. Leis, K. D. Klika, K. Pihlaja and M. Karelson.
High Inversion Barrier in *N*-Acylated 1,2-Dihydrobenzo(*h*)quinolines,
Tetrahedron, 000, 000–000, 1998 (submitted).

Dynamic Processes in *N*-Acylated 1,2-dihydro-2,2,4-trimethylbenzo(*h*)quinoline: A Comparative Study by NMR Spectroscopy and Quantum Mechanics

Jaan Leis^a, Karel D. Klika^b, Kalevi Pihlaja^b and Mati Karelson^{a*}

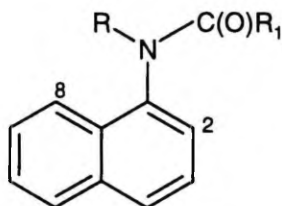
^aDepartment of Chemistry, University of Tartu, 2 Jakobi St., Tartu, EE2400, Estonia

^bDepartment of Chemistry, University of Turku, FIN-20014, Turku, Finland

Abstract: The results of the conformational studies on several *N*-acyl derivatives of 1,2-dihydro-2,2,4-trimethylbenzo(*h*)quinoline are reported. A comparative study by NMR spectroscopy and semiempirical quantum chemical modelling with the AM1 SCF method revealed that the nitrogen atom is pyramidal with a substantial out-of-plane torsion of the acyl group, and the molecules adopt the *E* conformation in the ground state. Also, the ¹H NMR signals revealed the inter-conversion of a pair of enantiomers for all compounds studied, with $\Delta G^\ddagger = 13.4\text{--}17.7 \text{ kcal mol}^{-1}$. A good correlation exists between the above ΔG^\ddagger values and the energy barriers, E_A , predicted by the semiempirical AM1 SCF model.

INTRODUCTION

Semiempirical quantum chemical calculations have shown the racemisation of *N*-1-naphthylamides [1, 2] (Scheme 1) to occur *via* a planar transition state with passage of the acyl group preferred over the position (2) of the naphthyl ring rather than the position (8) [2].

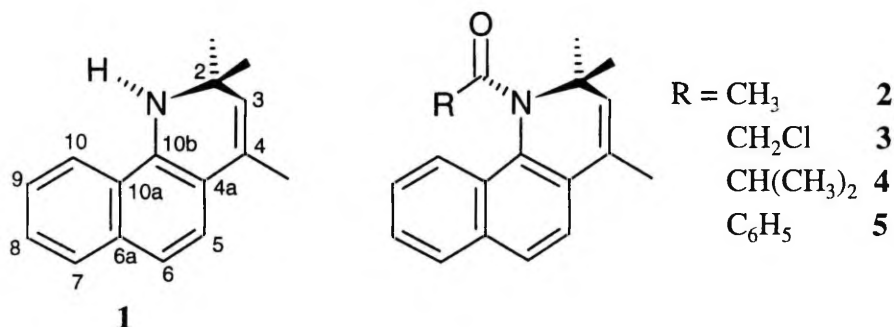


Scheme 1

Passage over the position (8) cause a considerable out-of-plane deformation of the amide group and therefore, it would be energetically less favoured. Conse-

quently, the factors reducing the sp^2 character of the amide nitrogen destabilise the ground state of the molecule and both directions of rotation along the N-aryl bond should become competitive. The rotation of the acyl group past over the position (8) of naphthylamides has been modelled with *N*-tosylbenzo(*h*)quinolone derivatives as models [3, 4]. Due to the steric restrictions, the latter are characterised by high inversion barriers and hence by unusually slow inversion rates.

In this paper, the results of stereochemical studies on several *N*-acylated 1,2-dihydrobenzoquinolines (cf. Scheme 2) are reported. The substituents at the carbonyl carbon were chosen to find out the possible effects of the size, electronegativity and π - π conjugation on the inversion barriers.



Scheme 2

RESULTS AND DISCUSSION

It is known that the *N,N*-unsymmetrically-substituted amides may adopt both the *cis*- and *trans* conformation due to the hindered rotation around the N-C partial double bond [5]. However, at room temperature the proton and carbon-13 NMR spectra of each of the title compounds displayed only a single set of signals, most probably due to the fast rotation around the N-C(O) bond. This is supported by the semiempirical AM1 SCF calculations, which predict low rotational barriers. The calculated E_A values were 3.3, 4.6, 4.7 and 4.5 kcal mol⁻¹ for **2**–**5**, respectively, which after empirical correction [6] correspond to the ΔG^\ddagger values of 9.8, 11.9, 12.0 and 11.7 kcal mol⁻¹, respectively. These calculations also predict that the nitrogen atom is highly pyramidalised in ground state of the molecules with the significantly longer N-C(O) bonds (*ca.* 1.41 Å) than the usual C-N partial double bond (~ 1.35 Å [1]) in amides. The AM1 calculated torsion angles defined by the three C-N bonds are 154.2°, 158.3°, 162.5° and 163.4° in **2**–**5**, respectively.

The semiempirical AM1 calculations also predict the *E* conformer of compounds **2–5** (in analogy with the *N*-1-naphthylamides [1] the oxygen is *trans* to the aromatic ring) to be 2–4 kcal mol⁻¹ more stable than the *Z* conformer. Thus, even at slow exchange rates, only a single set of signals would be observed in the NMR spectra due to the predominance of the *E* conformer. However, solvent effects may substantially alter the conformer populations as shown for the tertiary *N*-1-naphthylamides [7].

The quantumchemically predicted preference for the *E* conformer is supported by the measured NOE enhancements presented in Table 1 which indicate the protons of the acyl group to be closer to the hydrogen at the *peri* position, H(10), than to the hydrogens of the geminal methyl groups. Several factors may affect the conformational preference in acylated benzo(*h*)quinolines, including (1) the less effective size of oxygen as compared to the alkyl groups, (2) the weak intramolecular O...H₃C interaction and (3) the bipolar repulsion between the carbonyl group and the π -electron system of the aromatic ring. None of these effects appears to talk against predominance of the *E* conformer.

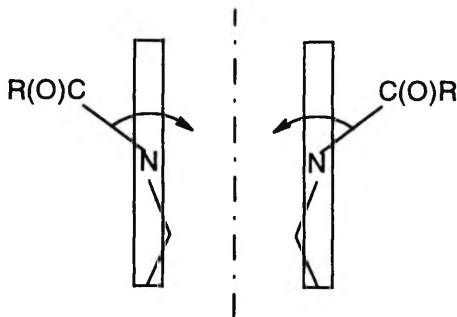
Table 1. The NOE enhancements for compounds **2–5**, expressed as a percentage of the original signals of the denoted protons upon irradiation of the protons of the geminal methyls and acyl groups. H(3) and H(10) denote the hydrogen atoms at the respective positions of the benzo(*h*)quinoline ring (Scheme 2) and (+) and (–) indicate the up- and downfield signals, respectively.

Compound	Observed protons	Irradiated protons				
		CH ₃ (–)	CH ₃ (+)	C(O)CH ₃ C(O)CH	ClCH(+) CHCH ₃ (+)	ClCH(–) CHCH ₃ (–)
2^a	H(10)	1.4	1.5	1.7	–	–
	H(3)	8.5	4.9	0	–	–
	CH ₃ (+)	–58.2	–100	0	–	–
	CH ₃ (–)	–100	–55.7	0	–	–
3^b	H(10)	0.5	2.0	–	0	7.6
	H(3)	7.7	2.0	–	0	0
	CH ₃ (+)	0	–100	–	0	0
	CH ₃ (–)	–100	0	–	0	0
4^c	H(10)	0.8	1.4	4.7	0.9	2.0
	H(3)	7.9	4.0	0	0.3	0
	CH ₃ (+)	–35.1	–100	0	0	0
	CH ₃ (–)	–100	–31.2	0	0	0
5^d	H(10)	0.1	0.8	–	–	–
	H(3)	4.0	1.1	–	–	–
	CH ₃ (+)	–3.4	–100	–	–	–
	CH ₃ (–)	–100	–2.1	–	–	–

^a NOE experiments performed at 5.5°C; ^b at –20°C; ^c at 25°C and ^d at –60°C.

Inversion barriers estimated by the dynamic NMR spectroscopy.

At room temperature, a pair of slightly broadened signals for the geminal methyl groups was observed for the acylated benzo(*h*)quinoline derivatives, with the exception of the benzoyl derivative. This implies the existence of a nonplanar molecule (Scheme 3). The flip of the acyl group from one side of the benzoquinoline ring to the other (called inversion below) should lead from one enantiomer to the other. The dynamic exchange process is evident from the temperature dependent NMR signals of the geminal methyl groups [8].



Scheme 3

At the coalescence temperature, the barrier to inversion (Table 2) was calculated using equation (1a) for an uncoupled two-site system or equation (1b) when a coupling was present [8].

$$\Delta G^\ddagger = 4.575 \cdot 10^{-3} T_c [9.972 + \log (T_c / \delta\nu)] \quad (1a)$$

$$\Delta G^\ddagger = 4.575 \cdot 10^{-3} T_c [9.972 + \log (T_c / \sqrt{\delta\nu^2 + 6J_{AB}^2})] \quad (1b)$$

where T_c is the coalescence temperature in K, $\delta\nu$ [Hz] is the difference between resonance frequencies of the A and B sites under the conditions of slow exchange, and J_{AB} is the coupling constant in Hz.

In compound 3, there are two prochiral centres: C(2) and the chloromethyl group. Therefore, two coalescences were observed as expected: that of the methyl groups at C(2) and that of the hydrogens of the chloromethyl group (Fig. 1). In the *N*-isobutyryl substituted compound, 4, also two coalescences were observed corresponding to the geminal methyl signals and methyl signals of the isopropyl group (Table 2).

Table 2. The activation energies (ΔG^\ddagger) of nitrogen inversion for the compounds **2–5**, calculated at the coalescence temperature (T_c). The difference of the resonance frequencies ($\delta\nu$) of the geminal methyl groups, and the frequency of NMR is indicated.

Compound d	$\delta\nu$ (Hz)	T_c (K)	ν_{NMR} (Hz)	solvent	ΔG^\ddagger (kcal mol ⁻¹)
2	379 (303 K)	342.0	400	TCE ^a	15.51
3	368 (298 K)	363.0	400	TCE	16.56
	84 ^b (298 K) (J_{HH} 13.8 Hz)	342.4	400	TCE	16.53
4	337 (298 K)	383.5	400	TCE	17.59
	65 ^c (298 K)	360.8	400	TCE	17.69
5	306 (213 K)	294.0	400	CDCl ₃	13.39

^a Tetrachloroethane; ^b Separation of hydrogens of the chloromethyl group; ^c Separation of methyls of the isopropyl group.

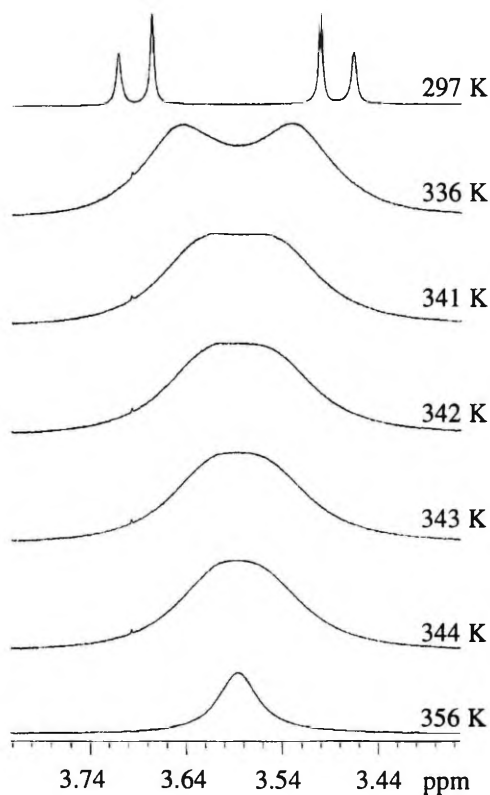


Figure 1. A selected part of the dynamic NMR spectra of compound **3** showing the coalescence of the AB-quartet of the methylene protons at 342 K.

Potential energy surface (PES) of inversion.

The semiempirical AM1 SCF method [9] was used to model the potential energy surface of the inversion. The passage of the carbonyl group over the *peri* position, *i.e.*, C(10), was modelled by varying the torsion angle C(O)-N-C(10a)-C(6a) in steps of 5 or 10 degrees and in smaller steps (0.5 or 1.0 degrees) around the transition state. The final transition state geometry of inverting molecules was confirmed by the single point calculations at the fixed reaction coordinate. For comparison, the inversion dynamics in *N*-*para*-tosylbenzo(*h*)quinolone (**6**) was also investigated. The AM1 SCF calculated heats of formation for ground and transition states of the compounds **1–6** are given in Table 3.

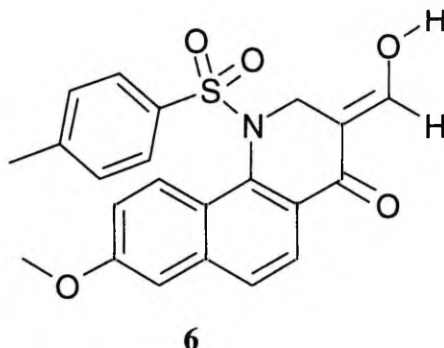


Table 3. The AM1 SCF calculated heats of formation for the *E* (E_{GS1}) and *Z* conformers (E_{GS2}), the transition state of inversion (E_{TS}) and the energy barriers for inversion ($E_{A(INV)}$) and rotation ($E_{A(Z-E)}$) along the N-C(O) bond.

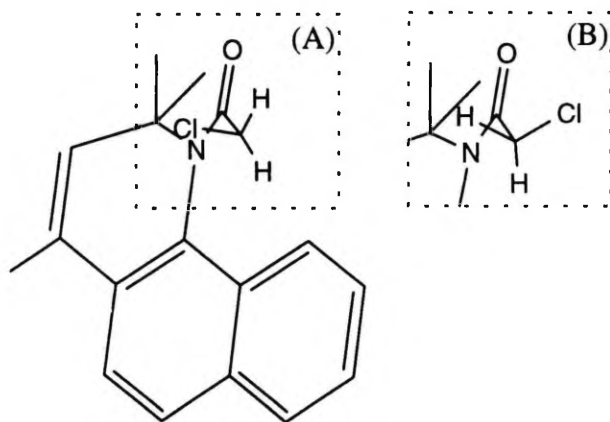
Compound	E_{GS1}^a (kcal mol ⁻¹)	E_{GS2}^b (kcal mol ⁻¹)	E_{TS}^c (kcal mol ⁻¹)	$E_{A(INV)}^d$ (kcal mol ⁻¹)	$E_{A(Z-E)}^e$ (kcal mol ⁻¹)
1		49.15	49.35	0.2	–
2	25.80	28.96	34.9	9.1	3.3
3	20.53	24.95	30.8	10.3	4.6
4	16.45	20.78	28.6	12.2	4.7
5	62.80	64.13	69.9	7.1	4.5
6	–83.55	–80.29	–70.9	12.6	–

^a Corresponds to the *E* conformation in the amides, **2–6**; ^b Corresponds to the *Z* conformation in the amides, **2–6**; ^c Corresponds to the maximum point on the potential curve for inversion; ^d The inversion barrier in respective compounds; ^e The rotation barrier for the *Z-E* interconversion.

Evidently, the nitrogen atom in **1** undergoes a rapid inversion with a very small energy barrier ($E_{A(AM1)} = 0.2$ kcal/mol). Also, the benzo(*h*)quinoline ring in **1** has almost planar geometry in the transition state, with a symmetric potential

curve as expected for classical nitrogen inversion. However, acylation of the nitrogen substantially increases the inversion barrier, as shown in Table 3.

For the *E* conformer of compound **3**, rotation around the chloromethyl-C(O) bond produced two different energy minima on PES. The rotamers are depicted in Scheme 4.



Scheme 4

Therefore, the grid search for the transition state of inversion was carried out for both the (A) and (B) rotamers. It was found that the calculated activation energy was higher for the more stable rotamer. Since the AM1 SCF calculated barrier for the $3E\text{-(A)} \rightarrow 3E\text{-(B)}$ interconversion was rather low, i.e., $2.1 \text{ kcal mol}^{-1}$, it was presumed that the inversion is accompanied by the simultaneous rotation of chloromethyl group. The full PES of isopropyl derivative (**4**) is even more complicated due to the conformationally flexible acyl group. The precision of the semiempirically calculated rotational barriers for the large and flexible molecules is rather sensitive to the choice of the initial geometry. To establish the most probable geometry of **4** in the ground state we used the experimentally determined NOE ratios (for the method see in ref. [10] and [11]). The NOE enhancements (η) of the NMR proton signals of the isopropyl group on irradiation of the H(10) proton of the benzo(*h*)quinoline ring are presented in Fig. 2.

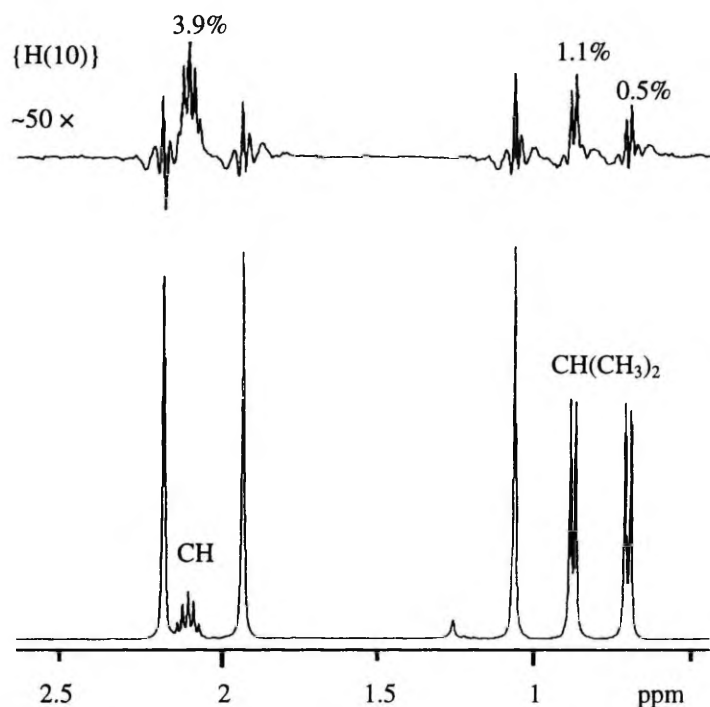
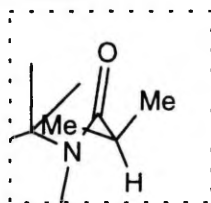


Figure 2. Aliphatic region of the 400 MHz NOE difference spectrum (above), vertically amplified *ca.* 50 times with respect to the reference spectrum (below) of compound **4** obtained upon irradiation of H(10).

The results of the NOE analysis were in accordance with the conformation predicted by the AM1 SCF calculations:



It is wellknown that the AM1 method significantly underestimates the intramolecular conformational transition barriers in the amides [2, 6, 9]. However, for certain dynamic processes, a satisfactory correlation between the calculated and experimentally obtained transition barriers have been obtained. In particular, a good linear relationship has been found for the amide bond rotation barriers in amides and their thioderivatives [6].

In this work, a good correlation between the computed inversion barriers, E_A , and the experimentally determined activation free energies, ΔG^\ddagger , was obtained (Fig. 3):

$$\Delta G_{\text{exp}}^\ddagger = 0.87E_A (\text{AM1}) + 7.38 \quad (\text{kcal mol}^{-1}) \quad (2)$$

$$R^2 = 0.985; s = 0.28$$

From equation (2), the compound **1** should have the free energy of activation $7.5 \text{ kcal mol}^{-1}$, which is close to the experimental barriers for nitrogen inversion in ammonia and simple alkyl-substituted amines [12] ($\sim 6 \text{ kcal mol}^{-1}$). Our results also display the increase of the inversion barriers with the increasing effective size of the acyl substituent ($\text{Ph} < \text{Me} < \text{CH}_2\text{Cl} < {}^i\text{Pr}$). A substantially smaller barrier for **5** ($R = \text{Ph}$) is unexpected from the simple consideration of steric interactions. However, it can be related to the destabilising repulsion of aromatic π -electron systems of aromatic rings in the ground state conformation. Alternatively, the effective size of carbonyl group in **5**, interacting with the other parts of molecule, could be reduced in the transition state due to the possible electron delocalisation between the phenyl and $\text{C}=\text{O}$ groups.

Inv. barriers (kcal mol^{-1})	2	3	4	5	6^a
$E_a (\text{AM1})$	9.1	10.3	12.3	7.1	12.6
$\Delta G^\ddagger (\text{EXP})$	15.5	16.6	17.7	13.4	18.5

^a the experimental ΔG^\ddagger is calculated from the kinetic data reported in ref. [4]

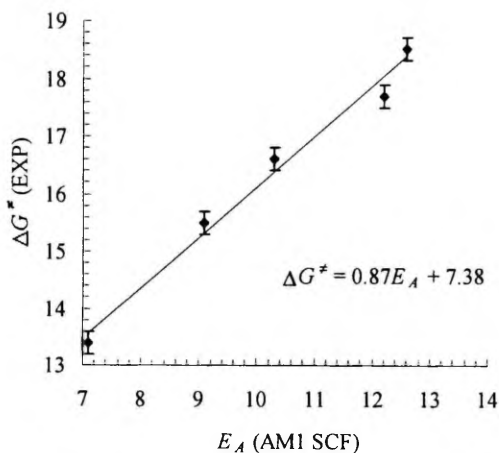


Figure 3. Graphical plot of the experimental $\Delta G_{\text{exp}}^\ddagger$ vs. computed E_a inversion barriers for the compounds **2–6**.

Induction effects raise the rotational barrier about the amide N-C(O) bond [14]. Consequently, the inversion barrier in **3** should be increased due to the concerted rotation about the N-C(O) bond. However, this effect, while important in the gas phase, is usually rather small in liquids [14]. Therefore, the higher inversion barrier in *N*-chloroacetyl derivative (**3**) as compared to the *N*-acetyl derivative (**2**) is a result of steric effects.

EXPERIMENTAL

The proton and carbon-13 NMR spectra were recorded on JEOL LAMBDA 400 (400 MHz) and JEOL ALPHA 500 (500 MHz) spectrometers in CDCl₃ at 298 K. The chemical shifts are given in ppm relative to TMS used as an internal standard. The temperature in dynamic NMR measurements performed in C₂D₂Cl₄ or CDCl₃, was calibrated using the ethylene glycol thermometer for high temperature and the methanol thermometer for low temperature. The infrared (IR) spectra were recorded on a GALAXY Series FT-IR 6030 (Mattson Instruments). The electron ionization mass-spectra were recorded on a VG 7070E (VG Analytical) spectrometer with direct inlet and the electron impact energy 70 eV. The accurate mass measurements were performed on a ZabSpec spectrometer using the peak matching technique at a resolution of 8000–9000.

The semiempirical AM1 SCF [9] calculations were performed using the MOPAC 6.0 program package [15].

The title compounds were prepared by acylation of 1,2-dihydro-2,2,4-trimethylbenzo(*h*)quinoline (**1**) with the respective (commercially available) acyl chloride. The synthesis of **1** is described elsewhere [16], whereas the other reagents were commercially available. The synthesis of *N*-acetyl-1,2-dihydro-2,2,4-trimethylbenzo(*h*)quinoline (**2**) is described as a general method for the preparation of the *N*-acylated compounds (**2**–**5**). The syntheses were carried out at room temperature and the yields ranged between 38 and 58%. An exception was the synthesis of **4** which was accelerated by heating of the reaction mixture for 48 hours at 60°C to give the product in 9.3% yield.

N-Acetyl-1,2-dihydro-2,2,4-trimethylbenzo(*h*)quinoline (**2**).

A magnetically stirred mixture of 0.5 g (2.2 mmol) of 1,2-dihydro-2,2,4-trimethylbenzo(*h*)quinoline (**1**) and 0.1 ml (1.4 mmol) of acetyl chloride in 10 ml of dioxane was left to react for 48 hours at room temperature, at which time the reaction mixture was quenched with 10 ml of water and extracted with ether. The ether extracts were collected, dried over sodium sulphate and concentrated at reduced pressure to yield 0.63 g of yellow oil. The crude product was passed through a silica gel column to yield 0.14 g (37.7 %) of *N*-acetyl-1,2-

dihydro-2,2,4-trimethylbenzo(*h*)quinoline (2) as a slightly yellow oil and 0.27 g of starting material (1).

IR (cm⁻¹): 3060, 2966, 2919, 2849, 1731, 1673 (C=O), 1558, 1508, 1463, 1363, 1310, 1265, 1243, 1175, 826, 752; MS (EI, 70 eV): 265 (M⁺, [C₁₈H₁₉NO], 9%), 250 ([M-CH₃]⁺, 9%), 222 ([M-C₂H₃O]⁺, 8%), 208 ([M-C₃H₅O]⁺, 100%), 43 ([CH₃CO]⁺, 15%); ¹H NMR (400 MHz, CDCl₃, 25°C): 7.91 (br d, J³ 8.4, 1H, H(10)), 7.83 (br d, J³ 8.1, 1H, H(7)), 7.74(d, J³ 8.4, 1H, H(6)), 7.52 (m, J³ 8.4, 6.8, J⁴ 1.4, 1H, H(9)), 7.50 (d, J³ 8.5, 1H, H(5)), 7.45 (m, J³ 8.1, 6.8, J⁴ 1.3, 1H, H(8)), 5.82 (q, J⁴ 1.5, 1H, H(3)), 2.17 (d, J⁴ 1.5, 3H, =CCH₃), 2.01 (br s, 3H, CH₃), 1.59 (s, 3H, C(O)CH₃), 1.05 (br s, 3H, CH₃); ¹³C NMR (100 MHz, CDCl₃, 25°C): 173.7 (C(O)), 138.5 (C(3)), 133.6 (C(10b)), 133.2 (C(6a)), 130.7 (C(10a)), 128.9 (C(4)), 128.3 (C(7)), 128.1 (C(4a)), 126.8 (C(9)), 125.9 (C(6)), 125.7 (C(8)), 123.7 (C(10)), 121.1 (C(5)), 58.5 (C(2)), 28.0 (CH₃), 26.4 (CCH₃CO), 25.3 (CH₃), 18.0 (=CCH₃). (Found for [C₁₈H₁₉NO]⁺: 265.1467. Calcd.: 265.1469.).

N-Chloroacetyl-1,2-dihydro-2,2,4-trimethylbenzo(h)quinoline (3):

a yellow viscous oil; IR (cm⁻¹): 3059, 2974, 1690 (C=O), 1349, 1219, 828, 752, 677; MS (EI, 70 eV): 299 (M⁺, [C₁₈H₁₈NOCl], 10.5%), 284 ([M-CH₃]⁺, 24.8%), 222 ([M-C₂H₂ClO]⁺, 8.4%), 208 ([M-C₃H₅ClO]⁺, 100%), 28 (CO⁺); ¹H NMR (400 MHz, CDCl₃, 25°C): 7.87 (br d, J³ 8.4, 1H, H(10)), 7.86 (br d, J³ 8.1, 1H, H(7)), 7.78(d, J³ 8.4, 1H, H(6)), 7.55 (m, J³ 8.4, 6.9, J⁴ 1.4, 1H, H(9)), 7.51 (d, J³ 8.5, 1H, H(5)), 7.48 (m, J³ 8.1, 6.8, J⁴ 1.1, 1H, H(8)), 5.83 (q, J⁴ 1.5, 1H, H(3)), 3.67 (d, J² 13.6, 1H, CH₂), 3.47 (d, J² 13.5, 1H, CH₂), 2.18 (d, J⁴ 1.5, 3H, =CCH₃), 2.00 (br s, 3H, CH₃), 1.08 (br s, 3H, CH₃); ¹³C NMR (100 MHz, CDCl₃, 25°C): 169.0 (C(O)), 138.1 (C(3)), 133.3 (C(6a)), 131.2 (C(10b)), 130.3 (C(10a)), 129.1 (C(4)), 128.9 (C(4a)), 128.6 (C(7)), 127.7 (C(9)), 126.7 (C(6)), 126.0 (C(8)), 122.5 (C(10)), 121.2 (C(5)), 59.3 (C(2)), 45.3 (CH₂), 27.6 (CH₃), 24.9 (CH₃), 18.0 (=CCH₃). (Found for [C₁₈H₁₈NOCl]⁺: 299.1077. Calcd.: 299.1080.)

N-Isobutyryl-1,2-dihydro-2,2,4-trimethylbenzo(h)quinoline (4):

m.p. 135–137°C (hexane-dichloromethane); IR (cm⁻¹): 3062, 2968, 2931, 2869, 1680 (C=O), 1557, 1508, 1466, 1379, 1299, 1208, 1175, 1080, 836, 787; MS (EI, 70 eV): 293 (M⁺, [C₂₀H₂₃NO], 19.6%), 278 ([M-CH₃]⁺, 10.9%), 222 ([M-C₄H₇O]⁺, 45.1%), 208 ([M-C₅H₉O]⁺, 100%), 71 (C₄H₇O⁺), 43 (C₃H₇⁺); ¹H NMR (500 MHz, CDCl₃, 25°C): 7.88 (d, J³ 8.6, 1H, H(10)), 7.82 (d, J³ 8.1, 1H, H(7)), 7.70 (d, J³ 8.5, 1H, H(6)), 7.49 (m, J³ 8.5, 6.9, J⁴ 1.4, 1H, H(9)), 7.49 (d, J³ 8.5, 1H, H(5)), 7.44 (m, J³ 8.1, 6.8, J⁴ 1.2, 1H, H(8)), 5.76 (q, J⁴ 1.5, 1H, H(3)), 2.17 (d, J⁴ 1.5, 3H, =CCH₃), 2.10 (sept., J³ 6.7, 1H, CH), 1.93 (s, 3H, CH₃), 1.06 (s, 3H, CH₃), 0.87 (d, J³ 6.5, 3H, CH₃), 0.70 (d, J³ 7.0, 3H, CH₃); ¹³C NMR (125 MHz, CDCl₃, 25°C): 181.8 (C(O)), 137.7 (C(3)), 133.2 (C(6a)), 133.1 (C(10b)), 131.1 (C(10a)), 128.9 (C(4)), 128.2 (C(7)), 127.9 (C(4a)),

126.8 (C(9)), 125.7 (C(8)), 125.4 (C(6)), 123.3 (C(10)), 121.1 (C(5)), 58.3 (C(2)), 35.4 (CH), 28.1 & 25.0 (2xCH₃), 20.1 & 17.4 (2x CH₃) 18.0 (=CCH₃). (Found for [C₂₀H₂₃NO]⁺: 293.1780. Calcd.: 293.1783.)

N-Benzoyl-1,2-dihydro-2,2,4-trimethylbenzo(h)quinoline (5):

m.p. 92–93.5°C (hexane-dichloromethane); IR (cm⁻¹): 3063, 2972, 2928, 2861, 1656 (C=O), 1557, 1510, 1467, 1383, 1314, 1276, 1177, 844, 788, 713; MS (EI, 70 eV): 327 (M⁺, [C₂₃H₂₁NO], 21.4%), 312 ([M-CH₃]⁺, 34.5%), 222 ([M-C₇H₅O]⁺, 20.3%), 207 ([M-C₈H₈O]⁺, 10.6%), 105 ([C₇H₅O]⁺, 100%), 77 (C₆H₅⁺, 36.4%); ¹H NMR (500 MHz, CDCl₃, 25°C): 7.90 (d, J³ 8.6, 1H, H(10)), 7.54 (d, J³ 8.2, 1H, H(7)), 7.53 (d, J³ 8.4, 1H, H(6)), 7.45 (d, J³ 8.4, 1H, H(5)), 7.27 (m, J³ 8.5, 6.9, J⁴ 1.3, 1H, H(9)), 7.20 (m, 2H, H(2') & H(6')), 7.19 (m, J³ 8.1, 6.8, J⁴ 1.2, 1H, H(8)), 6.99 (tt, J³ 7.4, J⁴ 1.3, 1H, H(4')), 6.89 (m, 2H, H(3') & H(5')), 5.83 (q, J⁴ 1.5, 1H, H(3)), 2.26 (d, J⁴ 1.5, 3H, =CCH₃), 2.03[#] (s, 3H, CH₃), 1.27[#] (s, 3H, CH₃); ¹³C NMR (125 MHz, CDCl₃, 25°C): 172.6 (C(O)), 138.6 (C(1')), 136.7 (C(3)), 133.8 (C(10b)), 133.3 (C(6a)), 130.2 (C(4')), 130.0 (C(10a)), 128.8 (C(4)), 128.7 (C(2') & C(6')), 127.7 (C(7)), 127.2 (C(3') & C(5')), 126.8 (C(4a)), 125.8 (C(9)), 125.3 (C(6)), 125.3 (C(8)), 123.9 (C(10)), 120.8 (C(5)), 58.5 (C(2)), 27.8[#] (CH₃), 24.4[#] (CH₃), 18.3 (=CCH₃). (Found for [C₂₃H₂₁NO]⁺: 327.1623. Calcd.: 327.1623.)

ACKNOWLEDGMENT

We thank Dr. Aino Pihl (University of Tartu) for the co-working and help in the synthesis of the benzo(h)quinoline derivatives studied. Also we thank Vladimir Ovcharenko (University of Turku) for recording the mass spectra.

REFERENCES

1. Leis, J.; Karelson, M.; Schiemenz, G.P. *ACH-Mod. Chem.* **1998**, *135*, 157.
2. Leis, J.; Maran, U.; Schiemenz, G.P.; Karelson, M. *ACH-Mod. Chem.* **1998**, *135*, 173.
3. Speckcamp, W.N.; Pandit, U.K.; Huisman, H.O. *Tetr. Lett.* **1964**, 3279.
4. Speckcamp, W.N.; Pandit, U.K.; Korver, P.K.; van der Haak, P.J.; Huisman, H.O. *Tetrahedron* **1966**, *22*, 2413.
5. Stewart, W.E., Siddall, T.H. *Chem. Rev.* **1970**, *70*, 517.
6. Feigel, M.; Strassner, T. *THEOCHEM* **1993**, *102*, 33.

[#] observed at 213 K

7. Leis, J.; Klika, K.D.; Karelson, M. *Tetrahedron*, **1998**, 54, 7497.
8. Sandström, J. *Dynamic NMR Spectroscopy*; Academic Press, London, 1982.
9. Dewar, M.J.S.; Zebisch, E.G.; Healy, E.F.; Stewart, J.J.P. *J. Am. Chem. Soc.* **1985**, 107, 3902.
10. Casarini, D.; Lunazzi, L.; Pasquali, F.; Gasparrini, F.; Villani, C. *J. Am. Chem. Soc.* **1992**, 114, 6521.
11. Casarini, D.; Lunazzi, L.; Macciantelli, D. *J. Chem. Soc., Perkin Trans. 2*, **1992**, 1363.
12. Lambert, J.B. *Top. Stereochem.* **1971**, 6, 19.
13. Ross, B.D.; Wong, L.T.; True, N.S. *J. Phys. Chem.* **1985**, 89, 836.
14. Suarez, C.; Tafazzoli, M.; True, N.S.; Gerrard, S.; LeMaster, C.B.; LeMaster, C.L. *J. Phys. Chem.* **1995**, 99, 8170.
15. Stewart, J.J.P. *MOPAC 6.0*, QCPE No. 455, **1989**.
16. Leis, J.; Pihl, A.; Pihlaja, K.; Karelson, M. *ACH-Mod. Chem.* **1998**, 135, 573.

CURRICULUM VITAE

JAAN LEIS

Born: March 6, 1967 in Jõgeva, Estonia
Citizenship: Estonian
Marital Status: Married, 2 children
Address: Institute of Chemical Physics, Phone: +372 7 375 254
University of Tartu, Fax: +372 7 375 264
2 Jakobi Str., E-mail: jaan@chem.ut.ee
Tartu 51014, Estonia

EDUCATION

1985–1992 Student, Department of Chemistry, University of Tartu, Estonia; B.S. (chemistry) in 1992;
1992–1994 Graduate Student, Department of Chemistry, University of Tartu, Estonia; M.Sc. (chemistry) in 1994;
1994–present PhD student, Department of Chemistry, University of Tartu, Estonia, doctoral advisor Prof. Mati Karelson.

PROFESSIONAL EXPERIENCES

1993–1995 (12 months) Visiting Scholar, Department of Organic Chemistry, University of Kiel, Germany; in the group of Prof. Günther-Paulus Schiemenz;
1995–1996 (6 months) Visiting Scholar, Department of Organic Chemistry, University of Uppsala, Sweden; in the group of Prof. Olle Matson and Dr. Svante Axelsson;
1997 (6 months) Visiting Scholar, Department of Physical Chemistry, University of Turku, Finland; in the group of Prof. Kalevi Pihlaja.

SCIENTIFIC WORK

1. **J. Leis**, K. Pihlaja and M. Karelson. Sintez 1-fenil-3,4-dimetilfosfoli, dimera 1-fenil-3,4-dimetilfosfol-1-oksida i 1-fenil-3,4-dimetil-2,5-digidrofosfol-1-oksida. *Zh. Org. Khim.* **1996**, 32, 446–448.
2. **J. Leis**, M. Karelson, G.-P. Schiemenz. Stereochemistry of Arylamides 1. NMR Spectra of Some *N*-(1-Naphthyl)amides. *ACH — Models in Chemistry* **1998**, 135 (1–2), 157–171.
3. **J. Leis**, U. Maran, G.-P. Schiemenz, M. Karelson. Stereochemistry of Arylamides 2. AM1 SCF and SCRF Quantum Chemical Modelling of Some *N*-(1-Naphthyl)amides. *ACH - Models in Chemistry* **1998**, 135 (1–2), 173–181.

4. **J. Leis**, A. Pihl, K. Pihlaja, M. Karelson. Reaction of 1-Naphthyl Amine with Methyl Ketones: A Possible Route to The One-Pot Syntheses of Substituted 1,2-Dihydrobenzo(*h*)quinolines. *ACH-Models in Chemistry* **1998**, 135 (4), 573–581.
5. **J. Leis**, K. D. Klika, M. Karelson. Solvent Polarity Effects on the *E/Z* Conformational Equilibrium of *N*-1-naphthylamides. *Tetrahedron* **1998**, 54, 7497–7504.

CONFERENCES & MEETINGS

1. **J. Leis**, M. Karelson. Hindered *N*-Arylamides: Structure and Isomerism. XXII-th Estonian Chemistry Days, Tartu, 1996 (abstract + poster).
2. S. Axelsson, **J. Leis**. ¹¹C/¹⁴C-Kinetic Isotope Effects of the Monoamine Oxidase (MAO) Catalysed Deamination of Benzylamine. Reaction Mechanism meeting, Canterbury, England, 1996 (abstract + poster).
3. **J. Leis**, M. Karelson, K. D. Klika. Effects of the Polarity of the Environment to the *E/Z* Conformational Equilibria of *N*-Arylamides. XXIII-th Estonian Chemistry Days, Tallinn, 1997 (abstract + poster).
4. **J. Leis**, M. Karelson. Dynamic Processes in *N*-Acylated 1,2-Dihydro-2,2,4-trimethylbenzo(*h*)quinolines. XXIV-th Estonian Chemistry Days, Tartu, 1998 (abstract + poster).

ELULOOKIRJELDUS

JAAN LEIS

Sündinud: 6. märtsil 1967 Jõgeval
Kodakondsus: Eesti
Perekonnaseis: abielus, 2 last
Aadress Keemilise füüsika instituut, Tel.: (27) 375 254
Tartu Ülikool, Faks: (27) 375 264
Jakobi 2, E-post: jaan@chem.ut.ee
Tartu 51014, Eesti

HARIDUS

1985–1992 Tartu Ülikooli keemiaosakonna üliõpilane, *B.S.* (keemia) 1992. aastal;
1992–1994 Tartu Ülikooli keemiaosakonna magistrant, *M.Sc.* (keemia) 1994. aastal;
1994 – tänap. Tartu Ülikooli keemiaosakonna doktorant, juhendaja prof. Mati Karelson.

ERIALASED KOGEMUSED

1993–1995 Kieli Ülikooli orgaanilise keemia osakonna külalisteadur prof. (12 kuud) Günther-Paulus Schiemenzi grupis;
1995–1996 Uppsala Ülikooli orgaanilise keemia osakonna külalisteadur (6 kuud) prof. Olle Matsoni ja dr. Svante Axelssoni grupis;
1997 Turu Ülikooli füüsikalise keemia osakonna külalisteadur prof. (6 kuud) Kalevi Pihlaja grupis.

TEADUSPUBLIKATSIOONID

1. **J. Leis**, K. Pihlaja and M. Karelson. Sintez 1-fenil-3,4-dimetilfosfoli, dimera 1-fenil-3,4-dimetilfosfol-1-oksida i 1-fenil-3,4-dimetil-2,5-digidrofosfol-1-oksida. *Zh. Org. Khim.* **1996**, 32, 446–448.
2. **J. Leis**, M. Karelson, G.-P. Schiemenz. Stereochemistry of Arylamides 1. NMR Spectra of Some *N*-(1-Naphthyl)amides. *ACH — Models in Chemistry* **1998**, 135 (1–2), 157–171.
3. **J. Leis**, U. Maran, G.-P. Schiemenz, M. Karelson. Stereochemistry of Arylamides 2. AM1 SCF and SCRF Quantum Chemical Modelling of Some *N*-(1-Naphthyl)amides. *ACH — Models in Chemistry* **1998**, 135 (1–2), 173–181.
4. **J. Leis**, A. Pihl, K. Pihlaja, M. Karelson. Reaction of 1-Naphthyl Amine with Methyl Ketones: A Possible Route to The One-Pot Syntheses of Substi-

tuted 1,2-Dihydrobenzo(*h*)quinolines. *ACH-Models in Chemistry* **1998**, 135, 573–581.

5. **J. Leis**, K. D. Klika, M. Karelson. Solvent Polarity Effects on the *E/Z* Conformational Equilibrium of *N*-1-naphthylamides. *Tetrahedron* **1998**, 54, 7497–7504.

OSALEMINE KONVERENTSIDEL

1. **J. Leis**, M. Karelson. Hindered *N*-Arylamides: Structure and Isomerism. XXII-th Estonian Chemistry Days, Tartu, 1996 (abstract + poster).
2. S. Axelsson, **J. Leis**. $^{11}\text{C}/^{14}\text{C}$ -Kinetic Isotope Effects of the Monoamine Oxidase (MAO) Catalysed Deamination of Benzylamine. Reaction Mechanism meeting, Canterbury, England, 1996 (abstract + poster).
3. **J. Leis**, M. Karelson, K. D. Klika. Effects of the Polarity of the Environment to the *E/Z* Conformational Equilibria of *N*-Arylamides. XXIII-th Estonian Chemistry Days, Tallinn, 1997 (abstract + poster).
4. **J. Leis**, M. Karelson. Dynamic Processes in *N*-Acylated 1,2-Dihydro-2,2,4-trimethylbenzo(*h*)quinolines. XXIV-th Estonian Chemistry Days, Tartu, 1998 (abstract + poster).

DISSERTATIONES CHIMICAE UNIVERSITATIS TARTUENSIS

1. Toomas Tamm. Quantum-chemical simulation of solvent effects. Tartu 1993, 110 p.
2. Peeter Burk. Theoretical Study of gas-phase acid-base equilibria. Tartu 1994, 96 p.
3. Victor Lobanov. Quantitative structure-property relationships in large descriptor spaces. Tartu 1995, 135 p.
4. Vahur Mäemets. The ^{17}O and ^1H nuclear magnetic resonance study of H_2O in individual solvents and its charged clusters in aqueous solutions of electrolytes. Tartu 1997, 140 p.
5. Andrus Metsala. Microcanonical rate constant in nonequilibrium distribution of vibrational energy and in restricted intramolecular vibrational energy redistribution on the basis of Slater's theory of unimolecular reactions. Tartu 1997, 150 p.
6. Uko Maran. Quantum-mechanical study of potential energy surfaces in different environments. Tartu 1997, 137 p.
7. Alar Jänes. Adsorption of organic compounds on antimony, bismuth and cadmium electrodes. Tartu 1998, 219 p.
8. Kaido Tammeveski. Oxygen electroreduction on thin platinum films and the electrochemical detection of superoxide anion. Tartu 1998, 139 p.
9. Ivo Leito. Studies of Brønsted acid-base equilibria in water and nonaqueous media. Tartu 1998, 101 p.



ISSN 1406-0299
ISBN 9985-56-363-8